


5-2009

Identifying biomarkers for resistance to novel cisplatin analogues in human lung, breast and prostate cancers

Becky Michelle Hess
University of Nevada, Las Vegas

Follow this and additional works at: <https://digitalscholarship.unlv.edu/thesesdissertations>

 Part of the [Biochemistry Commons](#), [Chemicals and Drugs Commons](#), [Medicinal-Pharmaceutical Chemistry Commons](#), and the [Molecular Biology Commons](#)

Repository Citation

Hess, Becky Michelle, "Identifying biomarkers for resistance to novel cisplatin analogues in human lung, breast and prostate cancers" (2009). *UNLV Theses, Dissertations, Professional Papers, and Capstones*. 992.

<https://digitalscholarship.unlv.edu/thesesdissertations/992>

This Thesis is protected by copyright and/or related rights. It has been brought to you by Digital Scholarship@UNLV with permission from the rights-holder(s). You are free to use this Thesis in any way that is permitted by the copyright and related rights legislation that applies to your use. For other uses you need to obtain permission from the rights-holder(s) directly, unless additional rights are indicated by a Creative Commons license in the record and/or on the work itself.

This Thesis has been accepted for inclusion in UNLV Theses, Dissertations, Professional Papers, and Capstones by an authorized administrator of Digital Scholarship@UNLV. For more information, please contact digitalscholarship@unlv.edu.

IDENTIFYING BIOMARKERS FOR RESISTANCE TO NOVEL CISPLATIN
ANALOGUES IN HUMAN BREAST, LUNG AND PROSTATE CANCERS

by

Becky Michelle Hess

Bachelor of Science
University of Nevada, Las Vegas
2006

A thesis submitted in partial fulfillment
of the requirements for the

Masters of Science Degree in Biochemistry
Department of Chemistry
College of Sciences

Graduate College
University of Nevada, Las Vegas
May 2009

UMI Number: 1472415

INFORMATION TO USERS

The quality of this reproduction is dependent upon the quality of the copy submitted. Broken or indistinct print, colored or poor quality illustrations and photographs, print bleed-through, substandard margins, and improper alignment can adversely affect reproduction.

In the unlikely event that the author did not send a complete manuscript and there are missing pages, these will be noted. Also, if unauthorized copyright material had to be removed, a note will indicate the deletion.

UMI[®]

UMI Microform 1472415
Copyright 2009 by ProQuest LLC
All rights reserved. This microform edition is protected against
unauthorized copying under Title 17, United States Code.

ProQuest LLC
789 East Eisenhower Parkway
P.O. Box 1346
Ann Arbor, MI 48106-1346

Copyright by Becky Michelle Hess 2009
All rights reserved



Thesis Approval
The Graduate College
University of Nevada, Las Vegas

February 20, 2009

The Thesis prepared by
Becky Michelle Hess

Entitled
Identifying Biomarkers for Resistance to Novel Cisplatin Analogues in
Human Breast, Lung and Prostate Cancers

is approved in partial fulfillment of the requirements for the degree of
Masters of Science in Biochemistry

Examination Committee Chair

Dean of the Graduate College

Examination Committee Member

Examination Committee Member

Graduate College Faculty Representative

ABSTRACT

Identifying Biomarkers for Resistance to Novel Cisplatin Analogues in Human Lung, Breast and Prostate Cancers

by

Becky Michelle Hess

Dr. Bryan L. Spangelo, Examination Committee Chair
Professor of Chemistry
University of Nevada, Las Vegas

Cisplatin is a common therapeutic agent used in cancer treatment. Unfortunately, resistance to cisplatin in addition to severe side effects limits its use in cancer treatment. Two novel cisplatin analogues, 4DB and 4TB were shown to have varying cytotoxicity in lung, breast and prostate cancer cells. The hypothesis for this study states that the differences in 4DB and 4TB cytotoxicity among different tissue types is due to the type and efficiency of DNA repair mechanisms involved in response to these drugs.

To test the hypothesis, proteins involved in the rate limiting step of nucleotide excision repair (NER) and mismatch repair (MMR) mechanisms were disrupted using stable shRNA transfectants. Survival assays using these cell lines revealed that suppression of MMR enhanced survival in breast and lung cancer cells with respect to cisplatin treatment. Suppression of NER enhanced sensitivity of prostate cancer cells to 4TB.

Microarray analysis of 4DB treated cells showed repeated over expression of the CHOP gene, indicating DNA damage signalling. Repeated over expression of ZNT1 and MT-1L genes were identified in lung and prostate cells in response to cisplatin and 4TB treatment, indicating their capacity to mitigate drug cytotoxicity in these tissue types.

TABLE OF CONTENTS

ABSTRACT.....	iii
LIST OF FIGURES.....	vii
LIST OF TABLES.....	ix
ABBREVIATIONS.....	x
ACKNOWLEDGEMENTS.....	xi
CHAPTER 1 INTRODUCTION.....	1
Purpose of the Study.....	1
Significance of the Study.....	2
Research Questions.....	3
CHAPTER 2 REIEW OF RELATED LITERATURE.....	4
Cisplatin.....	4
Second Generation Cisplatin Analogues.....	6
Gene Expression Profiles.....	10
Genes of Interest.....	11
Hypothesis.....	15
CHAPTER 3 MATERIALS AND METHODS.....	17
Cell Culture.....	17
Z1 Beckman Coulter Particle Counter.....	18
Preparation of Cisplatin and Cisplatin Analogues.....	18
Transient Short Hairpin RNA.....	19
Stable Short Hairpin RNA or Expression Plasmid Transfection.....	20
Colony Formation Assay.....	22
RNA Extractions.....	23
RNA Quantification and Verification of Purity.....	24
Microarray Analysis.....	25
Western Blot Analysis.....	26
Cell Cycle Analysis.....	28
Intracellular Antigen Staining.....	29

Fluorescent Microscopy.....	31
DNA Extractions	33
DNA Quantification and Purity Verification	33
Determining Platinum Concentration by ICP-MS	34
Statistical Analysis	37
CHAPTER 4 FINDINGS OF THE STUDY	38
CHAPTER 5 SUMMARY, CONCLUSIONS AND RECOMMENDATIONS	95
REFERENCES	110
VITA.....	113

LIST OF FIGURES

Figure 1.	Structure of cisplatin.....	5
Figure 2.	Mechanism of GpG adduct formation.....	6
Figure 3.	Structures of carboplatin, oxaliplatin and nedaplatin.....	7
Figure 4.	Structures of novel cisplatin analogues.....	8
Figure 5.	Structures of 4DB and 4TB.....	9
Figure 6.	Binding of HMGB1 to DNA containing a Pt-DNA adduct.....	12
Figure 7.	Mechanism of DNA Mismatch Repair.....	13
Figure 8.	Mechanism of DNA Nucleotide Excision Repair.....	14
Figure 9.	Procedure for developing stable cell lines expressing shRNA.....	22
Figure 10.	Clonogenic survivals of MDA-MB-435, A-549 and DU-145 cells.....	40
Figure 11.	Standard curves of DNA mass verses cell number.....	43
Figure 12.	ICP-MS analysis of protocol optimization experiments.....	47
Figure 13.	ICP-MS analysis of percentage of drug uptake in whole cells and nuclear extracts of MDA-MB-435, A-549 and DU-145 cells.....	49
Figure 14.	ICP-MS analysis of mass of platinum per mass of protein in MDA-MB-435, A-549 and DU-145 cells.....	51
Figure 15.	ICP-MS analysis of mass of platinum per mass of DNA in MDA-MB-435, A-549 and DU-145 cells.....	54
Figure 16.	ICP-MS analysis of percentage of drug remaining in MDA-MB-435, A-549 and DU-145 whole cells.....	56
Figure 17.	ICP-MS analysis of percentage of drug bound to DNA remaining in MDA-MB-435, A-549 and DU-145 cells.....	58
Figure 18.	Fluorescent microscopy analysis of MDA-MB-435 cells treated with 4DB.....	60
Figure 19.	Flow cytometry analysis of MDA-MB-435 cells treated with 4DB.....	62
Figure 20.	Western blot analysis of MDA-MB-435, A-549 and DU-145 wild type cells.....	82
Figure 21.	Expression vector map for shRNA constructs.....	83
Figure 22.	Western blot analysis of transiently transfected MDA-MB-435, A-549 and DU-145 cells.....	84
Figure 23.	Intracellular antigen staining analysis of MDA-MB-435 cells.....	85
Figure 24.	Western blot analysis of wild type and all shRNA constructs for MDA-MB-435 cells.....	86
Figure 25.	Western blot analysis of wild type and transfected MDA-MB-435.....	88

Figure 26.	Western blot analysis of wild type and transfected A-549.....	88
Figure 27.	Western blot analysis of wild type and transfected DU-145.....	89
Figure 28.	Clonogenic survivals of MDA-MB-435 transfected cells.....	90
Figure 29.	Clonogenic survivals of A-549 transfected cells.....	92
Figure 30.	Clonogenic survivals of DU-145 transfected cells.....	93

LIST OF TABLES

Table 1.	EC ₅₀ values determined by Van Vo.....	38
Table 2.	EC ₅₀ values determined in the current study.....	41
Table 3.	Platinum concentration in wash control samples.....	44
Table 4.	Platinum concentration in each EC ₅₀ concentration.....	45
Table 5.	Protocol development summary for ICP-MS analysis.....	46
Table 6.	Microarray analysis of MDA-MB-435 cells treated with 4DB.....	64
Table 7.	Microarray analysis of MDA-MB-435 cells treated with 4TB.....	68
Table 8.	Microarray analysis of MDA-MB-435 cells treated with 4TB.....	70
Table 9.	Microarray analysis of A-549 cells treated with 4DB.....	71
Table 10.	Microarray analysis of A-549 cells treated with 4TB.....	73
Table 11.	Microarray analysis of A-549 cells treated with Cisplatin.....	75
Table 12.	Microarray analysis of DU-145 cells treated with 4DB.....	77
Table 13.	Microarray analysis of DU-145 cells treated with 4TB.....	79
Table 14.	Microarray analysis of DU-145 cells treated with Cisplatin.....	80
Table 15.	Nomenclature of cell lines developed using stable transfection of shRNA.	87
Table 16.	EC ₅₀ values of MDA-MB-435 wild type and transfected cell lines.....	94
Table 17.	EC ₅₀ values of A-549 wild type and transfected cell lines.....	94
Table 18.	EC ₅₀ values of DU-145 wild type and transfected cell lines.....	94

ABBREVIATIONS

Abbreviation	Definition
4DB	dichloro(4,4'-dibutyl-2,2'-bipyridine)platinum
4TB	dichloro(4,4'-ditertbutyl-2,2'-bipyridine)platinum
BCA	bicinchoninic acid
BSA	bovine serum albumin
CDDP	cisplatin
cDNA	complementary deoxyribonucleic acid
CEL	GDAS file extension
CLDN4	Caludin 4
cRNA	complementary ribonucleic acid
DMSO	dimethyl sulfoxide
DNA	deoxyribonucleic acid
EC ₅₀	Effective concentration, 50%
EDTA	ethylenediaminetetraacetic acid
ERCC1	Excision Repair Cross Complement 1
G1 phase	gap 1 phase of the cell cycle
G2 phase	gap 2 phase of the cell cycle
GCRMA	Gene Chip Robust Multiple Array
HSPs	heat shock proteins
GDAS	Gene Chip DNA Analysis Software
GFP	green fluorescence protein
HBSS	Hank's Balanced Salt Solution
HEPES	4-(2-hydroxyethyl) piperazine-1-ethanesulfonic Acid
ICP-MS	Inductively Coupled Plasma-Mass Spectrometry
MEM	Minimum Essential Medium
M-PER	Mammalian Protein Extraction Reagent
MSH2	MutS Homolog 2
NER	nucleotide excision repair
PBS	Phosphate Buffered Saline
RNA	ribonucleic acid
SDS	sodium dodecyl sulfate
SDS-PAGE	sodium dodecyl sulfate-polyacrylamide gel electrophoresis
shRNA	short hair pin ribonucleic acid
TBST	Tris-buffered saline Tween-20

ACKNOWLEDGEMENTS

This thesis is in dedication to Dr. Stephen W. Carper who taught me how to be a scientist, a successful student and a better person. I am forever indebted to him for the guidance he so freely gave and his seemingly unlimited amount of patience with me. I am honored that I had the opportunity to work for him and will always cherish his memory. I would also like to thank Dr. Bryan Spangelo for assuming the role of my advisor, especially under such difficult circumstances. I appreciate his guidance, support, and believing in my abilities to finish this project. I would like to thank Dr. Lindle for managing the research grant, which supported my work, and ensuring the Carper lab was able to continue in its daily operations. I am deeply grateful to Ms. Casey Hall for both her technical support in this project as well her emotional support. I must also thank Ms. Shauna Durocher for her willingness to listen to my issues surrounding my project and sharing her experiences with me to enrich my research. Shauna has been such a good friend to me and her support was an invaluable part of my experience in the laboratory. I appreciate all the time and effort put forth by each member of my committee. Finally, I would like to thank my family for their love, patience and support throughout my graduate studies. My parents, Dr. and Mrs. Campbell made my continued education possible. My sister, Jeanette Palmer, for making sure I always had a place to stay. My

husband, John, who has been extremely ill throughout my graduate studies, I thank him for being more supportive, understanding and loving than I could have ever imagined.

CHAPTER 1

INTRODUCTION

1.1 Purpose of the Study

Cancer is currently the second leading cause of death in the United States. The American Cancer Society reported that approximately 1.5 million new cases of cancer were diagnosed in 2008 and half of those diagnosed are expected to die from the disease. Of these new cases, approximately 185,000 will be diagnosed with breast cancer, 215,000 will be diagnosed with lung cancer and 186,000 will be diagnosed with prostate cancer. Treatments for these cancers include surgical resection of the tumor, chemotherapy, radiation and, in the cases of breast and prostate cancer, hormone therapy (American Cancer Society, 2008).

Multiple chemotherapeutic drugs are currently available and these drugs are known to have inconsistent efficacy among different patients (Anguiano et al., 2008). Additionally, these drugs induce various side effects including fatigue, hair loss and nausea. A specific chemotherapeutic drug, cisplatin, has been used in the successful treatment of testicular, ovarian, bladder and neck cancers. Unfortunately, severe side effects with this drug have been reported including renal toxicity, hearing loss and nerve damage. In addition to these severe side effects, cisplatin is ineffective in the

treatment of many malignant tumours including lung carcinomas, colon and rectal adenocarcinomas (Elwell 2006). For these reasons, the development of more effective chemotherapeutic drugs with fewer side effects is needed. A complete understanding of drug function on the cellular level will support the development of customizing drug treatment to individual patients based on protein expression profile, thus avoiding the current trial-and-error method of prescribing chemotherapeutic drugs.

1.2 Significance of the Study

The characterization of drug uptake, DNA repair response and overall survival of different cancer types to two novel cisplatin analogues, 4,4'-ditertbutyl 2,2'-bipyridine dichloroplatinum (4TB) and 4,4'-dibutyl 2,2'-bipyridine dichloroplatinum (4DB), can provide detailed protein expression profiles that are ultimately related to successful chemotherapeutic treatment. The data derived from these experiments can have the potential to determine the protein biomarkers that lead to either poor or successful outcomes with each drug type. Understanding the protein expression profiles would allow screening of individual patient protein biomarkers to determine a patient's sensitivity or resistance to a chemotherapeutic drug. Ultimately, physicians will individualize patient treatment by selecting the drug that is most likely to successfully treat the patient's cancer.

1.3 Research Questions

In order to determine potential biomarkers and other factors responsible for variations in lethality observed upon treatment with cisplatin and cisplatin analogues in different cancer tissue types, the following study will generate data related to the following tasks:

- 1) Characterize drug uptake and drug clearance over time in whole cells in wild type breast, prostate and lung cancer cell lines;
- 2) Determine the levels of platinum-DNA adducts formed over time with each drug in all wild type cell lines;
- 3) Determine by microarray analysis which genes are expressed in the wild type cell lines in response to drug treatment;
- 4) Suppress DNA repair mechanisms, nucleotide excision repair and mismatch repair, using short hairpin RNA, to determine the effects on drug efficacy.

CHAPTER 2

REVIEW OF RELATED LITERATURE

2.1 Cisplatin

Cisplatin (*cis*-diaminodichloroplatinum, CDDP), illustrated in Figure 1, is a compound with a platinum center bound to two ammonia and two chlorine groups in a *cis* conformation. Cisplatin was first approved for use as an anticancer drug in 1979, and it is still being used today in the treatment of cancer (Elwell et al., 2006). Although shown to be effective against testicular, ovarian and bladder cancers, the drug has limited efficacy in lung and colon cancers (Stewart, 2007). The drug also has severe, dose-limiting, side effects including neuropathies, renal toxicity and ototoxicity (Elwell et al., 2006). An additional drawback to the use of cisplatin is the propensity of patients to develop resistance to the drug, which requires physicians to prescribe alternate chemotherapeutics in a “trial and error” approach (Anguiano et al., 2008).

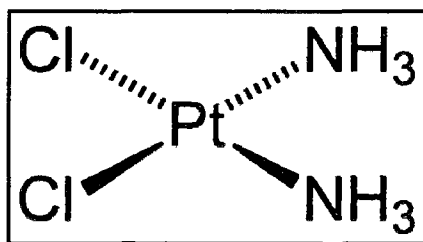


Figure 1: Structure of the chemotherapeutic drug, cisplatin <http://upload.wikimedia.org/>.

The cytotoxic effects of cisplatin are the result of the covalent adduct formation between the platinum center of the drug and either DNA or proteins (Eastman, 1987). When the drug enters solution, the chlorides are easily displaced by water molecules, resulting in a $[\text{Pt}(\text{NH}_3)_2(\text{OH}_2)_2]^{2+}$ or $\text{Pt}(\text{NH}_3)_2(\text{OH})_2$ intermediate compounds. However, these newly formed hydroxyl and water ligands are labile and can be easily displaced, thus allowing the formation of covalent adducts between the platinum molecule and a cellular target (Chaney et al., 2005). The primary cause of cisplatin cytotoxicity is hypothesized to be the formation of DNA intrastrand or interstrand cross links as follows: intrastrand (GpG), intrastrand (ApG), intrastrand (GpNpG) or interstrand (G-G). Of the aforementioned cross linkages formed, intrastrand GpG adducts predominate (Figure 2).

Elucidation of the structure of cisplatin bound to DNA reveals that adduct formation results in a 60 to 80° bend in the DNA which is in the direction of the major groove, resulting in minor groove widening (Chaney et al., 2005). Although these adducts are believed to be responsible for the lethality of cisplatin, only 1% of the administered drug results in DNA adduct formation. One of the reasons for the low percentage of drug binding the DNA is because cisplatin can also bind intracellular proteins. Formation of adducts with intracellular proteins in the cytosol limits the amount of drug that ultimately

gains access to DNA. Once in the nucleus, cisplatin can also bind nuclear proteins, including histones, which has been shown to prevent the remodeling of chromatin, thereby preventing transcription (Mymryk et al., 1995). The insult to these genomic structures and other intracellular proteins results in programmed cell death, or apoptosis (Wang et al., 2005).

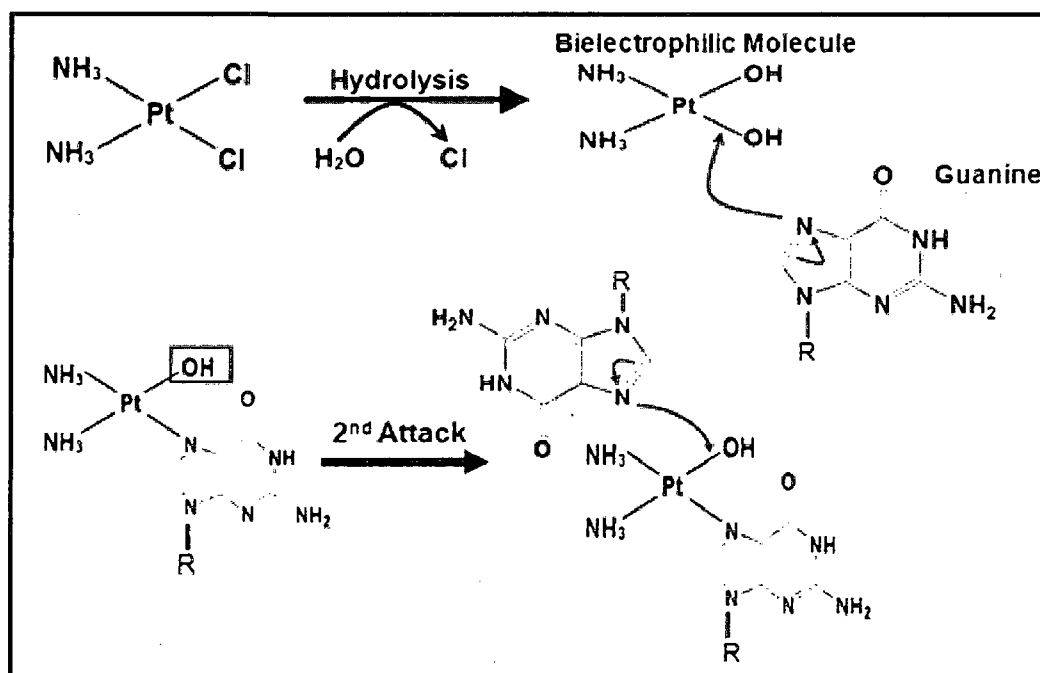


Figure 2: Mechanism of formation of an intrastrand GpG adduct.

2.2 Second Generation Analogues

Acquired drug resistance coupled with the severe side effects of cisplatin sparked interest in the development of second generation cisplatin analogues. Several of these new drugs are currently prescribed as chemotherapeutics. These drugs were all designed

with a central platinum atom and include carboplatin, oxaliplatin and nedaplatin (Wang et al., 2005). Each of the analogues is thought to function in the same manner as cisplatin, with the central platinum forming adducts with intracellular proteins and with DNA. These drugs induce less severe and more tolerable side effects; unfortunately, all three of these analogues have been shown to be less effective than cisplatin in the treatment of cancer (Marcel Gielen et al., 2005). Due to the limited success of oxaliplatin (Figure 3A), carboplatin (Figure 3B) and nedaplatin (Figure 3C), the need for continual development of cisplatin analogues with increased efficacy and reduced general toxicity was realized (Elwell et al., 2006).

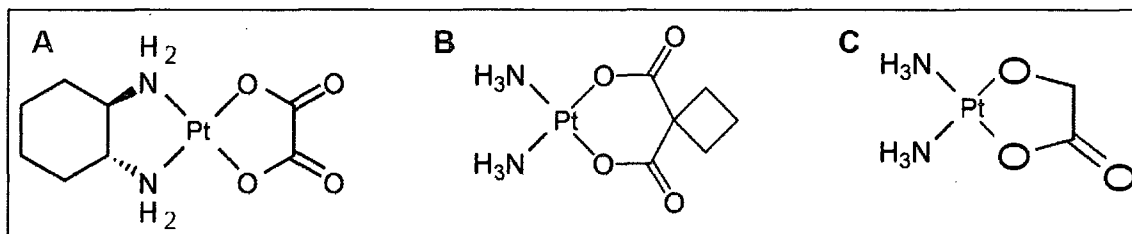


Figure 3: Structures of second generation cisplatin analogues, oxaliplatin (A), carboplatin (B) and nedaplatin (C) <http://upload.wikimedia.org/>.

Synthesis of more complicated chemotherapeutics containing a bipyridine ring structure began in 1992 with fluorinated alkyl groups at the 4 and 4' positions (Garelli et al., 1992b); however, these drugs were not reported to have increased efficacy over cisplatin (Garelli et al., 1992a). More recent studies have shown that the addition of short

alkyl groups, as shown in Figure 4, at the 4 and 4' positions induce significantly increased apoptosis in lung, breast and prostate cancers (Elwell et al., 2006).

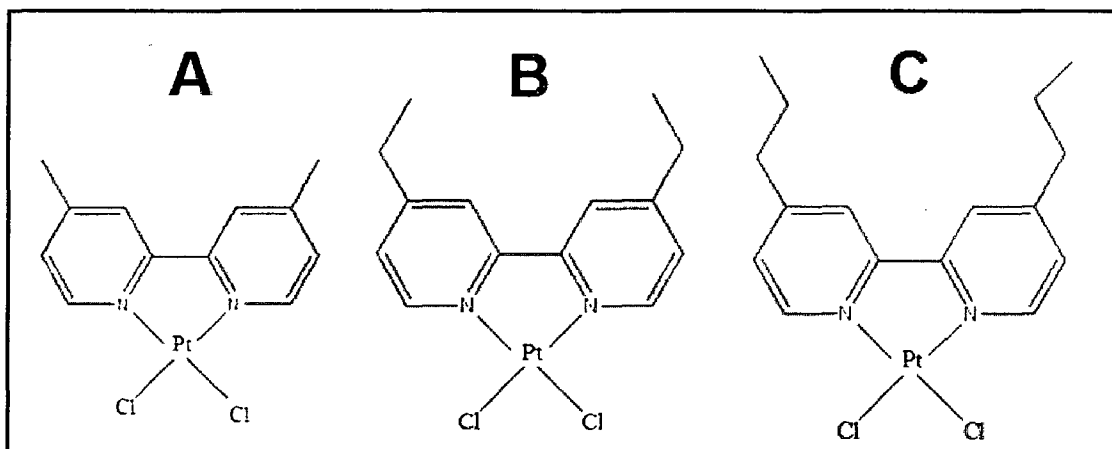


Figure 4: Structures of cisplatin analogues containing a bipyridine ring system, dichloro(4,4'-dimethyl-2,2'-bipyridine)platinum (A), dichloro(4,4'-diethyl-2,2'-bipyridine)platinum (B), and dichloro(4,4'-dipropyl-2,2'-bipyridine)platinum.

The initial success of these analogues lead to the production of dichloro(4,4'-diterbutyl-2,2'-bipyridine)platinum (4TB) and dichloro(4,4'-dibutyl-2,2'-bipyridine)platinum (4DB) (Figure 5) within the current laboratory group to determine the effects of bulkier or lengthier alkyl groups extending from the bipyridine ring system.

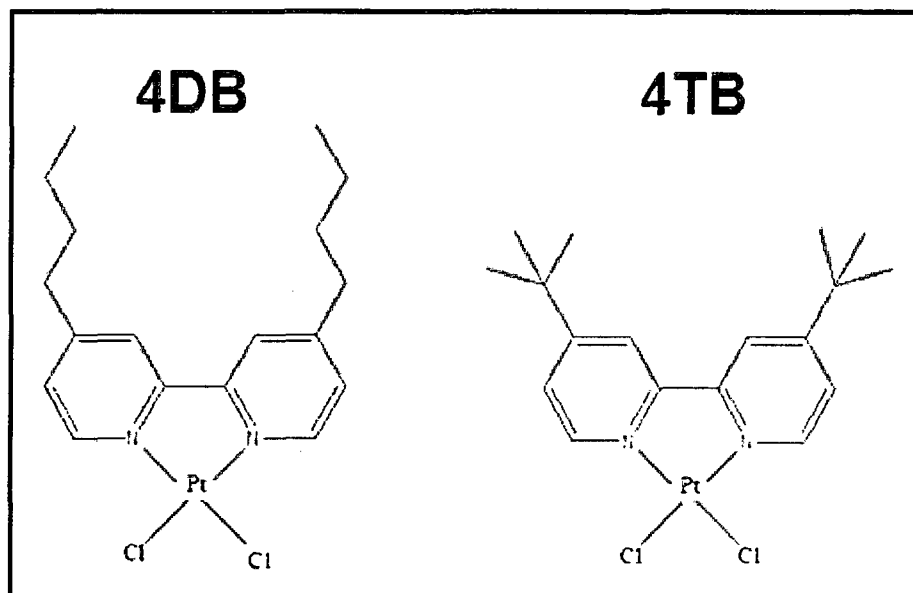


Figure 5: Structures of cisplatin analogues containing a bipyridine ring system, dichloro(4,4'-dibutyl-2,2'-bipyridine)platinum (4DB) and dichloro(4,4'-tertbutyl-2,2'-bipyridine)platinum (4TB).

Clonogenic survival assays with these compounds in lung, prostate and breast cancer cell lines conducted by Vo et al. revealed that the 4DB chemotherapeutic drug was more efficacious than cisplatin in all cell lines. The 4TB drug had different results among the three tissue types. In the lung cancer cell line, the drug was shown to ineffective at all concentrations. In the prostate cancer cell line, 4TB was more efficacious than cisplatin, but less efficacious than 4DB. In the breast cancer cell line, 4TB was as efficacious as 4DB which was nearly 125 times more potent than cisplatin. The findings from these assays raised important questions regarding the rational design of cisplatin analogues. Understanding the different factors in each tissue type that result in the observed cytotoxicity to each drug can lead to the rational drug design of new generation chemotherapeutics. In addition, these data would support more individualized treatment

regimens. Completing gene and protein expression profiles of patient tumours and matching them against the developed criteria for each drug would allow a physician to prescribe the most efficacious drug in the first round of patient therapy.

2.3 Gene Expression Profiles

Using microarray analysis, the genes involved in response to cisplatin have been elucidated for many tissue types (Stewart et al., 2006). In addition to cellular responses to the drug presence, proteins responsible for drug resistance or sensitivity have also been identified (Stewart et al., 2006). For example, in ovarian cancer cells characterized as resistant to cisplatin, Claudin 4 (CLDN4) was shown to be over expressed (Stewart et al., 2006). CLDN4 is a component in the formation of tight junctions between cells and is identified as an integral membrane protein; aberration of these junctions has been associated with the development of cancer (Gonzalez-Mariscal et al., 2003). In the current study, genes of interest include those that are involved in anti-apoptotic pathways, drug transport and modulation of cellular stress.

The use of gene profiling in lung, breast and prostate cancer cell lines with 4DB and 4TB *in vitro* has the potential to reveal the genes responsible for the observed cytotoxicity associated with these drugs. Understanding the mechanisms involved in the response to the drugs for each tissue type has the potential to improve cancer treatment success.

2.4 Genes of Interest

Cisplatin exerts its lethality through the formation of covalent adducts with DNA; however, these lesions can be repaired through two DNA repair mechanisms: nucleotide excision repair (NER) and mismatch repair (MMR) (Chang et al., 2005; Stojic et al., 2004). Therefore, proteins involved in these DNA repair mechanisms are of interest. Additionally, proteins directly involved in apoptosis are also of interest because over expression of either anti-apoptotic, specifically Bcl-2, or pro-apoptotic proteins, specifically; Bid, Bad and Bax; have been associated with general chemoresistance (Biswas et al., 2004).

Cisplatin adducts are poorly repaired, regardless of the repair mechanism involved, when the lesion is bound by high-mobility-group (HMG) proteins. When an HMG protein binds an adduct, its presence prevents recognition of the adduct by proteins involved in DNA repair processes (Jordan et al., 2000). HMG proteins bind nonspecifically to DNA and induce sharp bends in the DNA structure upon binding. For example, as shown in Figure 6, when HMGB1 binds the DNA it inserts a phenyl group into the groove created by cisplatin binding. Thus, these proteins preferentially bind to DNA that is already distorted which accounts for their propensity to bind to cisplatin-DNA adducts (Farid et al., 1996). Therefore, elevation of HMG protein levels in treated cells compared to untreated samples will be of interest in determining if these proteins play a role in cisplatin cytotoxicity.

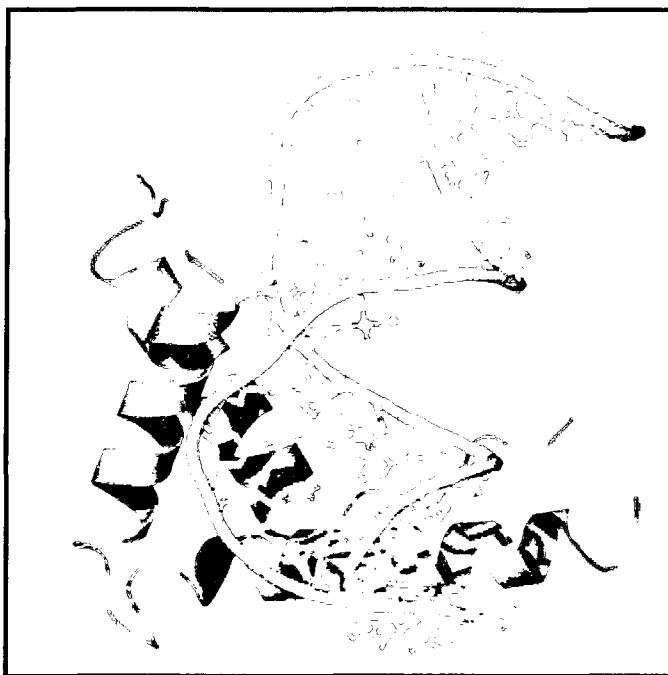


Figure 6: Binding of HMGB1 to DNA in a region containing a cisplatin-DNA adduct
<http://gibs.ws/cisplatin.com>.

The repair of cisplatin-DNA adducts is completed by the NER and MMR mechanisms. Each of these repair systems has rate limiting steps which provide genes of interest for this study. With respect to NER, the excision repair cross complement 1 (ERCC1) protein is responsible for the rate limiting step in the repair process, whereas the MutS Homolog 2 (MSH2) protein is responsible for the rate limiting step in the MMR process (Chang et al., 2005; Stojic et al., 2004). Both the rate and efficiency of each DNA repair process is thought to be critical to the successful removal of cisplatin-DNA adducts; therefore, the ERCC1 and MSH2 proteins are a focus in the current study.

Mismatches in DNA can be identified due to their lack of Watson-Crick base pairing, often resulting in modification of the overall DNA structure. MSH2 is responsible for recognizing mismatches in the DNA and initiating the MMR process. MSH2 forms a heterodimer with MSH6 which results in the formation of a sliding clamp. The MSH2/MSH6 complex formation recruits both MLH1 and PMS2 which forms a second heterodimer. This complete complex, as illustrated in Figure 7, can traverse DNA structures in both the forward and reverse directions to identify the compromised section of the strand (Stojic et al., 2004).

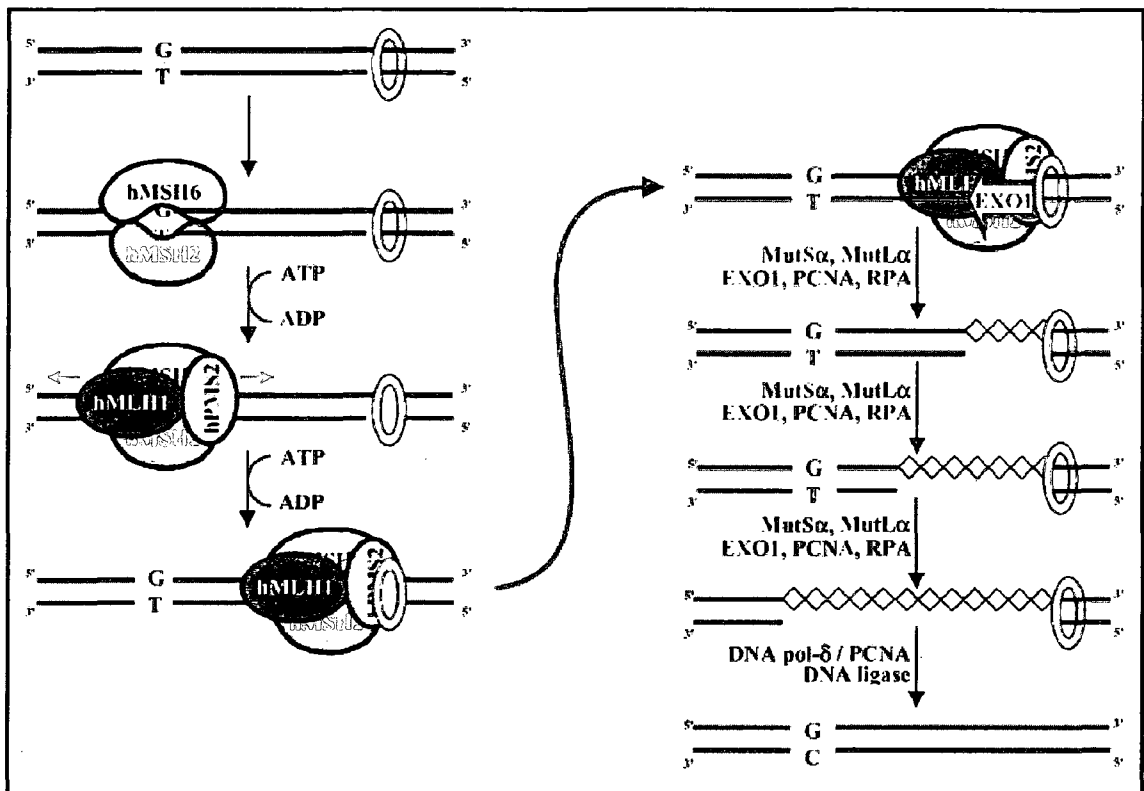


Figure 7: Mechanism of MMR, activated by the formation of cisplatin-DNA adducts (Stojic et al., 2004).

NER has been identified as the predominant DNA repair process which responds to the presence of cisplatin-DNA adducts. The NER mechanism, like MMR, is initiated by [1] damage recognition; [2] unwinding of the DNA strands; [3] exonuclease activities on either side of the lesion; and [4] removal of the damaged oligonucleotides and resynthesis of the removed section (Chang et al., 2005). As shown in Figure 8, there are multiple proteins involved, and although ERCC1 is not responsible for damage recognition, its initiation of the incision at the 5' end of the damage site is the rate limiting step of the DNA repair mechanism.

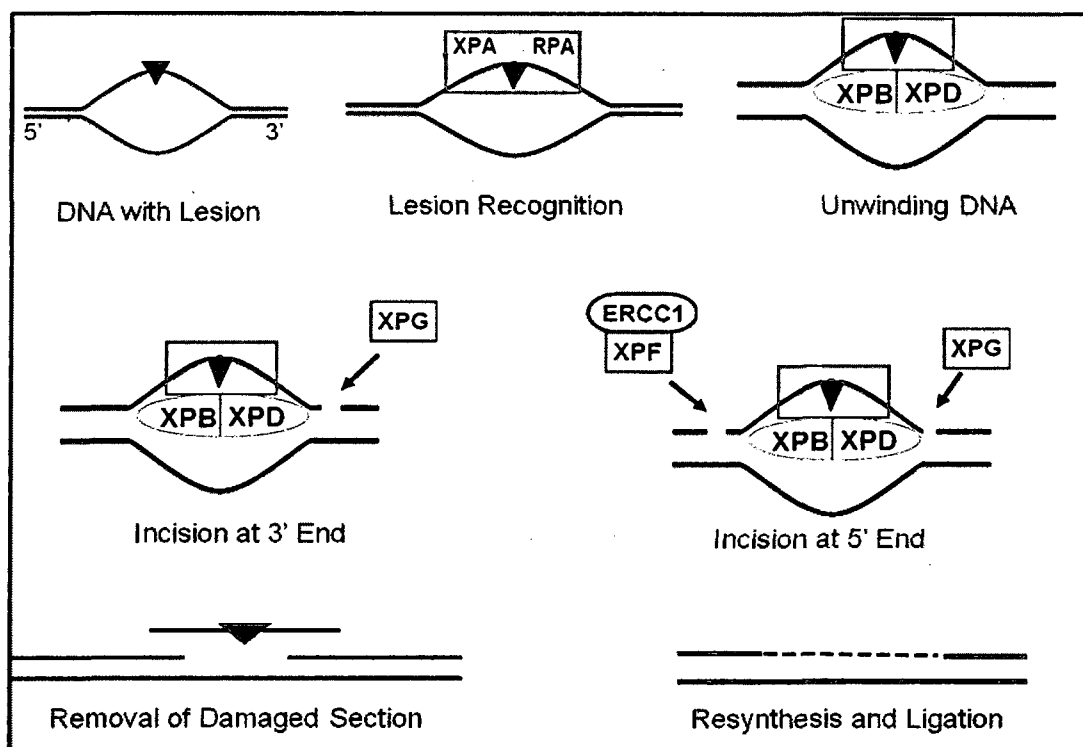


Figure 8: Mechanism of NER, activated by the formation of cisplatin-DNA adducts.

2.5 Hypothesis

Cisplatin has been widely used in the treatment of cancer, but severe dose-limiting side effects coupled with the propensity of patients to develop resistance to the drug warrants the development of more efficacious chemotherapeutics. Characterization of gene expression in response to the cisplatin analogues in different cancer types can lend insight into the mechanisms involved in cytotoxicity effectiveness. These data can be used in the rational drug design of future chemotherapeutic drugs. Further, understanding the response to each drug will allow the development of criteria for optimum drug usage. For example, if a drug is known to perform well in patients with suppressed NER activity, a patient can be screened for these related proteins in order to determine if the drug is an appropriate part of overall treatment.

The hypothesis for the current study is that *the differences in observed cytotoxicity between 4DB and 4TB among different tissue types is due to the type and efficiency of the DNA repair mechanisms involved in response to these drugs*. To test the hypothesis, the level of drug uptake as well as rate of repair of platinum-DNA adducts for cisplatin, 4DB and 4TB will be determined using inductively coupled plasma mass spectrometry (ICP-MS) in the wild type lung (A-549), breast (MDA-MB-435) and prostate (DU-145) cancer cell lines. Microarray analysis will also be conducted on the wild type cell lines following exposure to each of the three drugs to assess the genes involved in observed drug sensitivity or resistance. The MMR and NER mechanisms will be disrupted using short hairpin RNA (shRNA) against MSH2 or ERCC1 in each of the cell lines. Once these

transfected cell lines are developed, the cytotoxicity of each of the drugs will be determined using cell viability assays.

CHAPTER 3

MATERIALS AND METHODS

All chemicals and reagents used were of the highest quality grade. All cell lines were maintained at 95% humidity, 5% CO₂ and 37 °C unless otherwise stated. Ultrapure water was used in sample and drug preparations requiring the use of water.

3.1 Cell Culture

The human breast cancer cell line, MDA-MB-435, human prostate cancer cell line, DU-145, and human lung cancer cell line, A-549, was obtained from the American Type Culture Collection (Manassas, VA, USA). MDA-MB-435 and A-549 cells were both cultured in Minimum Essential Medium, Eagle (MEM) (Earle's Salts and L-glutamine, Invitrogen, USA) supplemented with 10% fetal bovine serum (Invitrogen, USA), 25mM HEPES pH 7.4 (Sigma-Aldrich, USA) and 1% penicillin-streptomycin (Invitrogen, USA). Transfected cell lines derived from A-549 or MDA-MB-435 were also cultured in MEM medium which contained 0.5µg/mL puromycin (Sigma-Aldrich, USA). DU-145 cells were culture in RPMI 1640 medium (Earle's Salts and L-glutamine, Invitrogen, USA) supplemented with 10% fetal bovine serum (Invitrogen, USA), 15mM HEPES pH 7.4 (Sigma-Aldrich, USA) and 1% penicillin-streptomycin (Invitrogen, USA). Transfected cell lines derived from DU-145 cells

were also cultured in RPMI 1640 medium which contained 0.5 μ g/mL puromycin. All cells were incubated at 37 °C in a 95% humidity environment containing 5% CO₂. Cell harvests were obtained by washing cells three times in phosphate buffered saline (PBS at pH 7.2) which did not contain CaCl₂ or MgCl₂ (Invitrogen, USA), followed by chemically detaching adherent cells by exposing the cells for 10 min to trypsin-EDTA (0.25% Trypsin with 53mM EDTA) in HBSS without calcium or magnesium (Invitrogen, USA). Fresh medium was added following the 10 min trypsin exposure to inactivate the trypsin. Cells counts were performed using a Z1 Beckman Coulter® Particle Counter (Fullerton, CA).

3.2 Z1 Beckman Coulter® Particle Counter

Cell suspension (0.1 mL) was added to 9.9 mL of an azide-free isotonic diluent (Isoton) solution (Val-Tech Diagnostics Inc., Pittsburgh, PA). The solution was stirred and placed in the Z1 Beckman Coulter® Particle Counter (Fullerton, CA). Two or three measurements were averaged and used to calculate the cell density of the solution.

3.3 Preparation of Cisplatin, Dichloro(4,4'-dibutyl-2,2'-biyprindine)platinum, Dichloro(4,4'-tertbutyl-2,2'-bipyridine)platinum and Puromycin

A 50 mM stock of cisplatin was prepared by dissolving 0.150 grams of 300.05 g/mol cisplatin (CDDP; Sigma-Aldrich, USA) in 10 mL of dimethyl sulfoxide (DMSO; Sigma-Aldrich, USA). The solution was sterile filtered using a syringe

(Becton Dickinson, USA) with an attached 0.2 μm nylon membrane syringe filter (PALL, Ann Arbor, MI). Serial dilutions were completed using 500 μL of the 50 mM stock diluted in 4.5 mL of sterile filtered DMSO.

A 5 mM stock of dichloro(4,4'-dibutyl-2,2'-bipyridine)platinum (4DB) or dichloro(4,4'-tertbutyl-2,2'-bipyridine)platinum (4TB), both kind gifts from Dr. Byron Bennett, were prepared by dissolving 0.0267 grams of 534.49 g/mol 4TB or 4DB in 10 mL of DMSO. The solutions were sterile filtered as described previously. Serial dilutions were completed using 500 μL of the 5 mM stock diluted in 4.5 mL of sterile filtered DMSO.

A 250 $\mu\text{g}/\text{mL}$ stock of puromycin (Sigma-Aldrich, USA) was prepared by diluting 0.125 mL of the 1 mg/mL stock solution in 4.875 mL of water. The solution was sterile filtered using a syringe (Becton Dickinson, USA) with an attached 0.2 μm polyethersulfone membrane syringe filter (VWR International, USA). Serial dilutions were made by using 1.0 mL of the 250 $\mu\text{g}/\text{mL}$ stock diluted in 9.0 mL of sterile filtered water.

3.4 Transient Short Hairpin RNA Transfection

Lyophilized short hairpin RNA (shRNA) constructs (OriGene, USA) against MutS Homolog 2 (MSH2) or excision repair cross complement 1 (ERCC1) were reconstituted in 50 μL of nuclease-free water (Qiagen, USA). Six well tissue culture plates (Becton Dickinson, USA) were seeded with 30×10^3 (MDA-MB-435) cells, 40×10^3 (A-549) cells or 45×10^3 (DU-145) cells and allowed to grow for 24 hr to

obtain a 50-60% confluent cell population. After the incubation period, on the day of transfection, the transfection complex was prepared by adding 3 μ L of TurboFectin 8.0 (OriGene, USA) to an RNase free tube containing 100 μ L of serum free medium (MEM for A-549 and MDA-MB-435 or RPMI-1640 for DU-145 cells). The solution was mixed by gentle pipetting and allowed to incubate at room temperature for 5 min. Following incubation, 3 μ g of the reconstituted construct was added to the TurboFectin-containing medium and the solution was mixed by gentle pipetting. This complete transfection complex was allowed to incubate at room temperature for 25 min. The transfection complex was added dropwise to the cells and the plate was gently rocked to evenly distribute the complex. The cells were incubated for 24 hr then harvested as described above and assayed for the protein of interest using Western Blot analysis to determine the appropriate construct to use for stable transfection.

3.5 Stable Short Hairpin RNA or Expression Plasmid Transfection

Six well tissue culture plates (Becton Dickinson, USA) were seeded with 30×10^3 (MDA-MB-435) cells, 40×10^3 (A-549) cells or 45×10^3 (DU-145) cells and allowed to grow for 24 hr to obtain a 50-60% confluent cell population. For all cell lines; MDA-MB-435, A-549 and DU-145; stable cell lines transfected with the empty expression vector and shRNA construct against green fluorescence protein (GFP) were developed. For the MDA-MB-435 cell line, MSH2 construct 25 and ERCC1 construct 65 were selected for stable transfection. For the A-549 cell line, MSH2

construct 27 and ERCC1 construct 67 were selected for stable transfection. For the DU-145 cell line, MSH2 construct 27 and ERCC1 construct 65 were selected for stable transfection. The complete transfection solution was prepared and addition of the complex to the cells was completed as described above. The cells were again incubated with the transfection complex for 24 hr. After the incubation period, the cells were harvested and passaged into T-12.5 cm² tissue culture flasks (Becton Dickinson, USA) containing complete culture medium and a final puromycin concentration of 0.5 µg/mL. The stable cell lines were developed as shown in Figure 9 below.

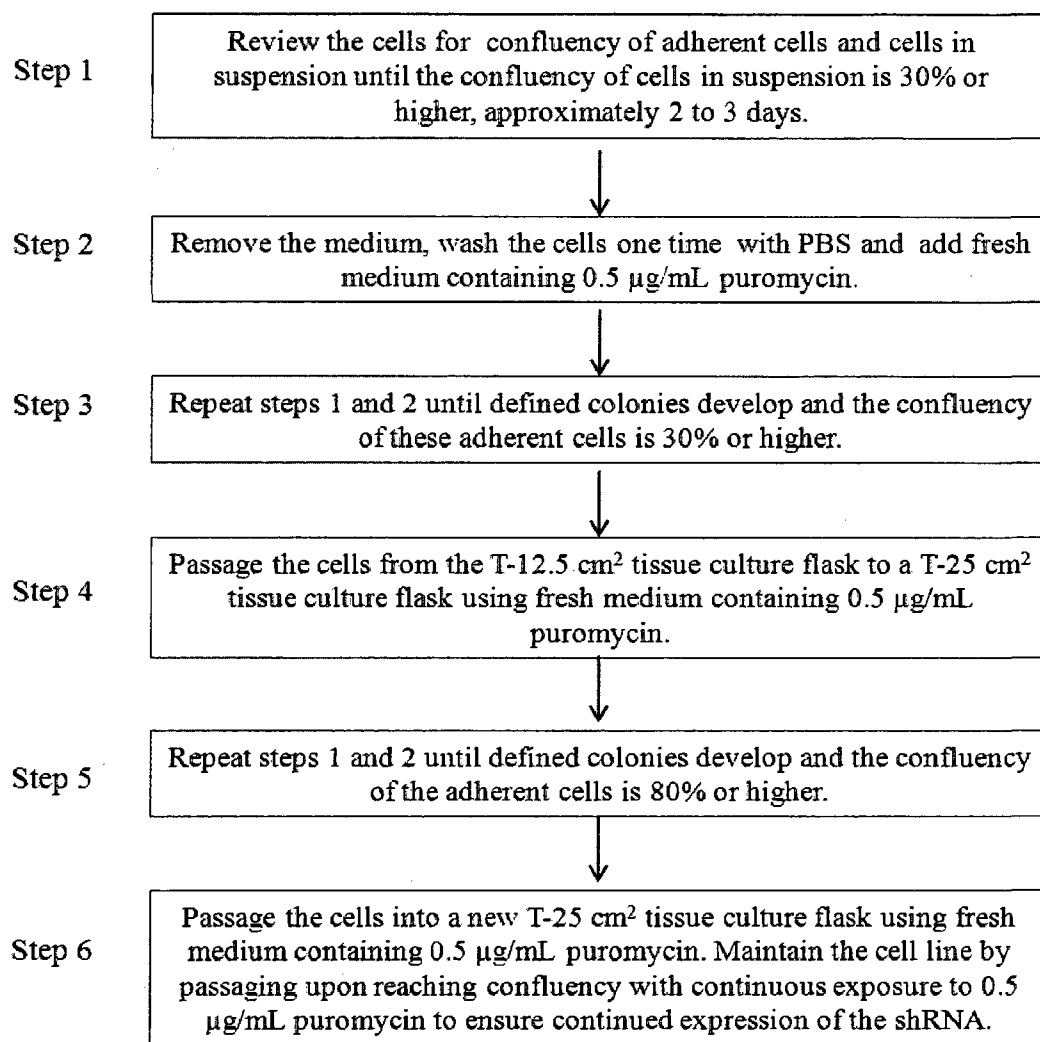


Figure 9: Procedure for the development of stable cell lines expressing shRNA. The incubation environment is maintained at 37 °C, 95% relative humidity and 5% CO₂.

3.6 Colony Formation Assay (Clonogenic Survival)

Parental MDA-MB-435 (100×10^3), transfected MDA-MB-435 (115×10^3), parental A-549 (120×10^3), transfected A-549 (135×10^3), parental DU-145 (130×10^3) or transfected DU-145 (135×10^3) cells were seeded into T-25 cm² tissue culture

flasks and maintained with a total volume of 5 mL of MEM or RPMI 1640 cell culture medium. The transfected cell lines were also supplemented with 100 μ L of 25 μ g/mL puromycin, resulting in a final concentration of 0.5 μ g/mL puromycin. After 24 hr of incubation, the cells were treated with varying concentrations of cisplatin, 4DB or 4TB and incubated for 1 hr whereas control samples were treated with the drug vehicle, DMSO. Cells were harvested, counted, and dilutions were prepared such that 150 cells (parental and transfected MDA-MB-435) or 200 cells (parental and transfected A-549 or DU-145) were sub-cultured in triplicate in 60 mm x 15 mm cell culture dishes (Corning Inc., USA). Dishes were incubated at 37 $^{\circ}$ C, 95% humidity and 5% CO₂ for 10 days, and stained with crystal violet (0.5% weight/volume crystal violet in 95% ethanol, Sigma-Aldrich, USA), and colonies ($n \geq 50$ cells) were counted. Percent survival compared to control cells was measured ($n = 3$).

3.7 RNA Extractions

Cells were passed at the same time each day for a total of three passages and maintained at 50-60% confluency. The cells were treated for 1 hr with the EC₅₀ concentration of cisplatin, 4DB or 4TB. Following treatment, samples designated at 0 hr were washed three times with 5 mL of PBS then harvested immediately as described below. Samples designated as 2 hr, 4 hr or 24 hr were washed three times with 5 mL of PBS and fresh medium was then added. The 2 hr, 4 hr or 24 hr samples were then harvested as described below. Media was removed from the triplicate flasks containing MDA-MB-435, A-549 or DU-145 cells and rinsed three times with 5 mL

of PBS. Cells were then harvested and transferred to a 15 mL conical vial. Total RNA extractions were then performed using the QIAGEN RNeasy MINI Kit (Qiagen, USA) purification system according to the manufacturer's instructions. The resulting solution was separated into aliquots for the purpose of microarray analysis, quantification, and verification of purity. The aliquots were immediately stored at -70 °C until further use.

3.8 RNA Quantification and Purity Verification Using the NanoDrop ND-1000

To ensure the integrity of the RNA, all samples remained on ice and were handled using RNase free materials. A 1:10 dilution of sample to Tris buffer was prepared for the purpose of verifying sample purity. The NanoDrop (ND-1000 spectrophotometer, Thermo Scientific, USA) instrument was set to zero using RNase free water prior to measuring the absorbance of the samples. A total of 2 μ L of sample was loaded onto the sensor to measure the absorbance at 260 and 280 nm. The sensor was thoroughly cleaned using RNase free water between sample readings. Each sample was measured twice and the average value was used in data analysis. Concentration of RNA was calculated by the NanoDrop software. To verify purity, the samples diluted in Tris buffer were measured and only samples with an A260/280 reading within 1.8-2.3 were used for microarray analysis.

3.9 Microarray Analysis

Affymetrix GeneChip Human Genome U133 Plus 2.0 Array (Affymetrix, Santa Clara, CA, USA) were used for the study which is a single array with over 47,000 transcript probe sets representing over 38,500 well-substantiated human genes. Windber followed the Affymetrix GeneChip® Expression Analysis Technical Manual for all GeneChip array procedures. Briefly, 1 µg of total RNA is used for reverse transcription to produce single strand cDNA followed by second strand synthesis to form double strand cDNA. After cDNA purification, biotin-labeled cRNA target is produced by an *in vitro* transcription (IVT) reaction using the cDNA template. After cRNA purification, an aliquot of the labelled cRNA is run on Agilent's Bioanalyzer as a quality control step and another aliquot is quantified using the NanoDrop UV/Vis spectrophotometer (NanoDrop). Only high quality RNA with a yield of more than 10 µg is fragmented and hybridized to Affymetrix GeneChip arrays overnight (18 hr) in a temperature-controlled hyb-oven. After hybridization, GeneChip arrays are loaded onto a Fluidic Station 450 for washing and staining using the standard Affymetrix procedure. After the final wash, the GeneChip arrays are scanned using the Affymetrix GeneChip scanner 3000 G7. Scanned images were analyzed using Affymetrix data analysis software (GDAS) to generate the raw data.

Data was analyzed using the GDAS software in order to generate relevant targets from each array. The CEL files were imported into GeneSpring microarray analysis software (Agilent). All arrays were subjected to GCRMA processing followed by subsequent processing using log transformation and global normalization to generate

normalized data. Probes with a raw signal intensity below 50 were eliminated, resulting in approximately 22,000 probe sets between replicate sample groups for further analysis. In order to identify differentially expressed genes for each compared group, fold changes of two or higher were used. Potential false positives were eliminated by identifying normalized signal values that were inconsistent between replicate sample groups. The t-test was used to further reduce false positive probe sets.

3.10 Western Blot Analysis

Parental MDA-MB-435 (265×10^3) cells, transfected MDA-MB-435 (290×10^3) cells, parental A-549 (300×10^3) cells, transfected A-549 (325×10^3) cells, parental DU-145 (300×10^3) cells or transfected DU-145 (325×10^3) cells were seeded into T-75 cm² tissue culture flasks and maintained with a total volume of 10 mL of MEM or RPMI 1640 cell culture medium. The transfected cell lines were also supplemented with 200 μ L of 25 μ g/mL puromycin, resulting in a final concentration of 0.5 μ g/mL puromycin. After 3 d of incubation, the adherent cells were washed three times with 10 mL of PBS, discarding each wash. Following the washing procedure, 2 mL of trypsin-EDTA was added to the flask and cells were harvested as described previously. The cells were centrifuged at 4° C for 5 min at 2,000x g and the resulting supernatant was discarded. To the remaining cell pellet, 500 μ L of M-PER cell lysis buffer (Pierce, Rockford, IL, USA) was added in addition to 20 μ L/mL protease and 10 μ L/mL EDTA (Pierce). The tube was then gently vortexed for 5 min. The cells

were then centrifuged at 14,000 x g for 15 min at 4 °C to pellet cellular debris. The resulting supernatant, containing all cellular proteins, was collected and stored at -20 °C until further analysis.

Protein concentrations were determined using the bicinchoninic acid (BCA) protein assay (Pierce, Rockford, IL) according to the manufacturer's instructions. Different masses of bovine serum albumin (BSA; Sigma-Aldrich, USA) protein standards (0, 25, 50, 100, 150, 200 µg) were used to generate a standard curve. Lysates were diluted by 35% by adding adding 25% sample loading buffer (PAGEgel, San Diego, CA) and 10% DDT reducer (PAGEgel). The samples were placed in boiling water for 3 min, and then samples with a volume of 35µL or less were loaded into the wells of a pre-casted 12% SDS-PAGE Western blot gel in duplicate (PAGEgel). A prestained protein ladder, SeeBlue plus (Invitrogen, USA) was used to ensure transfer of protein to membranes and served as a molecular weight marker. Electrophoresis was conducted in 1x PAGEgel SDS running buffer (PAGEgel) according to manufacturer's instructions. Briefly, electrophoresis was initiated at 80 mA/gel and the current was decreased by 10 mA/gel every 15 min until a current of 50 mA/gel is reached. The current is then reduced to 35 mA/gel and allowed to run for 20 min, or until the dye front reaches the base of the gel, resulting in a total run time of 75 to 90 min. Following electrophoresis, the protein is transferred from the gel to a 0.2 µm nitrocellulose membrane (PAGEgel) using a constant voltage of 20 V for 80 min while in Western transfer buffer (Tris-Glycine-SDS Run/Blot Stock Buffer, PAGEgel) and 20% v/v methanol (Sigma-Aldrich). Following the transfer, the

membranes are placed in blocking solution with TBST [Western wash, femto TBST 10X (G-Biosciences, St. Louis, MO)], 0.1% Tween-20 (Sigma-Aldrich, USA) and 5% nonfat milk (Nestle Carnation) for 1 hr, then rinsed three times using TBST until the solution was clear. The membrane was incubated in primary monoclonal IgG mouse anti-human antibody overnight at 4 °C. The primary antibodies were diluted to a concentration of 1:200 (MSH2), 1:100 (ERCC1), or 1:1000 (control, β -Actin) (Santa Cruz Biotechnology Inc., Santa Cruz, CA). All antibodies were diluted in TBST containing 5% BSA. After incubation, the primary antibody was removed and the membrane was subjected to a TBST wash while being rocked for 5 min at room temperature. The washing step is repeated a total of three times to ensure complete removal of unbound primary antibody. The membranes are then incubated in secondary monoclonal IgG goat anti-mouse antibody conjugated to a horseradish peroxidase (HRP) (1:2000) for 90 min at room temperature (Santa Cruz Biotechnology Inc.). After the incubation, the secondary antibody was removed and the membrane was washed three times with TBST as described above. Proteins were visualized on the Typhoon multipurpose imager using Enhanced chemiluminescence ECL-plus® detection reagent (Amersham, Piscataway, NJ).

3.11 Cell Cycle Analysis

Parental MDA-MB-435 (175×10^3) cells were seeded in a T-75 cm² tissue culture flask and allowed to grow for three days. To determine cell cycle phase distribution in parental MDA-MB-435 cells following treatment with 4DB, cells were treated for 1

hr with the EC₅₀ concentration of the drug whereas the control was treated with the drug vehicle, DMSO. Following drug exposure, the media was removed and the cells were rinsed three times with PBS. Fresh medium was then added and the cells were then incubated for 0, 2, 4 or 24 hr. Following the incubation period, cells were harvested and a cell pellet was obtained by centrifuging the cell solution at 4 ° C for 5 min at 2,000x g. Cells were washed with 5 mL PBS, centrifuged and resuspended in 100 µL of PBS. To fix the cells, 1 mL of cold 95% ethanol was added slowly while vortexing the sample gently. Samples were then stored at 4 ° C for at least 24h prior to being stained. To analyze the cells, propidium iodide staining was conducted. Fixed cells were washed with 2.0 mL of PBS and incubated with 0.1 mL Triton X 1% buffer and 0.1 mL RNase at 1 mg/mL for 10 min at room temperature. Propidium iodide stain (0.2 mL) at a concentration of 100 µg/mL was added and cells were incubated for 30 min in the absence of light at room temperature. Samples were analyzed on the Becton Dickinson FACSCalibur (Becton Dickinson, USA) and results were evaluated using ModFit LT Version 3.0 (Verity Software House, Topsham, ME).

3.12 Intracellular Antigen Staining

Parental MDA-MB-435 (265 x 10³) cells, transfected MDA-MB-435 (290 x 10³) cells, parental A-549 (300 x 10³) cells, transfected A-549 (325 x 10³) cells, parental DU-145 (300 x 10³) cells or transfected DU-145 (325 x 10³) cells were seeded into T-75 cm² tissue culture flasks and maintained with a total volume of 10 mL of MEM or RPMI 1640 cell culture medium. The transfected cell lines were also supplemented with 200 µL of 25

$\mu\text{g/mL}$ puromycin, resulting in a final concentration of $0.5 \mu\text{g}/\mu\text{L}$ puromycin. After 3 d of incubation, the adherent cells were washed three times with 10 mL of PBS, discarding each wash. Following the wash procedure, cells were harvested by exposure to 5mL of 0.2% EDTA in PBS for 10 min. Then, 5 mL of appropriate medium was added to neutralize the EDTA. A cell count was performed on the cell solution after which, the cell solution was separated in 1×10^6 cell aliquots.

The cell solution was centrifuged at 1000 rpm for 5 min at 4°C and the resulting supernatant was discarded. The cell pellet was then resuspended in 1 mL of fixation buffer (Santa Cruz Biotechnology Inc.) and incubated for 30 min at room temperature while gently being rotated. The cells were then centrifuged at 3000 rpm for 5 min at room temperature and the resulting supernatant was discarded. The pellet was then resuspended in 50mL of PBS and the resulting suspension was centrifuged at room temperature for 5 min at 2000 rpm. The supernatant was discarded and then 1 mL of cold permeabilization buffer (Santa Cruz Biotechnology, Inc.) was added dropwise while vortexing to the cell pellet. The sample was then incubated for 5 min at room temperature while being gently rotated followed immediately by centrifugation at room temperature for 5 min at 2500 rpm. The resulting supernatant was then discarded and the cell pellet was gently resuspended in 50 mL of PBS. The sample was then centrifuged at room temperature for 5 min at 2500 rpm and the resulting supernatant was discarded. The cell pellet was resuspended in 100 μL of wash buffer (Santa Cruz Biotechnology Inc.).

To all samples, 1 μg of primary antibody (MSH2 or ERCC1; Santa Cruz Biotechnology, Inc.) was added. To account for nonspecific binding, two samples of the

parental cell line were used as controls by treatment with the isoform antibody for ERCC1, normal mouse IgG_{2b}, or MSH2, normal mouse IgG₁. A third control, one that only contains secondary antibody to account for background signal, was also used. For this third control, the steps involving primary antibody staining (below) were omitted. The solutions were then vortexed briefly, covered and incubated on ice for 30 min. Then, 1.5 mL of Wash Buffer was added to the sample, followed by centrifugation at room temperature for 5 min at 4000 rpm and the resulting supernatant was discarded. The cell pellet is resuspended in 100 µL of wash buffer and 1 µg of secondary antibody conjugated to phycoerythrin (goat anti-mouse IgG; Santa Cruz Biotechnology, Inc.). The samples were then vortexed briefly, covered and incubated on ice for 30 min. Then, 1.5 mL of wash buffer was added to the sample followed by centrifugation at 4000 rpm for 5 min. The resulting supernatant was then discarded. The cell pellet was then resuspended in 500 µL of 1% paraformaldehyde in wash buffer and stored for a maximum of 24 hr in the absence of light prior to acquiring data.

Samples were analyzed on the Becton Dickinson FACSCalibur (Becton Dickinson) and results were evaluated using ModFit LT Version 3.0 (Verity Software House).

3.13 Fluorescent Microscopy

Parental MDA-MB-435 (40×10^3) cells were seeded on each slide of a 4-well chamber slide and allowed to grow for 24 hr in order to achieve a cell density of 65 to 70% confluency. The medium was then removed and the wells were washed with PBS.

Medium containing the EC₅₀ concentration of 4DB was then added to each well and drug exposure continued for 1 hr. Following treatment, the medium was removed and the cells were rinsed three times with PBS. Fresh medium was then added and the cells were incubated for 0, 2, 4 or 24 hr. At the indicated time point, the medium was removed and wells were washed with PBS and stained with 0.5 mL of Hoechst stain (2 µg/mL) and 0.5 mL of propidium iodide (10 µg/mL) diluted in PBS. The cells were incubated for 15 min and the images were acquired.

A bright field was obtained by visualizing cells with a phase lamp. Apoptotic cells were identified using a mercury lamp with an excitation wavelength of 300 -500 nm and an ultraviolet filter with an emission wavelength of 435-485 nm. Cells that have taken up the Hoechst stain were identified as apoptotic. Necrotic cells were identified using the mercury lamp and a green filter with an emission wavelength of 600-660 nm. Cells were positively identified as apoptotic by appearing red due to the presence of the propidium iodide stain being taken up by the cell. The images were obtained using a Photometrics Cool Snap CCD camera attached to a Nikon Eclipse TE2000-U microscope (Nikon Inc. Melville, NY) and analyzed using MetaVue software (Meta Series 6.0/6.1, Universal Imaging Corporation).

To determine the percentage of apoptosis or necrosis, the following equation was employed:

$$\left(\frac{\text{Number of positive apoptotic/necrotic cells}}{\text{Total number of cells in the bright field}} \right) \times 100\%$$

The three areas of the wells imaged were randomly selected and were scanned in each of the control and treated wells (n=3).

3.14 DNA Extractions

Following drug treatment, at the indicated time point, cells were washed three times using PBS. Cells were then harvested and transferred to a 15 mL conical vial. Total DNA extractions were then performed using the GenElute Mammalian DNA Miniprep Kit (Sigma-Aldrich, USA) according to the manufacturer's instructions. The resulting solution was separated into aliquots for the purpose of quantification, verification of purity and Inductively Coupled Plasma-Mass Spectroscopy analysis for total platinum concentration. Samples were stored in the -70 °C freezer until analysis.

3.15 DNA Quantification and Purity Verification using the NanoDrop ND1000

To ensure the integrity of the DNA, all samples remained on ice and were handled using nuclease-free materials. The ND-1000 spectrophotometer was set to zero using elution buffer (Sigma-Aldrich, USA) prior to measuring the absorbance of the samples. A total of 2 µL of sample was loaded onto the sensor to measure the absorbance at both 260 nm and 280 nm. The sensor was thoroughly cleaned using nuclease-free water between sample readings. Each sample was measured twice and the value was in data analysis. To verify purity, the A260/280 ratio was calculated by the NanoDrop software and only samples with an A260/280 ratio within 1.9-2.4 were used for further analysis.

3.16 Determining Platinum Concentration by Inductively Coupled Plasma – Mass Spectrometry (ICP-MS)

Parental MDA-MB-435 (430×10^3) cells, A-549 (500×10^3) cells and DU-145 (550×10^3) cells were seeded in T-150 cm² tissue culture flasks, maintained in 20 mL of either MEM or RPMI 1640 medium and allowed to grow for 3 days to obtain as 65 – 70% confluent cell population. After the incubation period, the cells were treated with the EC₅₀ concentration of cisplatin, 4DB or 4TB for two hours. A control sample for each treatment group was treated with the drug vehicle, DMSO. The drug or DMSO is washed from each flask by rinsing three times with 20 mL of PBS. For the 4 and 24 hr time points, fresh medium was added to the flask and the cells were incubated for the stated time period. For the 0 hr time point, flasks were harvested immediately following the 2 hr drug treatment. At the indicated time points, cells were harvested, counted and separated into two aliquots, one aliquot contained 1.0×10^6 cells and was designated as the whole cell sample, the second aliquot contained the remaining volume of cell solution and was designated as the genomic sample. For clarification, cell samples designated as the 0 hr sample were exposed to drug for 2 hr, washed, then immediately harvested. Samples designated as 4 hr or 24 hr were exposed to drug for 2 hr, washed, then incubated in fresh medium for 4 hr or 24 hr, respectively.

The cell solutions were centrifuged at 4° C for 5 min at 2000x g, and the resulting supernatant was discarded. The remaining cell pellet was washed three times using the following process: resuspend the cell pellet in 500 µL of cold PBS and centrifuge at 4° C for 5 min at 2000x g, and discard the resulting supernatant. After the final wash, 75 µL of

PBS was added for a total volume of 100 μL . The samples were then stored at $-70\text{ }^{\circ}\text{C}$ until further analysis.

The samples designated as whole cell were lysed using 200 μL of M-PER (Pierce) containing 20 $\mu\text{L}/\text{mL}$ Protease Inhibitor (Pierce) and 10 $\mu\text{L}/\text{mL}$ EDTA (Pierce). The sample was gently vortexed at room temperature for 5 min then centrifuged at $14,000 \times g$ for 15 min at $4\text{ }^{\circ}\text{C}$ to pellet the cell debris. A total of 30 μL of supernatant was removed for protein quantification using the bicinchoninic acid protein assay (Pierce) and the remaining sample was returned to the $-70\text{ }^{\circ}\text{C}$ freezer until digestion and subsequent ICP-MS analysis. The sample designated as the genomic extract was subjected to the DNA extraction procedure described previously. The resulting solution was separated into two aliquots, one for quantification and one for ICP-MS analysis. Quantification of the sample is conducted immediately using the ND-1000 as described previously. The sample designated for ICP-MS analysis was returned to the $-70\text{ }^{\circ}\text{C}$ freezer until digestion and subsequent ICP-MS analysis.

Prior to digestion, the volume of each sample was recorded. Samples were then digested by adding a total of 143 μL of 70% trace grade nitric acid (Fluka, USA) to the sample. The open vessels were placed in a $70\text{ }^{\circ}\text{C}$ heat block and were heated for 90 min. While continuing to heat, 20 μL of 30% hydrogen peroxide (Sigma-Aldrich, USA) was added to each sample. Heating was continued for an additional 3.5 hr for a total digestion period of 5 hr. Samples were then filtered using a syringe (Becton Dickinson) with an attached 0.45 μm polyethersulfone membrane syringe filter (VWR, USA). The total volume of the sample was brought to 10 mL and the final sample mass was determined

and recorded. Terbium was added to each sample such that the final concentration was 1 ppb to serve as the internal standard during analysis.

External platinum standards at concentrations of 20, 10, 5, 1 and 0.05 ppb were prepared gravimetrically by diluting the stock 1000 ppm platinum standard (Environmental Express, Mt. Pleasant, SC, USA) in 1% trace grade nitric acid (Fluka). Platinum standards for the purpose of continuous calibration verification were prepared gravimetrically by diluting the stock 1000 ppm platinum standard (High Purity Standards, Charleston, SC, USA) in 1% trace grade nitric acid (Fluka) to 10 and 5 ppb. The blank used during analysis was 1% trace grade nitric acid (Fluka). The digested samples were nebulized into the ICP-MS instrument without further dilution.

The following calculations were employed using the data generated from the aforementioned experiments:

$$\% \text{ Whole Cell Uptake} = \frac{\text{Concentration of Pt (ppb), 0 hr Whole Cell Sample}}{\text{Concentration of Pt (ppb) in the EC}_{50} \text{ Concentration}} \times 100\%$$

$$\% \text{ Drug Bound to DNA} = \frac{\text{Concentration of Pt (ppb), 0 hr Genomic Sample}}{\text{Concentration of Pt (ppb) in the EC}_{50} \text{ Concentration}} \times 100\%$$

$$\text{pg Pt} / \mu\text{g Protein} = \frac{\text{Mass of Pt (pg) in Respective Whole Cell Sample}}{\text{Mass of Protein (\mu g) in Respective Whole Cell Sample}}$$

$$\text{pg Pt} / \mu\text{g DNA} = \frac{\text{Mass of Pt (pg) in Respective Genomic Sample}}{\text{Mass of DNA (\mu g) in Respective Genomic Sample}}$$

$$\% \text{ Intracellular Pt Remaining} = \frac{\text{pg Pt} / \mu\text{g Protein in Respective Whole Cell Sample}}{\text{pg Pt} / \mu\text{g Protein in 0 hr Whole Cell Sample}} \times 100\%$$

$$\% \text{ Pt-DNA Adducts Remaining} = \frac{\text{pg Pt} / \mu\text{g DNA in Respective Genomic Sample}}{\text{pg Pt} / \mu\text{g DNA in 0 hr Genomic Sample}} \times 100\%$$

3.17 Statistical Analysis

Results were expressed as mean \pm standard deviation (SD), with groups consisting of three observations and each experiment was performed two or three times. Graph Pad Quick Calcs (www.graphpad.com) was used for Student's t test. P values less than 0.05 were considered significant. All graphical error bars are representative of standard deviation measurements.

CHAPTER 4

FINDINGS OF THE STUDY

4.1 Analysis of Results

The focus of the study is to determine the cause of varying responses to cisplatin and novel cisplatin analogues between different tissue types. Previous studies (Vo, 2009) discovered that the EC₅₀ for the 4TB analogue varied by a factor of 40 between breast (MDA-MB-435), prostate (DU-145) and lung (A-549) cancer cell lines. The EC₅₀ values determined by clonogenic survival are summarized in Table 1. Given that these values were the focus of this study, the first step in the research process was to ensure that the EC₅₀ values could be duplicated by a different researcher.

Agent (μM)	A549	DU-145	MDA-MB-435
Cisplatin	850	490.00 ± 169.71	311.96 ± 57.31
4DB	8.50 ± 0.56 *	2.53 ± 0.29 *	2.50 ± 0.33 *
4TB	>100	73.72 ± 36.21 *	2.41 ± 1.03 *

Table 1: EC₅₀ values determined by Vo using the clonogenic survival assay method.
*Statistically significant in comparison to cisplatin.

Clonogenic survivals using cisplatin, 4DB and 4TB with MDA-MB-435, A-549 or DU-145 cells are shown in Figures 10A, 10B and 10C, respectively. The cells were exposed to varying concentrations of each drug for 1 h. The calculated EC_{50} values from the experiments conducted for the current study are given in Table 2. The values obtained in the current study are equivalent to those obtained by Vo, and the trends of the data with respect to the lethality induced by each drug is consistent with the previous findings. The results from these initial clonogenic survival experiments supported further work in determining the factors responsible for the observed cytotoxicity induced by each drug in these different cell lines.

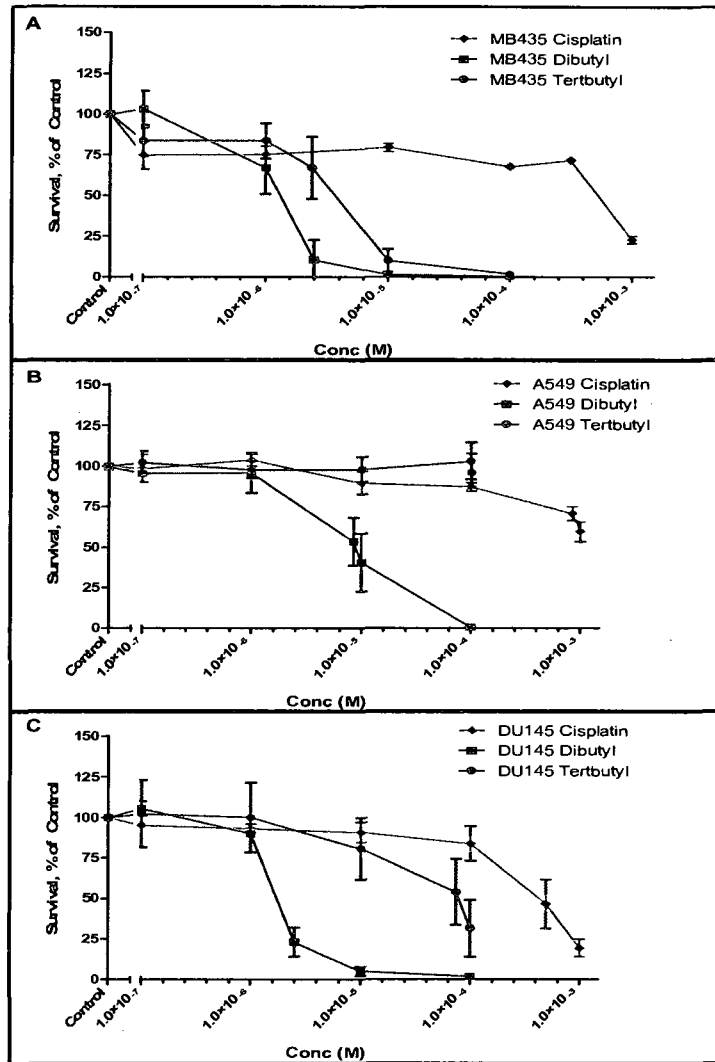


Figure 10: Clonogenic survival using cisplatin, 4DB or 4TB in MDA-MB-435 (A), A-549 (B) or DU-145 (C) cells. Cell survival was measured and compared to control cells after a 1 hr exposure to varying concentrations of the indicated drug. The above figures represent three trials each. Colonies were stained with crystal violet and viability was measured by counting colonies and comparing to the number of colonies in the control sample. A colony is a group of cells with $n \geq 50$.

Agent (μM)	A549	DU-145	MDA-MB-435
Cisplatin	900 \pm 4.28	490.00 \pm 15.20	523 \pm 13.79
4DB	9.41 \pm 2.79 *	1.85 \pm 0.089*	1.33 \pm 0.34 *
4TB	>100	79.10 \pm 18.41*	3.65 \pm 0.82*

Table 2: EC₅₀ values determined in the current study using the clonogenic survival assay method. *Statistically significant in comparison to cisplatin.

In addition to confirming the previous clonogenic survival data, the established EC₅₀ values were confirmed as an efficacious dose to test the rate of platinum-DNA adduct repair. Inductively coupled plasma-mass spectrometry (ICP-MS) analysis was employed to determine the concentration of drug taken up by the cells as well as rate of lesion repair. Initial protocol optimization required identifying the maximum number of cells that could be used to determine the rate of platinum-DNA (Pt-DNA) adduct repair for each cell line. Concentration of DNA is determined spectrophotometrically and is therefore subject to the Beer-Lambert Law. A standard curve of DNA mass verses cell number was constructed for each wild type cell line to ensure the concentration of DNA used in the ICP-MS studies could be accurately quantified. Wild type cells were seeded in T-150 cm² tissue culture flasks and were allowed to grow uninterrupted for three days, at which time the population density reached 70 to 75% confluency. The cells were then harvested, counted, divided into aliquots of increasing cell number and then subjected to DNA extraction. The DNA binding columns used in the extraction process can accommodate up to 5 x 10⁶ cells; therefore, cell numbers ranging from zero to 4.5 x 10⁶

cells were used. The concentration of DNA in each sample was quantified using the NanoDrop ND-100 as described previously. These studies revealed that for all cell lines, the mass of DNA up to 4.5×10^6 cells falls within the linear range of the standard curve and can be accurately quantified (Figure 11). Therefore, 4.5×10^6 cells was the maximum number of cells used in any genomic sample in the ICP-MS studies.

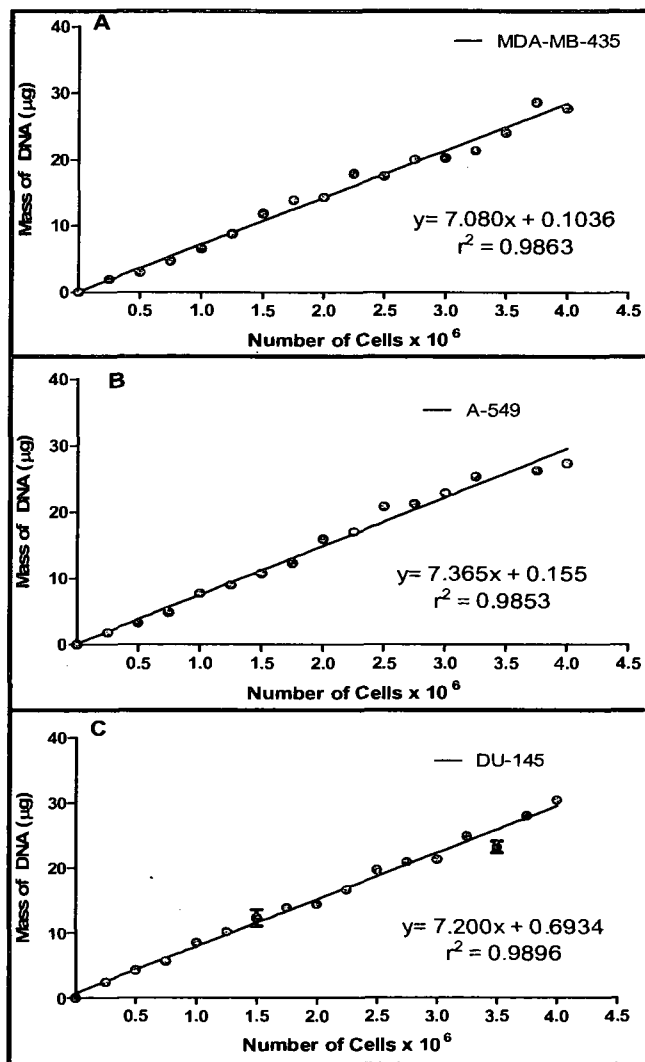


Figure 11: Standard curves of DNA mass versus cell number for MDA-MB-435 (A), A-549 (B) and DU-145 (C) cells. The ordinate represents the mass of DNA in micrograms and the abscissa represents the total number of cells in the sample. Values are representative of three independent experiments. Error bars, when not visible, are smaller than the symbols representing the measurement.

Another component of ICP-MS protocol optimization required determination of the total concentration of platinum that could potentially be present in the sample, but had not been taken up by the cells. In order to account for any residual platinum, “wash

controls” were analyzed for each cell line with each drug. The preparation of these samples involved exposing an equivalent cell population as a treatment sample to the same drug concentration for only 1 min, followed by the washing procedure described previously that was established for the treatment samples. The cells were then harvested, digested and analyzed for total platinum content by ICP-MS analysis. Total concentration of platinum remaining in comparison to total platinum concentration introduced yielded the percentage of platinum bound extracellularly which can then be subtracted from the total amount of platinum in the treatment samples. The results of the study, outlined in Table 3, revealed that the maximum concentration of platinum in the wash controls was 0.0161 ppb which was present in the A-549 sample treated with the EC₅₀ concentration of 4TB. The values obtained from the study reveal that the amount of extracellular platinum present in the sample was effectively removed using the developed washing procedure after drug treatment. For comparison, the concentration of platinum in each drug concentration is provided in Table 4.

Platinum (ppb)	MDA-MB-435	A-549	DU-145
Cisplatin	0.0088	0.0100	0.0116
4DB	0.0081	0.0140	0.0152
4TB	0.0137	0.0161	0.0160

Table 3: Concentration of platinum (ppb) in the wash control samples.

Platinum (ppb x 10 ³)	MDA-MB-435	A-549	DU-145
Cisplatin	60.84	165.75	95.55
4DB	0.49	1.66	0.49
4TB	0.47	19.50	14.37

Table 4: Concentrations of platinum (ppb x 10³) present in the EC₅₀ drug concentrations for each cell line.

After confirming that the protocol for washing the cells following drug treatment was sufficient, protocol optimization for treatment samples was conducted. The A-549 cell line and the 4DB drug were chosen as the model system. The identified variables in these experiments were the minimum number of cells to use for genomic samples, length of drug exposure, presence of an oxidizing agent during digestion, length of digestion and digestion temperature. A summary of the optimization process is provided in Table 5. As shown in Figure 12, obtaining repeatable results above the limit of detection (LOD) for the instrument required five different trials. Each trial had three treatment samples at each time point. The protocol provided in the Experimental Procedures section outlines the final, optimized protocol for ICP-MS analysis.

Trial	Drug Exposure	Cell Number in the Genomic Extract (GE)	Digestion	Results
1	1 hr	650,000	1 hr at 70 °C, no oxidizing agent	Platinum levels were above the LOD for the genomic samples; however, the standard deviation between trials was unacceptable.
2	1 hr	2.0×10^6	1 hr at 70 °C, no oxidizing agent	Platinum levels were above the LOD for the genomic samples; however, the standard deviation between trials was unacceptable.
3	1 hr	2.5×10^6	2 hr at 95 °C, no oxidizing agent	Platinum levels were above the LOD for the genomic samples; however, the standard deviation between trials was unacceptable.
4	3 hr	725,000	5 hr at 70 °C, no oxidizing agent	Platinum levels were below the LOD for the genomic samples; increased drug exposure decreased the number of cells in each sample.
5	2hr	2.5×10^6	5 hr at 70 °C, 15% H ₂ O ₂	Platinum levels were above the LOD for the genomic samples; acceptable standard deviation between trials.

Table 5: Summary of the protocol used and the results obtained from the optimization experiments for ICP-MS analysis using the A-549 cell with the 4DB drug as the model system.

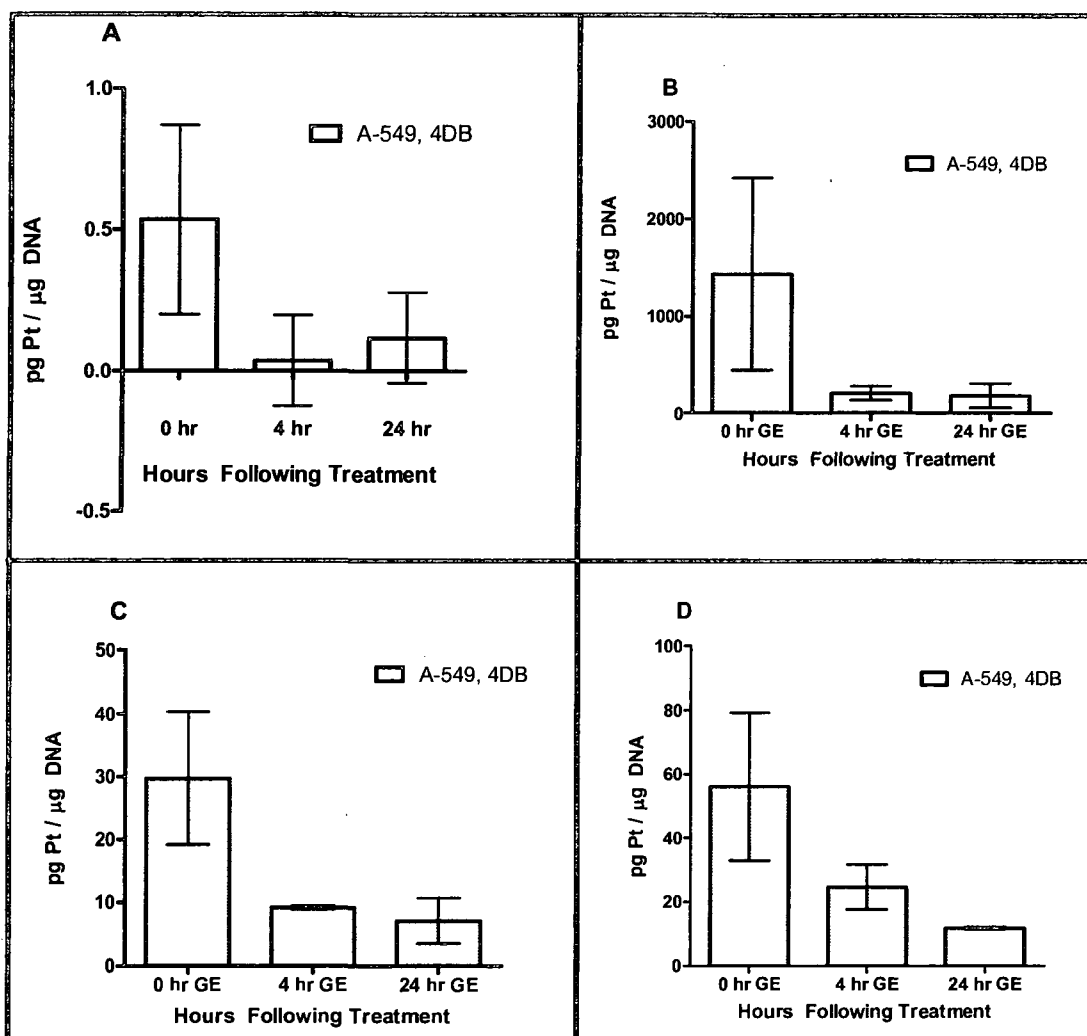


Figure12: Results of ICP-MS optimization trials 1 (A), 2 (B), 3 (C) and 5 (D) using A-549 and the respective EC_{50} concentration of 4DB. No data is shown for trial 4 per levels of platinum were below the limits of detection for the instrument. Values are representative of three independent experiments for each time point within each trial, and error bars are representative of standard deviation.

After optimizing the protocol for ICP-MS analysis, experiments were conducted with the MDA-MB-435, A-549 and DU-145 cell lines using the established EC_{50}

concentrations of cisplatin, 4DB and 4TB. Each cell line was exposed to the indicated drug for 2 hr, followed by washing then harvesting at the indicated time point.

Samples were analyzed for whole cell uptake of each drug by determining the concentration of platinum present in whole cells compared to the concentration of platinum in the EC₅₀ concentration immediately following drug exposure. Results are reported as a percentage of platinum taken up by the cell. The clearance rate of each drug was determined by analyzing the whole cell samples at 4 hr and 24 hr post drug exposure. The amount of drug that gained access to the DNA was determined by measuring the percentage of platinum present in the extracted DNA at the 0 hr time point compared to the concentration of platinum in the EC₅₀ concentration (Table 4).

Analysis of whole cell uptake for each cell line revealed that the drugs that were the most lethal were uniformly taken up by the cells at higher concentrations than the less efficacious drugs. As shown in Figure 13A, MDA-MB-435 cells had taken up 0.16% of cisplatin, 8.11% of 4TB and 23.25% of 4DB; A-549 cells had taken up 0.27% of cisplatin, 0.08% of 4TB and 4.24% of 4DB; DU-145 cells had taken up 0.15% of cisplatin, 2.70% of 4TB and 29.65% 4DB.

Analysis of genomic extracts for platinum revealed that there was an increase in the amount of Pt-DNA adducts formed immediately following drug treatment in the drugs that induced the highest level of cytotoxicity compared to the drugs that were less cytotoxic. As shown in Figure 13B, the percentage of the 4DB drug within the cell that formed Pt-DNA adducts was significantly increased in comparison to drugs that were less lethal. In the MDA-MB-435 cell line the percentage of drug that had formed Pt-DNA

adducts was 0.0093% with cisplatin, 0.21% with 4TB and 0.41% with 4DB. In the A-549 cell line, the percentage of drug that had formed Pt-DNA adducts was 0.17% with cisplatin, 0.0074% with 4TB and 0.98% with 4DB. In the DU-145 cell line, the percentage of drug that had formed Pt-DNA adducts was 0.0065% with cisplatin, 0.018% with 4TB and 0.27% with 4DB.

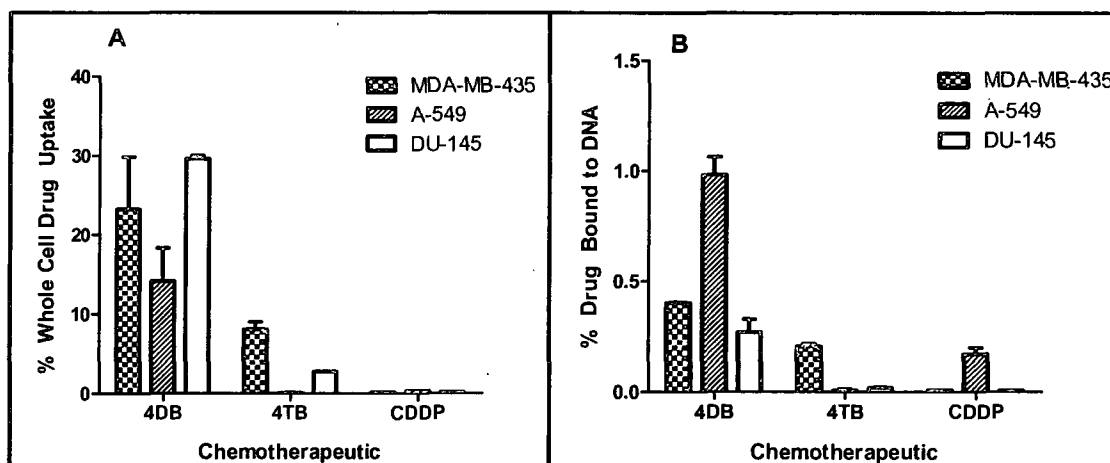


Figure 13: ICP-MS analysis of the percentage of drug uptake in whole cells and genomic extracts in wild type MDA-MB-435, A-549 and DU-145 cells. Panel A represents the percentage of the platinum remaining in whole cells immediately following drug treatment. Panel B represents the percentage of the platinum remaining in the genomic extracts immediately following drug treatment.

To confirm both the ability of the cell to export the drug and repair the formation of Pt-DNA adducts, the mass of platinum per mass of protein or DNA over time was determined. As shown in Figure 14, the mass of platinum per mass of protein for all cell lines with all drugs correlates to the given mass of platinum in each EC₅₀ concentration. Control samples represent exposure to the drug vehicle, DMSO, for 2 hr. The data also

shows that over time, all cell lines have the capacity to export the drug from the cell. With respect to the MDA-MB-435 cell line and the 4DB drug, the initial uptake of drug was 4332 pg Pt/ μ g protein which decreased over time to 3311 pg Pt/ μ g protein at 4 hr and 883 pg Pt/ μ g of protein at 24 hr post drug treatment. For the same cell line with the 4TB drug, uptake was determined to be 1472, 1032, and 566 pg Pt/ μ g protein at 0, 4 and 24 hr, respectively. Treatment with cisplatin yielded uptake values of 5118, 4064 and 1510 pg Pt/ μ g protein at 0, 4 and 24 hr, respectively. Given that the EC₅₀ concentration was the highest for cisplatin, then 4DB, then 4TB, the values of platinum per mass of protein correlate to the amount of platinum exposure. The data reveals that there were greater amounts of platinum in the cisplatin samples than the 4DB or 4TB samples.

In the A-549 cell line, treatment with 4DB yielded uptake values of 4322, 3311 and 883 pg Pt/ μ g protein at 0, 4 and 24 hr, respectively. Treatment in the A-549 cell line with 4TB yielded uptake values of 1472, 1032 and 556 pg Pt/ μ g protein at 0, 4 and 24 hr, respectively. Treatment with cisplatin yielded uptake values of 5118, 4064 and 1510 pg Pt/ μ g protein at 0, 4 and 24 hr, respectively.

In the DU-145 cell line, treatment with 4DB yielded uptake values of 7001, 6201 and 1348 pg Pt/ μ g protein at 0, 4 and 24 hr, respectively. Treatments with 4TB yielded uptake values of 16470, 14214 and 3904 pg Pt/ μ g protein at 0, 4 and 24 hr, respectively. Treatments with cisplatin in the DU-145 cell line yielded uptake values of 16255, 11219 and 4049 pg Pt/ μ g protein at 0, 4 and 24 hr, respectively.

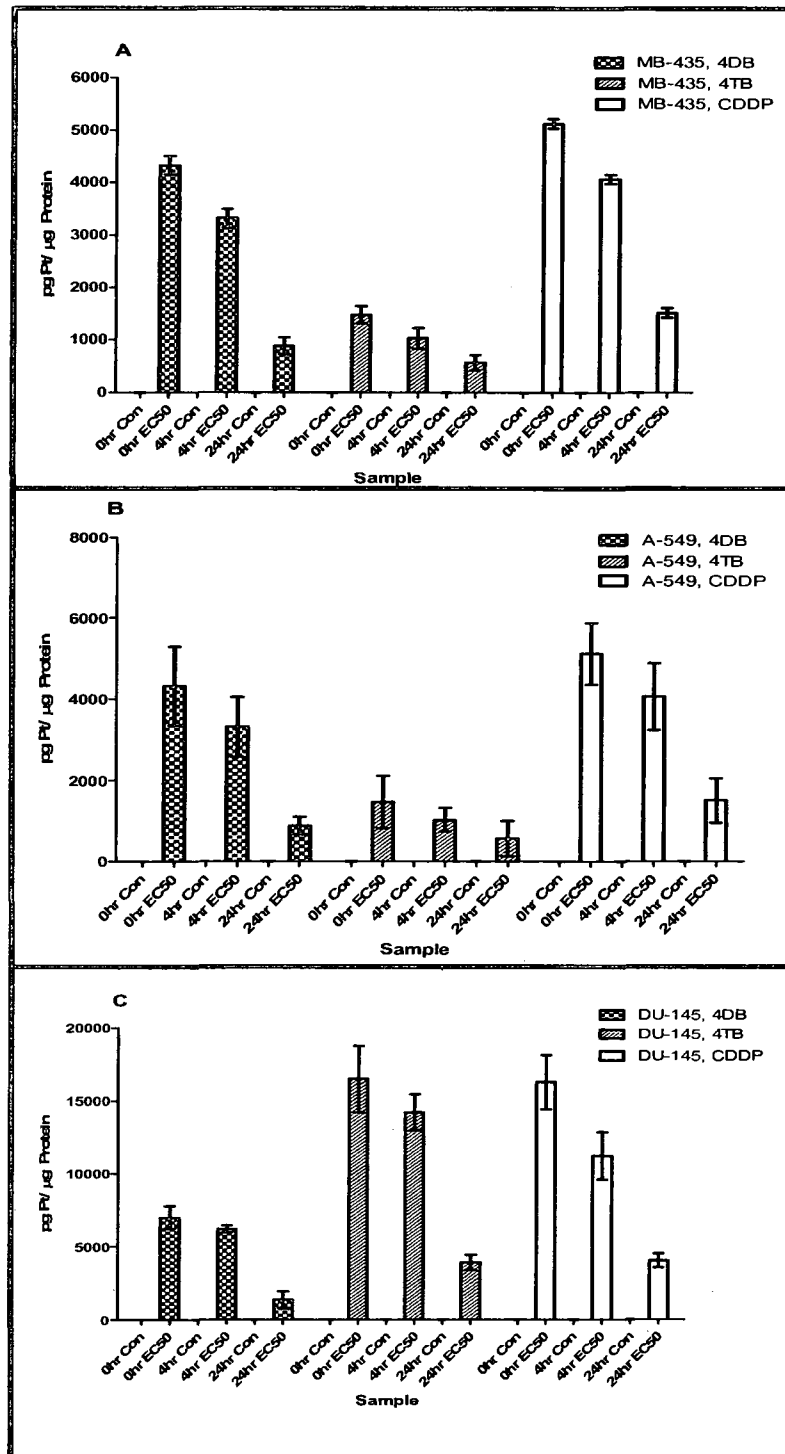


Figure 14: Mass of platinum per mass of protein in MDA-MB-435 (A), A-549 (B) or DU-145 (C) cells over time following exposure to the EC₅₀ concentration of the indicated drug. Values are representative of three independent experiments.

The trends observed in clearance of platinum from the whole cell were also observed in the removal of Pt-DNA adducts in each cell line with each drug. Control samples represent exposure to the drug vehicle, DMSO, for 2 hr. Rate of Pt-DNA adduct repair was determined by analyzing DNA extracts for concentration of platinum at 4 hr and 24 hr post drug exposure. As shown in Figure 15, the amount of Pt-DNA adducts is reduced over time and the amount of Pt-DNA adducts correlates to the original mass of platinum in the EC₅₀ concentration for each drug in all cell lines. For example, with the MDA-MB-435 cell line, the EC₅₀ concentration for cisplatin is 311 μ M versus 2.41 μ M with the 4TB drug. There were a greater number of Pt-DNA adducts formed in the cisplatin sample versus the 4DB samples. However, this trend was not unexpected given the drug concentrations used in the study. Specifically, in the MDA-MB-435 cell line, treatment with 4DB resulted in the formation of adducts in the amount of 795, 538 and 105 pg Pt/ μ g DNA at 0, 4 and 24 hr, respectively. Treatment with 4TB resulted in the formation of adducts in the amount of 447, 239 and 206 pg Pt/ μ g DNA at 0, 4 and 24 hr, respectively. Treatment with cisplatin resulted in the formation of adducts in the amount of 2611, 1485 and 1069 pg Pt/ μ g DNA at 0, 4 and 24 hr, respectively.

In the A-549 cell line, treatment with 4DB resulted in the formation of adducts in the amount of 795, 538 and 379 pg Pt/ μ g DNA at 0, 4 and 24 hr, respectively. Treatment in the A-549 cell line with 4TB resulted in the formation of adducts in the amount of 447, 239 and 206 pg Pt/ μ g DNA at 0, 4 and 24 hr, respectively. Treatment with cisplatin resulted in the formation of adducts in the amount of 2611, 1485 and 1069 pg Pt/ μ g DNA at 0, 4 and 24 hr, respectively.

In the DU-145 cell line, treatment with 4DB resulted in the formation of adducts in the amount of 792, 739 and 622 pg Pt/ μ g DNA at 0, 4 and 24 hr, respectively. Treatment with 4TB resulted in the formation of adducts in the amount of 1808, 1673 and 905 pg Pt/ μ g DNA at 0, 4 and 24 hr, respectively.

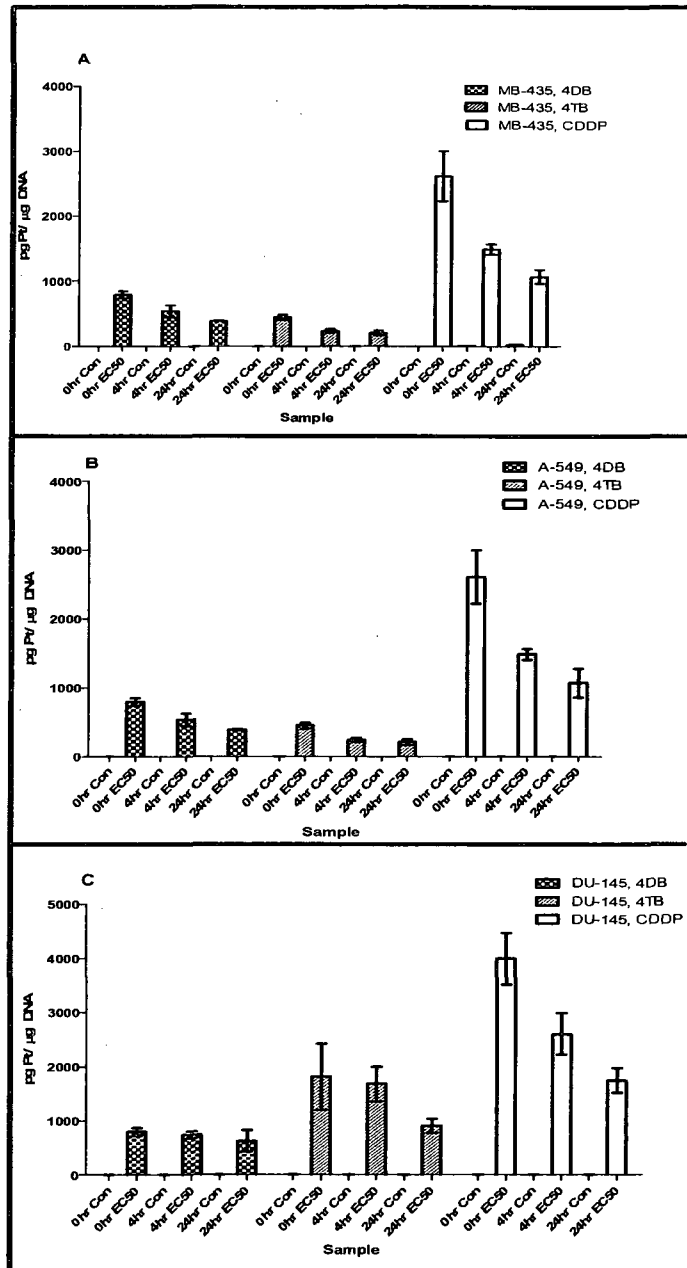


Figure 15: Mass of platinum per mass of DNA in MDA-MB-435 (A), A-549 (B) or DU-145 (C) cells over time following exposure to the EC₅₀ concentration of the indicated drug. Values are representative of three independent experiments.

In order to determine the rate of drug removal from the cells, the samples were analyzed for total mass of platinum versus total mass of protein. As described previously, cells were exposed to the drug then harvested at the indicated time point. Mass of protein in each sample was determined using the BCA assay. The mass of platinum in the original EC₅₀ concentration varied for each drug; therefore, in order to make a direct comparison with respect to rates of drug clearance between the three drugs within each cell line, the mass of platinum in picogram per microgram of protein in the 0 hr sample was calculated and considered as 100%. The subsequent time points at 4 hr and 24 hr were calculated in the same manner and compared to the value obtained for the 0 hr time point. The percentage of platinum remaining for MDA-MB-435, A-549 and DU-145 are shown in Figure 16. In the MDA-MB-435 cells treated with 4DB only 8% of the drug had been cleared at the 4 hr time compared to 23% clearance for 4TB and 21% clearance for cisplatin. At 24 hr post drug exposure, 64% of the drug had been cleared from whole cells with respect to 4DB and 4TB whereas 72% of cisplatin had been removed. With respect to the A-549 cell line, at 4 hr post drug treatment the clearance rates for 4DB, 4TB and cisplatin were 19%, 45% and 26%, respectively. The amount of drug cleared from the cells 24 hr post drug treatment for 4DB, 4TB and cisplatin were 53%, 57% and 70%, respectively. In the DU-145 cell line, at 4hr post drug treatment, the clearance rates for 4DB, 4TB and cisplatin were 11%, 6% and 32%, respectively. At 24 hr post drug treatment, the clearance rates in the DU-145 cell line for 4DB, 4TB and cisplatin were 71%, 76% and 75% respectively.

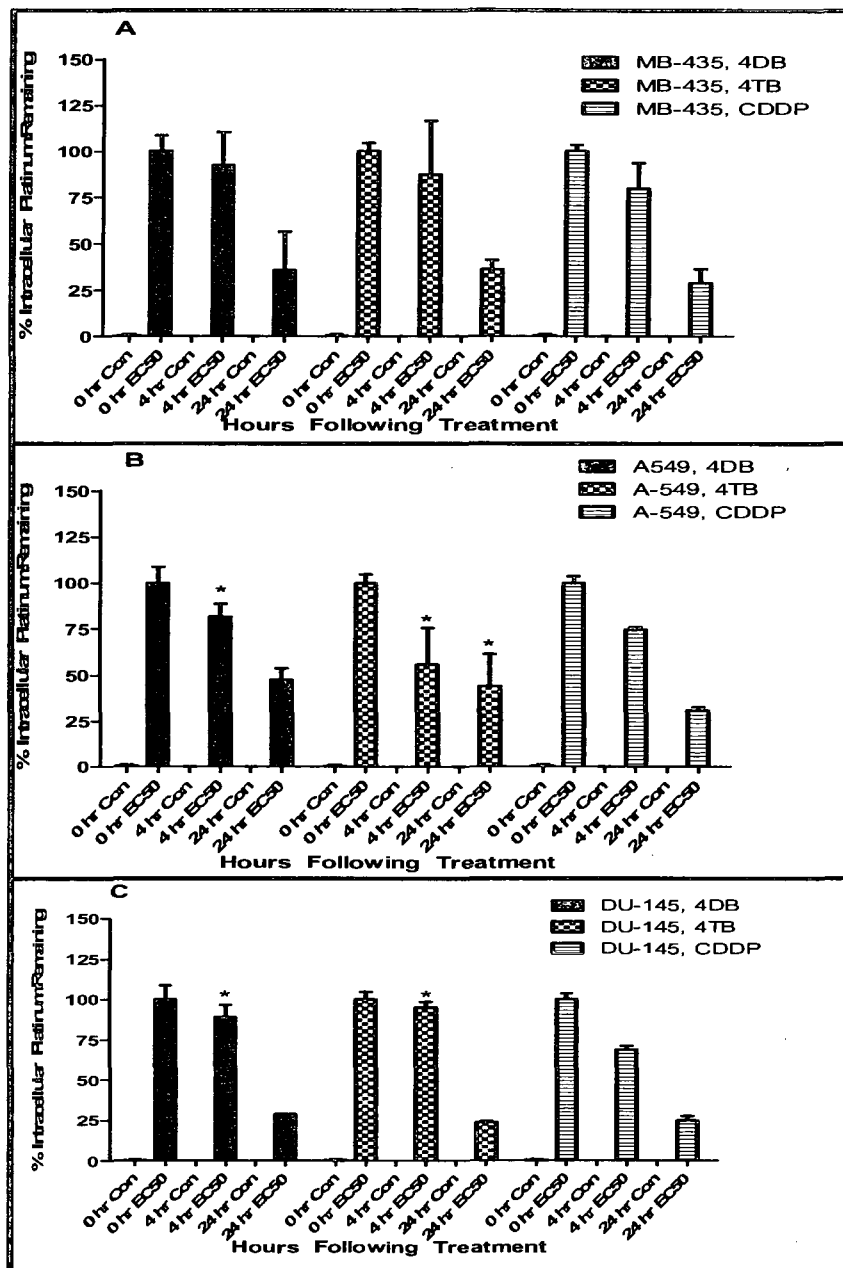


Figure 16: ICP-MS analysis of the percentage of drug remaining in whole MDA-MB-435 (A), A-549 (B) or DU-145 (C) cells over time following exposure to the EC₅₀ concentration of 4DB, 4TB or cisplatin. Values are representative of three independent experiments. *Statistically significant in comparison to cisplatin.

In order to determine the rate of Pt-DNA adduct repair, the samples were analyzed for total mass of platinum versus total mass of DNA. As described previously, cells were exposed to the drug then harvested at the indicated time point. Mass of DNA in each sample was determined by extracting the DNA using the GenElute kit and quantifying the DNA using the NanoDrop ND-1000 spectrophotometer. In order to make a direct comparison with respect to rates of Pt-DNA adduct repair between the three drugs within each cell line, the mass of platinum in picogram per microgram of DNA in the 0 hr sample was calculated and considered as 100%. The subsequent time points at 4 hr and 24 hr were calculated in the same manner and compared to the value obtained for the 0 hr time point. The percentage of platinum bound to DNA that remains over time for MDA-MB-435, A-549 and DU-145 cells are shown in Figure 17. Treating with 4DB in the MDA-MB-435 cell line revealed that only 33% of the lesions had been repaired compared to 47% repair for 4TB and 49% repair for cisplatin. At 24 hr post drug exposure, 52% of the adducts had been repaired with respect to 4DB and 4TB whereas 70% of adducts in the cisplatin treatment group had been repaired. With respect to the A-549 cell line, at 4 hr post drug treatment the repair rates for 4DB, 4TB and cisplatin were 37%, 64% and 55%, respectively. At the 24 hr time point, the percentage of lesions that had been repaired for 4DB, 4TB and cisplatin were 40%, 78% and 66%, respectively. In the DU-145 cell line, at 4hr post drug treatment, the percentage of adduct repair for 4DB, 4TB and cisplatin was 7%, 16% and 35%, respectively. At the 24 hr time point, the percentage of lesions that had been repaired for 4DB, 4TB and cisplatin were 20%, 38% and 44%, respectively.

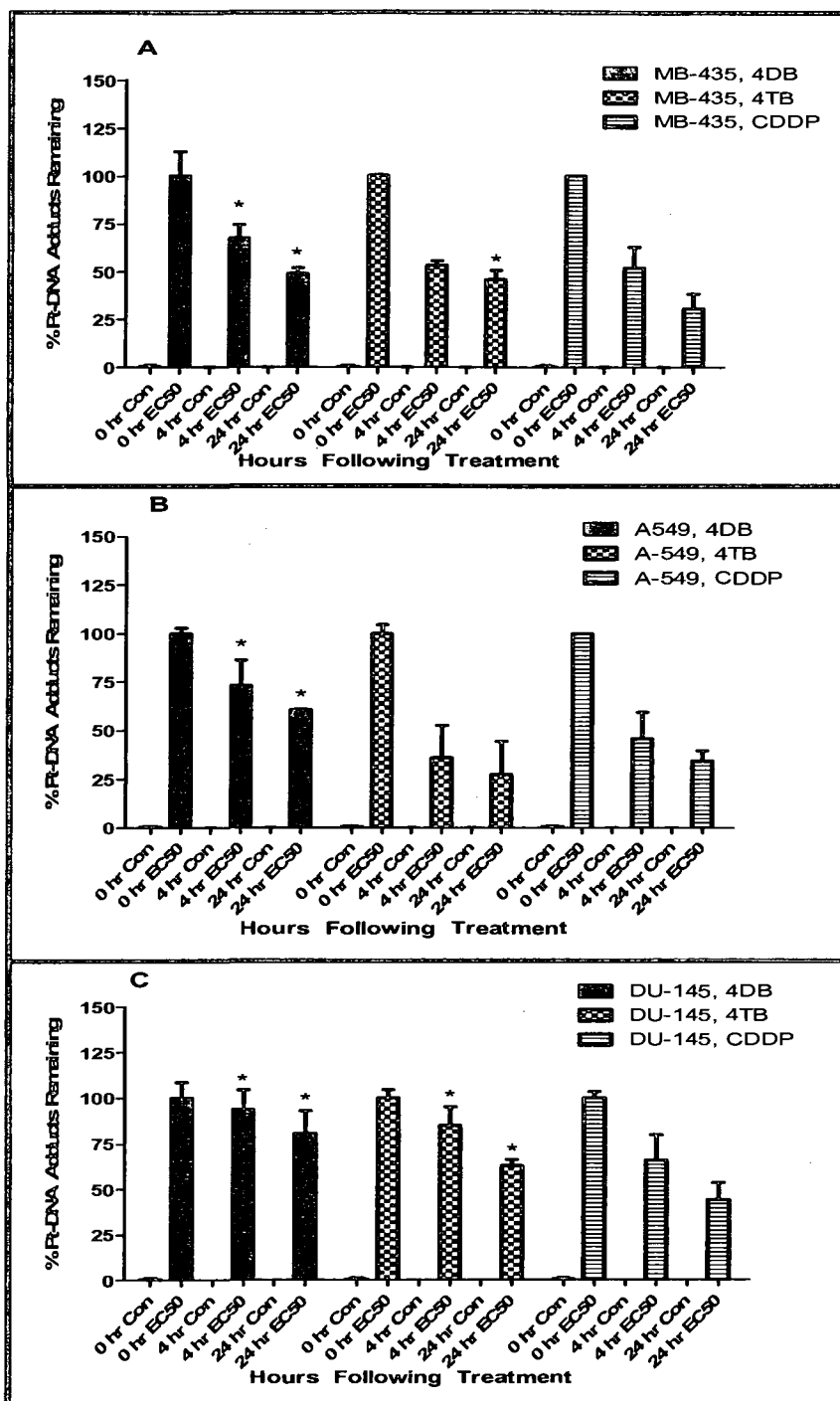


Figure 17: ICP-MS analysis of the percentage of drug remaining as Pt-DNA adducts in MDA-MB-435 (A), A-549 (B) or DU-145 (C) cells over time following exposure to the EC₅₀ concentration of 4DB, 4TB or cisplatin. Values are representative of three independent experiments. *Statistically significant in comparison to cisplatin.

Microarray analysis was employed to determine if the cytotoxicity of each drug within each cell line could be accounted for by changes in gene expression following drug exposure. MDA-MB-435, A-549 and DU-145 cell lines were exposed to each drug for 1 hr and then the drug was removed. A 1 hr exposure to DMSO for each cell line was used as the control sample. Cells were harvested and the RNA was extracted at 0 hr, 4hr or 24 hr post drug exposure. The RNA samples were analyzed by the Windber Research Institute (Windber, PA, USA) for gene expression changes as a result of exposure to each drug. In order to determine the genes that had significant changes in the level of expression, the 0 hr sample was compared to the control sample and the 4 and 24 hr samples were then compared to the 0 hr sample. The genes with the greatest change in protein expression, up to five, were identified for each drug and each cell line.

Unfortunately, RNA samples for the MDA-MB-435 cell line treated with 4DB at the 24 hr time point were too degraded for microarray analysis. The research staff at Windber Research Institute suggested that the reason the RNA was too degraded for analysis was due to the majority of the cells actively undergoing apoptosis. The research staff further suggested that it would be appropriate to analyze the MDA-MB-435 samples treated with 4DB at 0 hr, 2 hr and 4 hr post drug exposure for gene expression changes. Therefore, for the MDA-MB-435 cell line, samples treated with 4DB were analyzed at 2 hr and 4 hr post drug exposure instead of 4 hr and 24 hr post drug exposure. In order to confirm that the reason the RNA was too degraded at this time point due to cell death, fluorescent microscopy and flow cytometry analysis were employed. In the fluorescent

microscopy experiments, cells were exposed to the EC_{50} concentration of 4DB for one hour. The control sample was exposed to DMSO for 1 hr. Following treatment, the drug is removed from the cells and the samples were then incubated for 0, 2, 4 or 24 hr prior to obtaining images. At the indicated time point, the samples were stained with 1 $\mu\text{g}/\text{mL}$ Hoescht and 5 $\mu\text{g}/\text{mL}$ propidium iodide. After a 15 min exposure to the stain, the images were acquired. As shown in Figure 18, fluorescent microscopy analysis revealed that at the 4 hr time point, 28.7% of the cell population was undergoing apoptosis and 70.9% of the population was undergoing necrosis. These data reveal that 4 hr following drug treatment 99.6% of the population are in active stages of death. The experiment further revealed that at the 24 hr time point, 4.8% of the population was undergoing apoptosis and 25.5% of the population was undergoing necrosis.

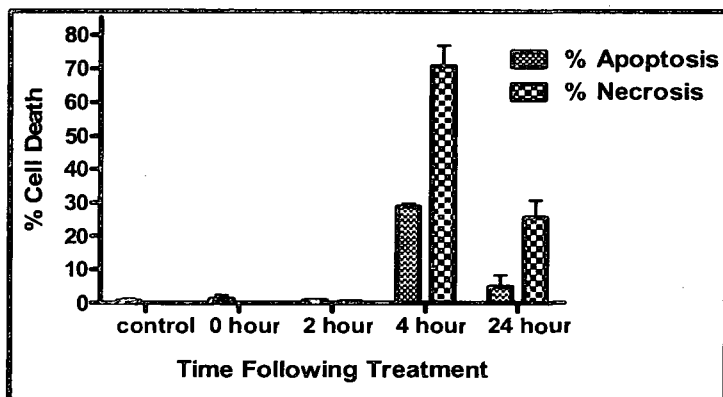


Figure 18: Fluorescent microscopy analysis of MDA-MB-435 cells exposed to the EC_{50} concentration of 4DB. Values are representative of two independent experiments.

Flow cytometry analysis of cell cycle distribution in the MDA-MB-435 cells following treatment with 4DB was also conducted. The cells were exposed to the EC₅₀ concentration of 4DB for 1 hr and the control sample was exposed to DMSO. Following drug exposure, the cells were washed and fresh medium was then added. The cells were incubated for 0, 2, 4 or 24 hr following exposure at which time they were harvested, pelleted and stained with 5 µg/mL propidium iodide. The samples were then analyzed as described previously using the flow cytometer. As shown in Figure 19, the data from the experiment revealed that at the 4 hr time point, approximately 48.3% of the cells were undergoing apoptosis and 64.7% of the cells were undergoing necrosis. These data reveal that 4 hr following drug treatment approximately 99% of the population are in active stages of death. The experiment further revealed that at the 24 hr time point, 6.6% of the population was undergoing apoptosis and 7.9% of the population was undergoing necrosis. Although the data from the fluorescent microscopy and flow cytometry experiments appear to suggest a decrease in cell death from the 4 hr to the 24 hr time point, the number of cells remaining at the 24 hr time point was extremely sparse given that the majority of the population was lost to cell death at the 4 hr time point. Therefore, these studies support the use of a 2 hr and 4 hr time point in the microarray analysis of MDA-MB-435 cells treated with the 4DB drug and removal of the 24 hr time point due to the inability to obtain pure RNA at 24 hr time point.

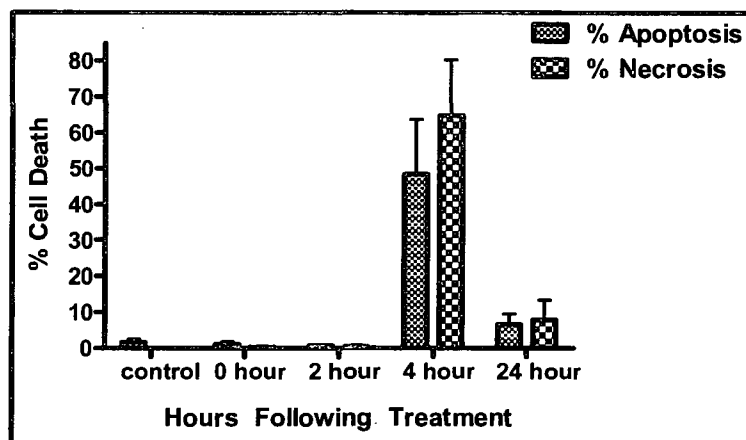


Figure 19: Flow cytometry analysis of apoptotic and necrotic events of MDA-MB-435 cells exposed to the EC₅₀ concentration of 4DB. Values are representative of two independent experiments.

The five genes with the greatest change in expression were identified by microarray analysis as described previously. Tables 6 through 14 provide the genes of interest for the MDA-MB-435, A-549 and DU-145 cells lines following treatment with 4DB, 4TB or cisplatin. A total of 93 genes were found to have increases in expression of at least three fold in response to the drug treatments. Of these 93 genes, 18 were found to occur in all three cell lines and all three drugs. One of the genes that was present in each cell line following treatment with 4DB was the CHOP gene which is a DNA damage inducible transcript which regulates progression through the cell cycle. Increased expression levels of this gene may play a role in decreased survival in all cell lines following treatment with 4DB due to the ability of CHOP to induce increased apoptotic signalling. Five of the 18 common genes were heat shock proteins, which have the

potential to lend protection against the cytotoxic effects of the drugs. Specifically, these heat shock proteins were HSP72, HSP70, HSP60, HSP40 and HSP32.

In addition to finding genes in common between the cell lines and treatment groups, identifying over expressed genes in the DU-145 and A-549 cell lines following treatment with 4TB that were not present in the MDA-MB-435 cell line was also of interest. The A-549 cell line is completely non-responsive to 4TB, and the drug has limited efficacy, compared to the MDA-MB-435 cell line, in the DU-145 cell line. Therefore, if varying genes can be found in the different cell lines, this information would allow identification of genes that potentially contribute to the observed cytotoxicity. After analyzing the genes present in each treatment group, three genes were identified that were common to both A-549 and DU-145 but absent from MDA-MB-435. These genes were identified as ZNT1, p21 and metallothionein 1L. The ZNTR1 gene is responsible for cation and drug uptake in the cell. The over expression of this gene in the A-549 and DU-145 cells versus no expression change in MDA-MB-435 cells may be a promising target in the examination of resistance to the 4TB drug. The data further revealed that metallothionein and p21 were over expressed following drug treatment in A-549 and DU-145 cells, but were not over expressed in the MDA-MB-435 cells. Metallothionein is of interest because this protein has been shown to bind heavy metals, such as platinum and provide protection against heavy metals toxicity as well as oxidative stress. The p21 gene is responsible for cell cycle regulation and acts as an inhibitor of apoptosis.

Gene Name	Sample	Fold Change	Activity	Function	Path-way	Cellular Location
c-fos v-fos FBJ murine osteosarcoma viral oncogene homolog	0 hr, Control	26.28	DNA methylation, regulation of transcription from RNA polymerase II promoter, inflammatory response, regulation of transcription, DNA-dependent	specific RNA polymerase II transcription factor activity	B cell receptor signalling pathway, MAPK signalling pathway, T cell receptor signalling pathway	Nucleus
HSPA6 heat shock 70kD protein 6 (HSP70B)	0 hr, Control	26.08	protein folding, response to unfolded protein	nucleotide binding, ATP binding	N/A	Cytoplasm
HO-1, HSP32, heme oxygenase (decycling) 1 (HMOX1)	0 hr, Control	13.57	heme oxidation, positive regulation of I-kappaB kinase/NF-kappaB cascade	heme oxygenase (decycling) activity, signal transducer activity iron ion binding, oxidoreductase activity, metal ion binding	Porphyrin metabolism	Plasma Membrane, endoplasmic reticulum

AP1, c-Jun v-jun avian sarcoma virus 17 oncogene homolog	0 hr, Control	10.46	regulation of transcription, DNA-dependent	transcription factor activity, RNA polymerase II transcription factor activity, transcription factor binding, protein binding, DNA binding, transcription factor activity	B cell receptor signalling pathway, MAPK signalling pathway, Renal cell carcinoma, T cell receptor signalling pathway	nuclear chromosome
HSP60, heat shock protein 60	0 hr, Control	9.09	protein folding response to unfolded protein, protein import into mitochondrial matrix	nucleotide binding, ATP binding, unfolded protein binding	N/A	Mitochondrial matrix
SHARP-2 basic helix-loop-helix domain containing, class B, 2 (BHLHB2)	0 hr, 2 hr	30.17	regulation of transcription, DNA-dependent	transcription factor activity, DNA binding	Circadian rhythm	Nucleus
HO-1, HSP32, heme oxygenase (decycling) 1 (HMOX1)	0 hr, 2 hr	10.14	heme oxidation, positive regulation of I-kappaB kinase/NF-kappaB cascade	heme oxygenase (decyclizing) activity, signal transducer activity iron ion binding, oxidoreductase activity, metal ion binding	Porphyrim metabolism	Plasma Membrane, endoplasmic reticulum
HSPA6 heat shock 70kD protein 6 (HSP70B)	0 hr, 2 hr	9.14	protein folding, response to unfolded protein	nucleotide binding, ATP binding	N/A	Cytoplasm

SKIP 1 phosphoprotein regulated by mitogenic pathways	0 hr, 2 hr	8.91	protein amino acid phosphorylation, cell proliferation, regulation of MAPK activity, protein amino acid phosphorylation	protein kinase activity, ATP binding, protein kinase activity, protein binding	N/A	Cytoplasm
MKNK2 G protein-coupled receptor kinase 7	0 hr, 2 hr	7.68	regulation of translation, protein amino acid phosphorylation, cell surface receptor linked signal transduction	nucleotide binding, protein serine/threonine kinase activity, protein-tyrosine kinase activity, ATP binding	Insulin signalling pathway	Cytoplasm
MCARP cardiac ankyrin repeat protein (CARP)	0 hr, 4 hr	22.25	Defense response, signal transduction	DNA binding	N/A	Nucleus
H11 protein kinase (H11)	0 hr, 4 hr	11.12	protein folding, response to unfolded protein	protein serine/threonine kinase activity, transferase activity, unfolded protein binding	N/A	Cytoplasm
SHARP-2 basic helix-loop-helix domain containing, class B, 2 (BHLHB2)	0 hr, 4 hr	10.26	regulation of transcription, DNA-dependent	transcription factor activity, DNA binding	Circadian rhythm	Nucleus
HSPA6 heat shock 70kD protein 6 (HSP70B)	0 hr, 4 hr	10.14	protein folding, response to unfolded protein	nucleotide binding, ATP binding	N/A	Cytoplasm

CHOP DNA- damage- inducible transcript 3	0 hr, 4 hr	8.85	regulation of progression through cell cycl	transcription factor activity, DNA binding, protein binding, RNA binding, zinc ion binding, metal ion binding	MAPK signalling pathway	Nucleus
---	------------	------	--	--	-------------------------------	---------

Table 6: Microarray analysis of MDA-MB-435 cells treated with 4DB. The table above provides up to five genes at each compared time point that exhibited the greatest change in expression.

Gene Name	Sample	Fold Change	Activity	Function	Pathway	Cellular Location
HSP72 heat shock 70kD protein 1A (HSPA1A)	0 hr, Control	9.54	protein folding, response to unfolded protein	nucleotide binding, ATP binding, unfolded protein binding	N/A	Nucleus, Cytoplas- m
HSPA1A, HSP70-2, heat shock 70kD protein 1B (HSPA1B)	0 hr, Control	4.24	protein folding, response to unfolded protein	nucleotide binding, ATP binding, unfolded protein binding	N/A	Nucleus, Cytoplas- m
HO-1, HSP32, heme oxygenase (decycling) 1 (HMOX1)	0 hr, Control	4.04	heme oxidation, positive regulation of I-kappaB kinase/NF-kappaB cascade	heme oxygenase (decyclizing) activity, signal transducer activity iron ion binding, oxidoreductase activity, metal ion binding	Porphyrin metabolism	Plasma Membr- ane, endoplas- mic reticulum
HSP40, heat shock 40kD protein 1 (HSPF1)	0 hr, Control	3.11	protein folding, response to unfolded protein	heat shock protein binding, unfolded protein binding	N/A	Nucleus, cytoplas- m
HO-1, HSP32, heme oxygenase (decycling) 1 (HMOX1)	0 hr, 4 hr	19.79	heme oxidation, positive regulation of I-kappaB kinase/NF-kappaB cascade	heme oxygenase (decyclizing) activity, signal transducer activity iron ion binding, oxidoreductase activity, metal ion binding	Porphyrin metabolism	Plasma Membr- ane, endoplas- mic reticulum
ZNTR1	0 hr, 4 hr	7.38	cation transport, zinc ion transport	Cation transporter activity	N/A	Plasma Membr- ane
GRO2 gro-beta	0 hr, 4 hr	6.60	chemotaxis, inflammatory response, G-protein coupled receptor protein signalling pathway	Chemokine and cytokine activity	Cytokine- cytokine receptor interaction	Extra- cellular Space
FTH	0 hr, 4 hr	6.03	iron ion transport	ferroxidase activity	Porphyrin metabolism	Plasma Membr- ane

AMCF-I interleukin 8 C- terminal variant (IL8)	0 hr, 4 hr	5.23	angiogenesis, cell motility, chemotaxis, cell cycle arrest, G- protein coupled receptor protein signalling pathway inflammatory response	interleukin-8 receptor binding	Cytokine- cytokine receptor interaction	Extra- cellular Space
MBAB aldo-keto reductase family 1, member C1	0 hr, 24 hr	3.25	lipid metabolism, steroid metabolism	aldo-keto reductase activity	Metabolism of xenobiotics by cytochrome P450	Cytopla- sm

Table 7: Microarray analysis of MDA-MB-435 cells treated with 4TB. The table above provides up to five genes at each compared time point that exhibited the greatest change in expression.

Gene Name	Sample	Fold Change	Activity	Function	Pathway	Cellular Location
HHL hairy (homolog (HRY)	0 hr, Control	2.66	regulation of transcription, DNA-dependent, nervous system development	DNA binding, transcription regulator activity	Maturity onset diabetes of the young	Nucleus
HO-1, HSP32, heme oxygenase (decyclizing) 1 (HMOX1)	0 hr, 4 hr	22.34	heme oxidation, positive regulation of I-kappaB kinase/NF-kappaB cascade	heme oxygenase (decyclizing) activity, signal transducer activity iron ion binding, oxidoreductase activity, metal ion binding	Porphyrin metabolism	Plasma Membr- ane, endopla- smic reticulum
ZNTR1	0 hr, 4 hr	8.88	cation transport, zinc ion transport	Cation transporter activity	N/A	Plasma Membr- ane
CP1B cytochrome P450, subfamily I (dioxin- inducible)	0 hr, 4 hr	6.57	visual perception	monooxygenase activity, oxygen binding	Metabolism of xenobiotics by cytochrome P450	Endopla- smic reticulum
P450-C cytochrome P450, subfamily I (aromatic compound- inducible)	0 hr, 4 hr	5.27	electron transport	iron ion binding, metal ion binding, heme binding monooxygenase activity	Metabolism of xenobiotics by cytochrome P450	Endopla- smic reticulum
G10P2	0 hr, 24 hr	3.19	immune response	binding	N/A	N/A

Table 8: Microarray analysis of MDA-MB-435 cells treated with Cisplatin. The table above provides up to five genes at each compared time point that exhibited the greatest change in expression

Gene Name	Sample	Fold Change	Activity	Function	Pathway	Cellular Location
GOS8 regulator of G-protein signalling 2	0 hr, Control	7.38	transmembrane receptor protein tyrosine kinase signalling pathway	signal transducer activity, calmodulin binding	Calcium regulation in cardiac cells	N/A
HSPA1A , heat shock 70kD protein 1B (HSPA1B)	0 hr, Control	5.89	protein folding, response to unfolded protein	nucleotide binding, ATP binding, unfolded protein binding	N/A	Nucleus, Cytoplasm
CHOP DNA-damage-inducible transcript 3	0 hr, Control	5.40	regulation of progression through cell cycle	transcription factor activity, DNA binding, protein binding, RNA binding, zinc ion binding, metal ion binding	MAPK signalling pathway	Nucleus
HSP40 , heat shock 40kD protein (HSPF1)	0 hr, Control	4.28	protein folding, response to unfolded protein	heat shock protein binding, unfolded protein binding	N/A	Nucleus, cytoplasm
TIS8 Early growth response 1	0 hr, Control	3.67	regulation of transcription, DNA-dependent	transcription factor activity	Ovarian infertility genes	Nucleus
GEM GTP-binding protein	0 hr, 4 hr	19.23	immune response, small GTPase mediated signal transduction	nucleotide binding, calmodulin binding	N/A	Membrane
HSP40 , heat shock 40kD protein 1 (HSPF1)	0 hr, 4 hr	12.31	protein folding, response to unfolded protein	heat shock protein binding, unfolded protein binding	N/A	Nucleus, cytoplasm
HO-1 , HSP32 , heme oxygenase (decycling) 1 (HMOX1)	0 hr, 4 hr	8.86	heme oxidation, positive regulation of I-kappaB kinase/NF-kappaB cascade	heme oxygenase (decycling) activity, signal transducer activity iron ion binding, oxidoreductase activity, metal ion binding	Porphyrim metabolism	Plasma Membrane, endoplasmic reticulum

MCARP cardiac ankyrin repeat protein (CARP)	0 hr, 4 hr	8.29	Defense response, signal transduction	DNA binding	N/A	Nucleus
ZNTR1	0 hr, 4 hr	7.85	cation transport, zinc ion transport	Cation transporter activity	N/A	Plasma Membr- ane
GCCR glucocortic oid receptor alpha	0 hr, 24 hr	10.10	inflammatory response, signal transduction, regulation of transcription	transcription factor activity, steroid binding, protein binding	Neuroactive ligand- receptor	Nucleus
MT-11 metallothio nein 1L (MT1L)	0 hr, 24 hr	5.93	response to metal ion, electron transport	copper ion binding, protection against metal toxicity and oxidative stress, transcription factor regulation	N/A	Cytopla- sm
KIR GTP- binding protein	0 hr, 24 hr	5.45	immune response, protein transport	nucleotide binding, calmodulin binding	N/A	Plasma Membr- ane
CPM carboxy- peptidase M (CPM)	0 hr, 24 hr	3.83	Proteolysis, aromatic compound metabolism	carboxypeptidase A activity, metal ion binding, metallopeptidase activity	N/A	Plasma Membr- ane
BPX nucleosom e assembly protein 1- like 2 (NAP1L2)	0 hr, 24 hr	3.61	nucleosome assembly	N/A	N/A	Nucleus

Table 9: Microarray analysis of A-549 cells treated with 4DB. The table above provides up to five genes at each compared time point that exhibited the greatest change in expression.

Gene Name	Sample	Fold Change	Activity	Function	Pathway	Cellular Location
N/A	0 hr, Control	N/A	N/A	N/A	N/A	N/A
HO-1, HSP32, heme oxygenase (decycling) 1 (HMOX1)	0 hr, 4 hr	7.36	heme oxidation, positive regulation of I-kappaB kinase/NF-kappaB cascade	heme oxygenase (decycling) activity, signal transducer activity iron ion binding, oxidoreductase activity, metal ion binding	Porphyrin metabolism	Plasma Membrane, endoplasmic reticulum
MT-11 metallothionein 1L (MT1L)	0 hr, 4 hr	5.03	response to metal ion, electron transport	copper ion binding, protection against metal toxicity and oxidative stress, transcription factor regulation	N/A	Cytoplasm
IGFBP3 insulin-like growth factor binding protein 3	0 hr, 4 hr	4.93	regulation of cell growth, negative regulation of signal transduction, positive regulation of apoptosis	insulin-like growth factor binding, protein tyrosine phosphatase activator activity	Smooth muscle contraction	Extra-cellular Region
SNK serum-inducible kinase	0 hr, 4 hr	4.37	protein amino acid phosphorylation, positive regulation of I-kappaB kinase/NF-kappaB cascade	protein-tyrosine kinase activity, signal transducer activity	N/A	Cytoplasm
G10P1 interferon-induced protein (IFIT1)	0 hr, 24 hr	4.92	immune response	Protein binding	N/A	Cytoplasm
FLJ40832 pyruvate dehydrogenase kinase, isoenzyme 4 (PDK4)	0 hr, 24 hr	4.56	protein amino acid phosphorylation	ATP binding	TCA Cycle	Mitochondria

FLRT3 fibronectin leucine rich transmembrane protein 3	0 hr, 24 hr	3.94	cell adhesion	receptor signalling protein activity	Cellular Adhesion	Extra- cellular Region
OPN nephropontin	0 hr, 24 hr	3.64	anti-apoptosis, cell- cell signalling	integrin binding, cytokine activity	Cell Signalling and Focal Adhesion	Extra- cellular Region

Table 10: Microarray analysis of A-549 cells treated with 4TB. The table above provides up to five genes at each compared time point that exhibited the greatest change in expression.

Gene Name	Sample	Fold Change	Activity	Function	Pathway	Cellular Location
N/A	0 hr, Control	N/A	N/A	N/A	N/A	N/A
HO-1, HSP32, heme oxygenase (decycling) 1 (HMOX1)	0 hr, 4 hr	12.87	heme oxidation, positive regulation of I-kappaB kinase/NF-kappaB cascade	heme oxygenase (decyclizing) activity, signal transducer activity iron ion binding, oxidoreductase activity, metal ion binding	Porphyrin metabolism	Plasma Membrane, endoplasmic reticulum
FRA1 FOS-like antigen-1	0 hr, 4 hr	4.59	regulation of transcription from RNA polymerase II promoter, positive regulation of cell proliferation	N/A	N/A	Nucleus
CDKN1 cyclin-dependent kinase inhibitor 1A (p21, Cip1)	0 hr, 4 hr	4.19	negative regulation of cell proliferation, cell cycle arrest	Cell Signalling	Apoptosis	Nucleus
YWHAS stratifin	0 hr, 4 hr	3.97	regulation of progression through cell cycle, negative regulation of protein kinase activity	Cell Signalling	Apoptosis	Nucleus
PHRIP pleckstrin homology-like domain, family A, member 1 (PHLDA1)	0 hr, 24 hr	3.68	Protein binding	N/A	N/A	Cytosol
GRO2 gro-beta	0 hr, 24 hr	3.68	chemotaxis, inflammatory response, G-protein coupled receptor protein signalling pathway	Chemokine and cytokine activity	Cytokine-cytokine receptor interaction	Extra-cellular Space

HEIR-1 inhibitor of DNA binding 3, dominant negative helix-loop- helix protein (ID3)	0 hr, 24 hr	3.37	regulation of transcription	transcription corepressor activity	TGF-beta signalling pathway	Nucleus
SSAT-1 Spermidine spermine N1- acetyltransf erase	0 hr, 24 hr	3.23	diamine N- acetyltransferase activity	Arginine and proline metabolism	Cell Migration	Cytopla- sm

Table 11: Microarray analysis of A-549 cells treated with Cisplatin. The table above provides up to five genes at each compared time point that exhibited the greatest change in expression.

Gene Name	Sample	Fold Change	Activity	Function	Pathway	Cellular Location
HSPA6 heat shock 70kD protein 6 (HSP70B)	0 hr, Control	13.10	protein folding, response to unfolded protein	nucleotide binding, ATP binding	N/A	Cytoplasm
c-fos v-fos FBJ murine osteosarcoma viral oncogene homolog	0 hr, Control	10.76	DNA methylation, regulation of transcription from RNA polymerase II promoter, inflammatory response, regulation of transcription, DNA-dependent	specific RNA polymerase II transcription factor activity	B cell receptor signalling pathway, MAPK signalling pathway, T cell receptor signalling pathway	Nucleus
ATF3 activating transcription factor 3 (ATF3)	0 hr, Control	6.23	Transcription, DNA-dependent	DNA binding	Smooth muscle contraction	Nucleus
CHOP DNA-damage-inducible transcript 3	0 hr, Control	4.79	regulation of progression through cell cycle	transcription factor activity, DNA binding, protein binding, RNA binding, zinc ion binding, metal ion binding	MAPK signalling pathway	Nucleus
HO-1, HSP32, heme oxygenase (decycling) 1 (HMOX1)	0 hr, Control	4.45	heme oxidation, positive regulation of I-kappaB kinase/NF-kappaB cascade	heme oxygenase (decyclizing) activity, signal transducer activity iron ion binding, oxidoreductase activity, metal ion binding	Porphyrin metabolism	Plasma Membrane, endoplasmic reticulum
HSPA6 heat shock 70kD protein 6 (HSP70B)	0 hr, 4 hr	38.31	protein folding, response to unfolded protein	nucleotide binding, ATP binding	N/A	Cytoplasm
ZNT1	0 hr, 4 hr	29.96	cation transport, zinc ion transport	Cation transporter activity	N/A	Plasma Membrane

THRM thrombomodulin	0 hr, 4 hr	23.89	calcium ion binding	transmembrane receptor activity	blood coagulation	Plasma Membrane
MT-11 metallothionein 1L (MT1L)	0 hr, 4 hr	14.82	response to metal ion, electron transport	copper ion binding, protection against metal toxicity and oxidative stress, transcription factor regulation	N/A	Cytoplasm
HFARP hepatic angiopoietin-related protein	0 hr, 24 hr	13.84	cellular response to starvation	Enzyme inhibitor activity	Angiogenesis Differentiation	Cytoplasm
GMCSF Granulocyte-macrophage colony-stimulating factor	0 hr, 24 hr	7.58	cellular defence response	cell surface receptor linked signal transduction, granulocyte macrophage colony-stimulating factor receptor binding	Cytokine-cytokine receptor interaction, Natural killer cell mediated cytotoxicity	Extra-cellular Region
MT-11 metallothionein 1L (MT1L)	0 hr, 24 hr	6.82	response to metal ion, electron transport	copper ion binding	N/A	Cytoplasm
CLGN matrix metalloproteinase 1 (interstitial collagenase) (MMP1)	0 hr, 24 hr	6.40	peptidoglycan metabolism, collagen catabolism	interstitial collagenase activity, calcium ion binding, metalloendopeptidase activity	PPAR Signalling	Extra-cellular Region
AGIF1 interleukin 11	0 hr, 24 hr	6.15	cell-cell signalling, B-cell differentiation	interleukin-11 receptor binding, growth factor activity	Cytokine-cytokine receptor interaction, JAK-STAT	Extra-cellular Region

Table 12: Microarray analysis of DU-145 cells treated with 4DB. The table above provides up to five genes at each compared time point that exhibited the greatest change in expression.

Gene Name	Sample	Fold Change	Activity	Function	Pathway	Cellular Location
N/A	0 hr, Control	N/A	N/A	N/A	N/A	N/A
ZNT1	0 hr, 4 hr	13.94	cation transport, zinc ion transport	Cation transporter activity	N/A	Plasma Membrane
DBA ribosomal protein S19	0 hr, 4 hr	8.69	protein biosynthesis	hemocyte development, RNA binding	Ribosome Reactome Events	Cytoplasm
AGIF1 interleukin 11	0 hr, 4 hr	8.55	cell-cell signalling, B-cell differentiation	interleukin-11 receptor binding, growth factor activity	Cytokine-cytokine receptor interaction, JAK-STAT	Extra-cellular Region
HO-1, HSP32, heme oxygenase (decycling) 1 (HMOX1)	0 hr, 4 hr	8.47	heme oxidation, positive regulation of I-kappaB kinase/NF-kappaB cascade	heme oxygenase (decyclizing) activity, signal transducer activity iron ion binding, oxidoreductase activity, metal ion binding	Porphyrin metabolism	Plasma Membrane, endoplasmic reticulum
TR Tomoregulin	0 hr, 24 hr	6.74	N/A	N/A	N/A	Plasma Membrane
DBA ribosomal protein S19	0 hr, 24 hr	6.06	protein biosynthesis	hemocyte development, RNA binding	Ribosome Reactome Events	Cytoplasm
HD-VDAC3 voltage-dependent anion channel 3	0 hr, 24 hr	5.01	Ion transport	voltage-gated ion-selective channel activity	Calcium signalling pathway	Mitochondria
MRPL52 cathepsin D (lysosomal aspartyl protease)	0 hr, 24 hr	4.63	N/A	Proteolytic cleavage	N/A	Ribosome

Table 13: Microarray analysis of DU-145 cells treated with 4TB. The table above provides up to five genes at each compared time point that exhibited the greatest change in expression.

Gene Name	Sample	Fold Change	Activity	Function	Pathway	Cellular Location
N/A	0 hr, Control	N/A	N/A	N/A	N/A	N/A
GMCSF Granulocyte-macrophage colony-stimulating factor	0 hr, 4 hr	44.7	cellular defence response	cell surface receptor linked signal transduction, granulocyte macrophage colony-stimulating factor receptor binding	Cytokine-cytokine receptor interaction, Natural killer cell mediated cytotoxicity	Extra-cellular Region
ZNTR1	0 hr, 4 hr	27.8	cation transport, zinc ion transport	Cation transporter activity	N/A	Plasma Membrane
HFARP hepatic angiopoietin-related protein (ANGPTL2)	0 hr, 4 hr	19.63	cellular response to starvation	Enzyme inhibitor activity	Angiogenesis Differentiation	Cytoplasm
HEGFL heparin-binding EGF-like growth factor	0 hr, 4 hr	16.27	signal transduction	heparin binding, receptor activity	GnRH signalling pathway	Extra-cellular Space, Membrane
GMCSF Granulocyte Macrophage colony-stimulating factor	0 hr, 24 hr	26.7	cellular defense response	cell surface receptor linked signal transduction, granulocyte macrophage colony-stimulating factor receptor binding	Cytokine-cytokine receptor interaction, Natural killer cell mediated cytotoxicity	Extra-cellular Region
DUSP6 dual specificity phosphatase 6	0 hr, 24 hr	10.86	regulation of progression through cell cycle	inactivation of MAPK activity, protein amino acid dephosphorylation	MAPK Signalling	Cytoplasm

IL-6 interleukin 6 (interferon, β -2)	0 hr, 24 hr	8.90	humoral immune response	cytokine activity	Cytokine- cytokine receptor interaction	Extracell ular Region
MKP1 dual specificity phosphatas e 1 (DUSP1)	0 hr, 24 hr	6.96	protein amino acid dephosphorylation	non-membrane spanning protein tyrosine phosphatase activity	MAPK Signalling	Cytoplas m
GRO2 gro-beta	0 hr,24 hr	6.65	chemotaxis, inflammatory response, G-protein coupled receptor protein signalling pathway	Chemokine and cytokine activity	Cytokine- cytokine receptor interaction	Extracell ular Space

Table 14: Microarray analysis of DU-145 cells treated with Cisplatin. The table above provides up to five genes at each compared time point that exhibited the greatest change in expression.

The final phase of the project employed disruption of DNA repair mechanisms using shRNA to determine if the efficacy of the drugs could be improved in each of the cell lines. The proteins involved in the rate limiting steps of both the NER and MMR processes were selected as targets for suppression of DNA repair activity. However, prior to beginning studies with shRNA, confirmation of ERCC1 and MSH2 protein expression in the wild type cell line was confirmed. As shown in Figure 20, Western blot analysis revealed that both MSH2 and ERCC1 can be successfully probed for using this technique. Nuclear HeLa extract, known to express both these proteins, was used as a positive control and β -actin was used as a loading control in the experiment.

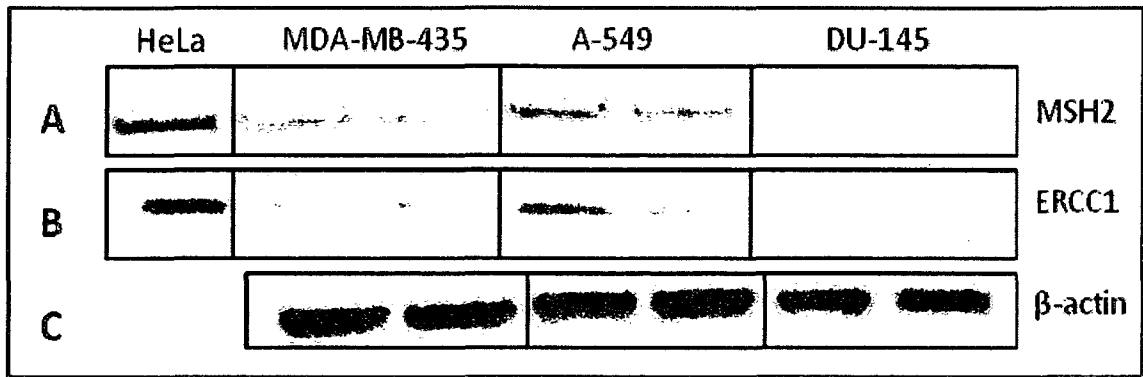


Figure 20: Western blot analysis for MSH2 (A), ERCC1 (B) and β -Actin (C) in wild type MDA-MB-435, A-549 and DU-145 cells. HeLa nuclear extract was used as a positive control. Each lane was loaded with 20 μ g of protein.

Disruption of the NER mechanism was accomplished by introducing shRNA against ERCC1 whereas disruption of the MMR mechanism was accomplished by introducing shRNA against MSH2. Two negative controls were used for these studies. The first negative control was the expression vector, shown in Figure 21, was used to ensure that the transfection process did not significantly change the response of the cell line to treatment. The second negative control was the expression vector with an ineffective shRNA insert against green fluorescence protein (GFP). This ineffective shRNA was used as a negative control to ensure that the presence of a non-effective shRNA does not have an effect on non-targeted protein expression.

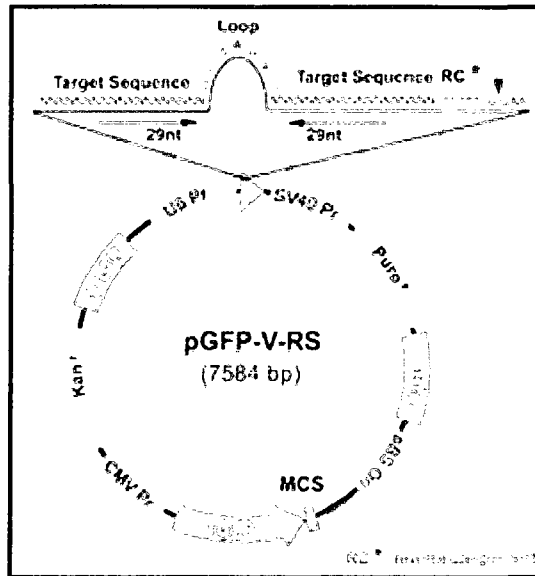


Figure 21: Expression vector for shRNA constructs. The negative control is the expression vector only, without a shRNA insert.

Four different constructs, targeting non-overlapping sequences of the gene of interest, were tested to determine which was the most effective in silencing each protein target. Each construct was tested in each cell line using the transient transfection procedure described previously. Western blotting analysis was employed to determine which construct was the most effective in reducing protein expression. In the A-549 cell line, construct 67 was most effective in silencing ERCC1 and construct 27 was most effective in silencing MSH2 (Figure 22A). In the DU-145 cell line, construct 65 was the most effective in silencing ERCC1 and construct 27 was the most effective in silencing MSH2 (Figure 22B). Transient transfection with MSH2 and ERCC1 constructs in the MDA-MB-435 cell line did not reveal an obvious construct to select for protein silencing with either target (Figure 22C).

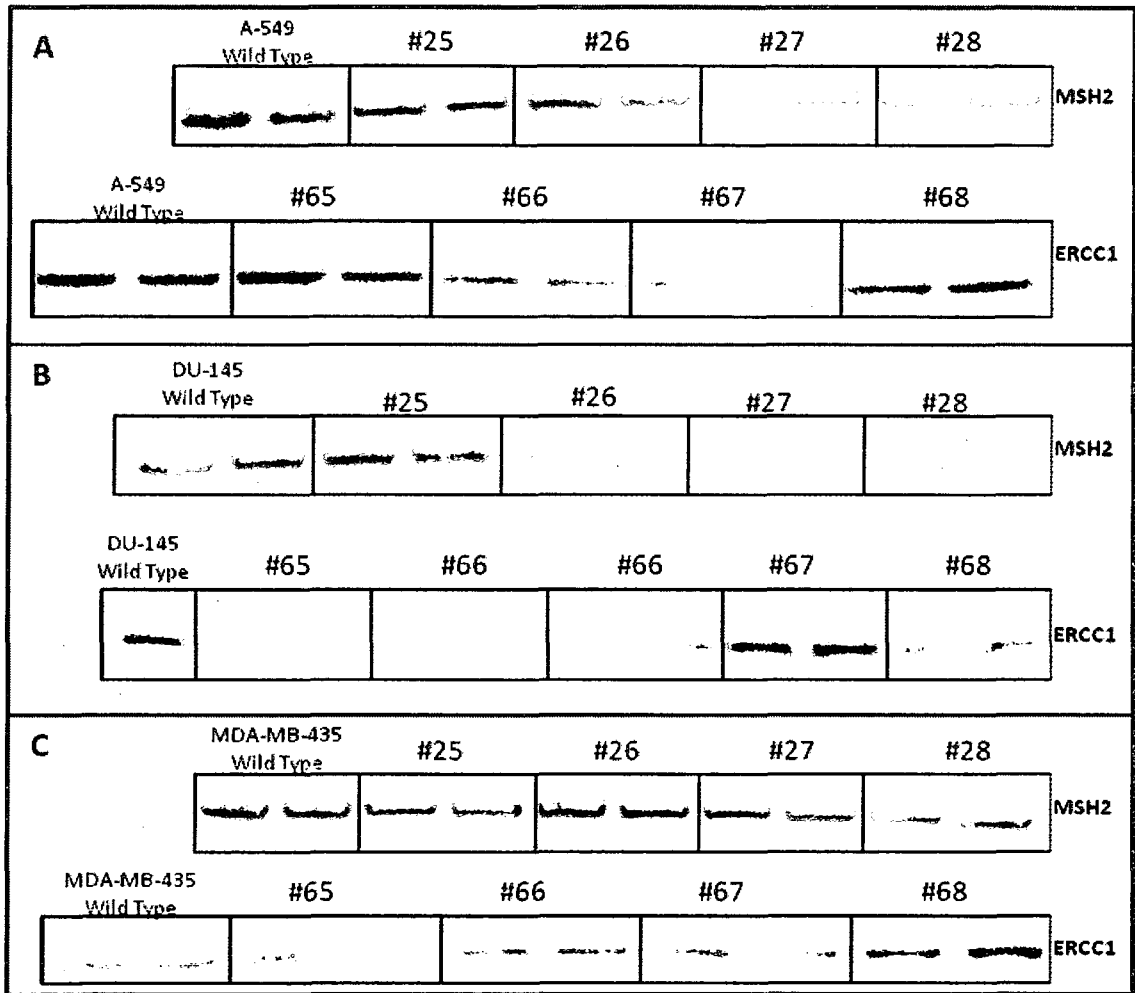


Figure 22: Results of Western blot analysis in wild type and transiently transfected A-549 (A), DU-145 (B) and MDA-MB-435 (C) cells probed for MSH2 or ERCC1. Each lane is loaded with 30 μ g of protein.

In order to effectively determine the appropriate constructs to use against each target, the stable transfection procedure was used for each target in the MDA-MB-435 cell line. These cells were then subjected to intracellular antigen staining as described previously and analyzed using the flow cytometer. As shown in Figure 23A, the MSH2 construct that resulted in the least amount of protein expression was construct 25. The

ERCC1 construct that resulted in the least amount of protein expression was construct 65, as shown in Figure 23B. Confirmation of the intracellular antigen staining results was achieved by repeating the Western blot analysis with all the stable transfects. As shown in Figure 24, Western blot and intracellular antigen staining experiments provide confirmation that construct 25 had the least amount of MSH2 expression whereas construct 65 had the least amount of ERCC1 expression.

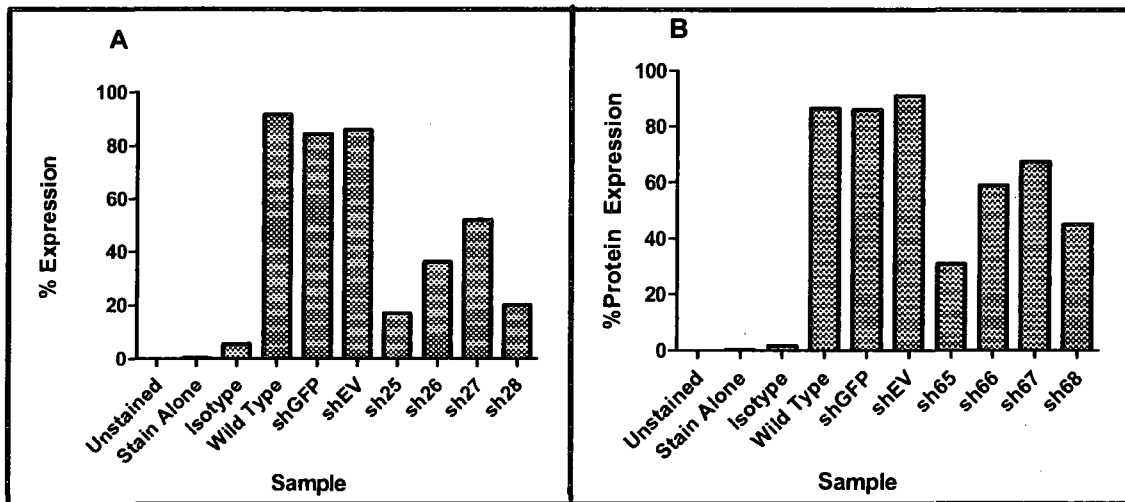


Figure 23: Intracellular antigen staining of MDA-MB-435 cells for MSH2 (A) or ERCC1 (B).

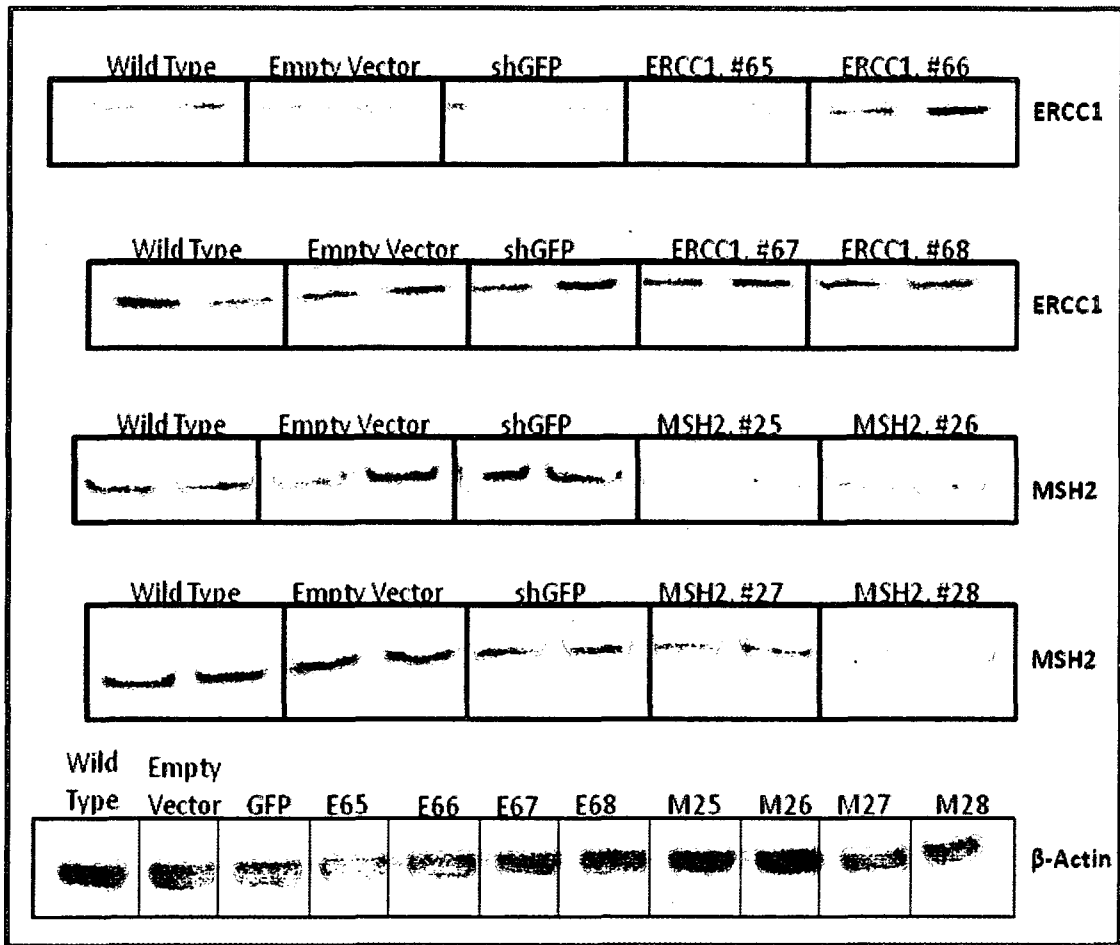


Figure 24: Western blot analysis of MDA-MB-435 stable transfects. Samples were probed for ERCC1, MSH2 or β -Actin. Each lane was loaded with 30 μ g of protein.

The selected constructs as well as positive and negative controls were used in the stable transfection procedure for all cell lines. The nomenclature for these newly developed cell lines utilized the beginning letter designation for each cell line, followed by the name of the target. The name of each cell line and its description are listed in Table 15.

Wild Type Cell Line	Transfected Cell Line Name	Transfected Cell Line Description
A-549	A-shEV	A-549 cell line transfected with the empty expression vector, negative control
A-549	A-shGFP	A-549 cell line transfected with ineffective shRNA against GFP, negative control
A-549	A-shMSH2	A-549 cell line transfected with effective shRNA against MSH2, construct 27
A-549	A-shERCC1	A-549 cell line transfected with effective shRNA against ERCC1, construct 67
DU-145	DU-shEV	DU-145 cell line transfected with the empty expression vector, negative control
DU-145	DU-shGFP	DU-145 cell line transfected with ineffective shRNA against GFP, negative control
DU-145	DU-shMSH2	DU-145 cell line transfected with effective shRNA against MSH2, construct 27
DU-145	DU-shERCC1	DU-145 cell line transfected with effective shRNA against ERCC1, construct 65
MDA-MB-435	MB-shEV	MDA-MB-435 cell line transfected with the empty expression vector, negative control
MDA-MB-435	MB-shGFP	MDA-MB-435 cell line transfected with ineffective shRNA against GFP, negative control
MDA-MB-435	MB-shMSH2	MDA-MB-435 cell line transfected with effective shRNA against MSH2, construct 25
MDA-MB-435	MB-shERCC1	MDA-MB-435 cell line transfected with effective shRNA against ERCC1, construct 65

Table 15: Nomenclature for cell lines expressing shRNA developed using stable transfection methods.

After stable transfections of all cell lines were completed, Western blot analysis was again conducted to ensure that the silencing of the ERCC1 and MSH2 targets was effective. Included in the analysis were the wild type cell line and both negative controls

(shGFP and shEV). Results of the Western blot experiments, Figures 25, 26 and 27, revealed that in all cell lines the shGFP and shEV samples had equivalent levels of protein expression in comparison to the wild type sample. All cell lines that were transfected with shRNA against ERCC1 or MSH2 had reduced levels of the intended target in comparison to the wild type and control samples.

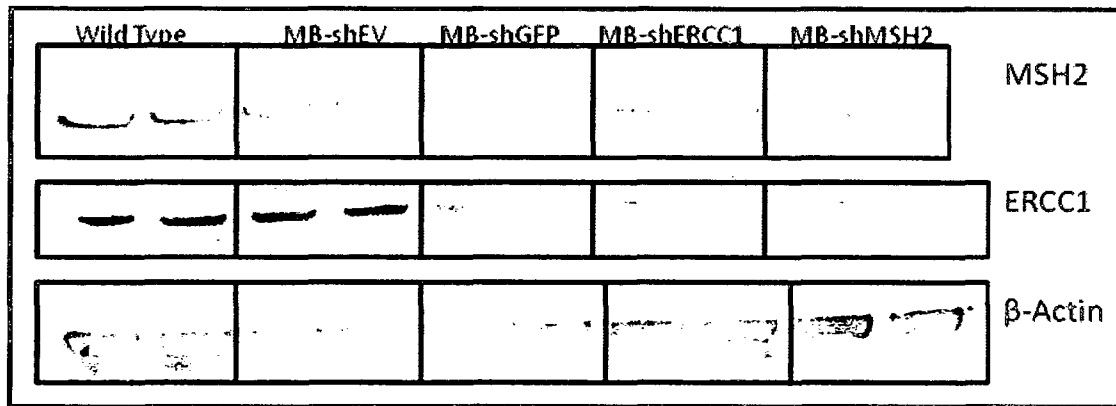


Figure 25: Western blot analysis of wild type and stable transfects of the MDA-MB-435 cell line. Samples were probed for MSH2, ERCC1 or β -Actin. Each lane was loaded with 30 μ g of protein.

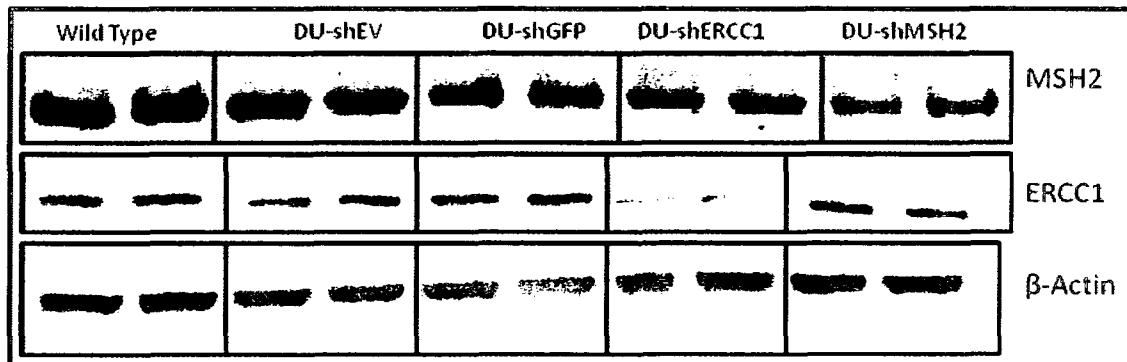


Figure 26: Western blot analysis of wild type and stable transfects of the DU-145 cell line. Samples were probed for MSH2, ERCC1 or β -Actin. Each lane was loaded with 30 μ g of protein.

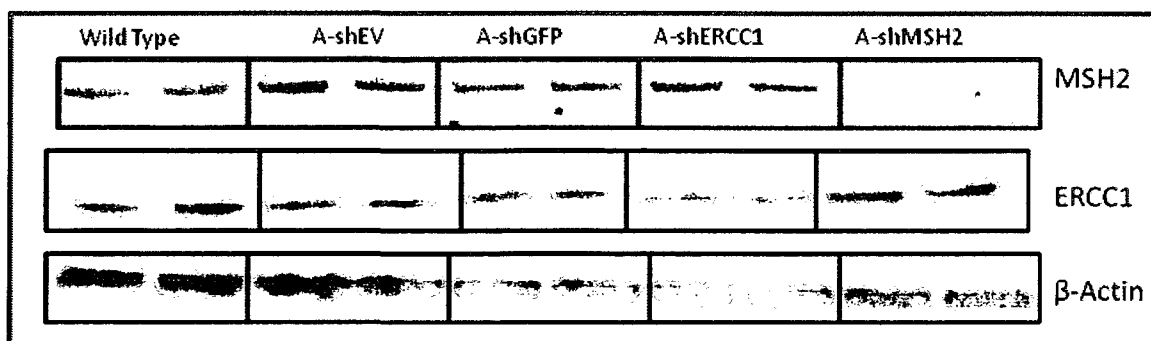


Figure 27: Western blot analysis of wild type and stable transfects of the A-549 cell line. Samples were probed for MSH2, ERCC1 or β -Actin. Each lane was loaded with 30 μ g of protein.

After confirming that the developed cell lines had decreased expression levels of proteins of interest, clonogenic survivals with the shEV, shERCC1 and shMSH2 constructs for each cell line were conducted. The shGFP cell lines were not included in these studies because Western blot analysis confirmed that levels of protein expression did not change with the transfection of ineffective shRNA. As described previously, cells were exposed to varying concentrations of the indicated drug for 1 hr, washed, harvested, and then plated with the wild type control cell number. Cells were incubated for 10 days, stained with crystal violet and the resulting colonies were counted to determine survival. The EC_{50} values for each drug with each cell line were determined using the survival curves generated for the transfected cell lines. As shown in Figure 28, the only statistically significant difference, as compared to the related shEV and wild type cell lines, in the survivals conducted with the MDA-MB-435 transfected cell lines was observed in the MB-shMSH2 cell line upon exposure to 10^{-3} M cisplatin.

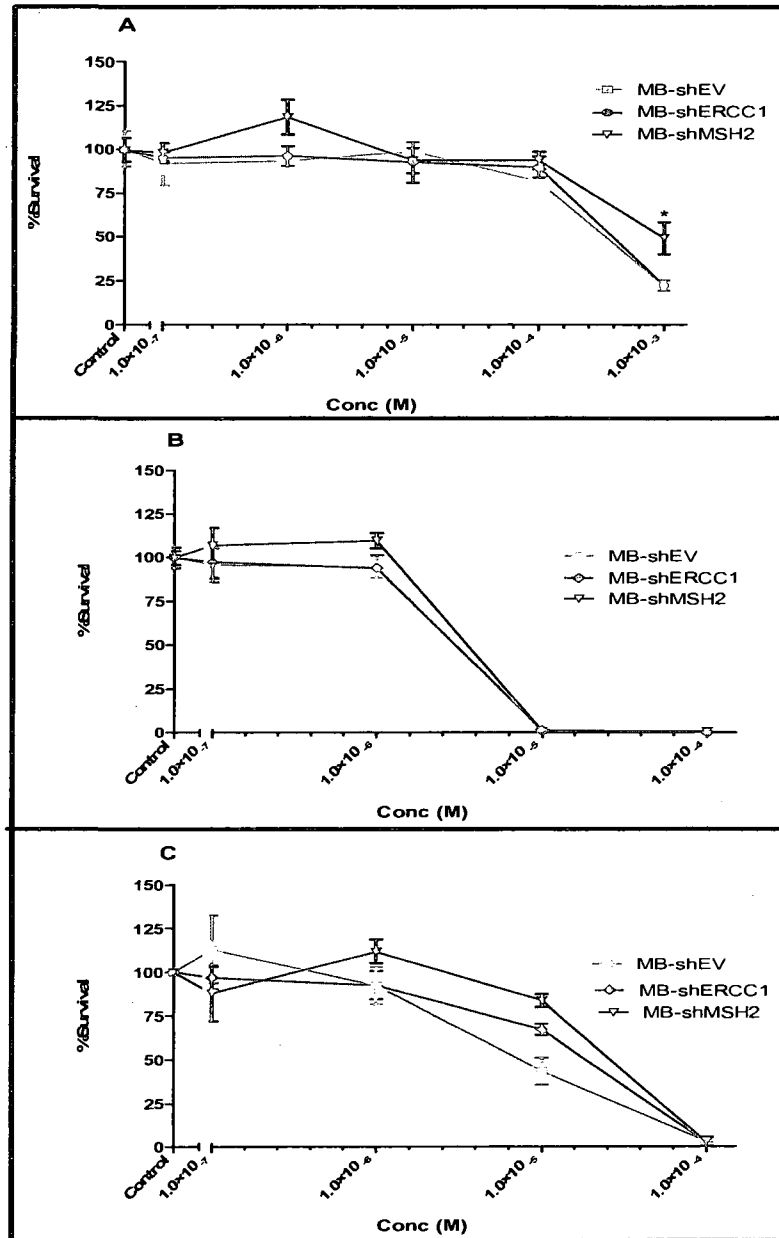


Figure 28: Clonogenic survival using cisplatin (A), 4DB (B) or 4TB (C) in MDA-MB-435 transfected cells. Cell survival was measured and compared to control cells after a 1 hr exposure to varying concentrations of the indicated drug. The above figures represent three trials each. Colonies were stained with crystal violet and viability was measured by counting colonies and comparing to the number of colonies in the control sample. A colony is a group of cells with $n \geq 50$.

Similar results were obtained with the A-549 and DU-145 transfected cell lines. As shown in Figure 29, the only statistically significant difference, as compared to the related shEV and wild type cell lines, in the survivals conducted with the A-549 transfected cell lines was observed in the A-shMSH2 cell line upon exposure to 10^{-3} M cisplatin. In the DU-145 transfected cell lines, as shown in Figure 30, the only statistically significant difference in survival, as compared to the related shEV and wild type cell lines, was observed in the DU-shERCC1 cell line upon exposure to 10^{-4} M 4TB. The EC_{50} values for each transfected cell line with each drug are reported in Tables 16, 17 and 18 for MDA-MB-435 transfected cells, A-549 transfected cells or DU-145 transfected cells, respectively. These data suggest that the relative efficiencies of the DNA repair mechanisms cannot, on their own, account for the observed differences in lethality between the three investigated chemotherapeutic drugs.

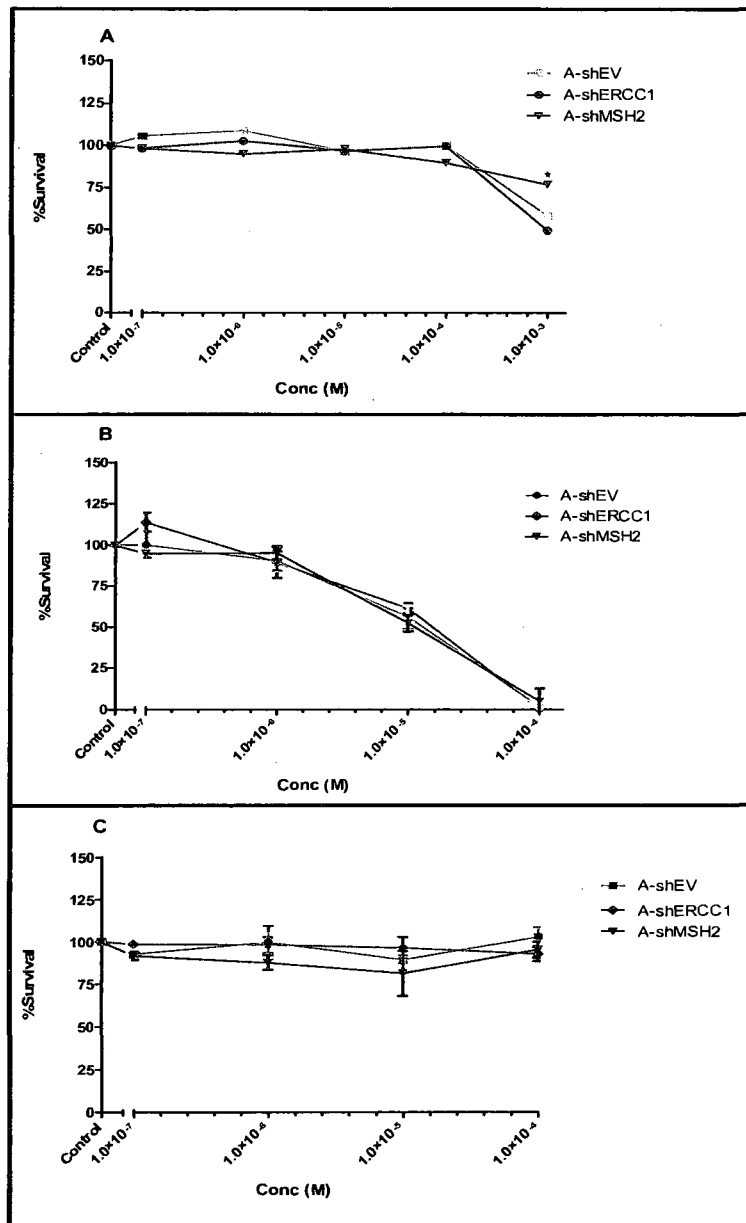


Figure 29: Clonogenic survival using cisplatin (A), 4DB (B) or 4TB (C) in A-549 transfected cells. Cell survival was measured and compared to control cells after a 1 hr exposure to varying concentrations of the indicated drug. The above figures represent three trials each. Colonies were stained with crystal violet and viability was measured by counting colonies and comparing to the number of colonies in the control sample. A colony is a group of cells with $n \geq 50$.

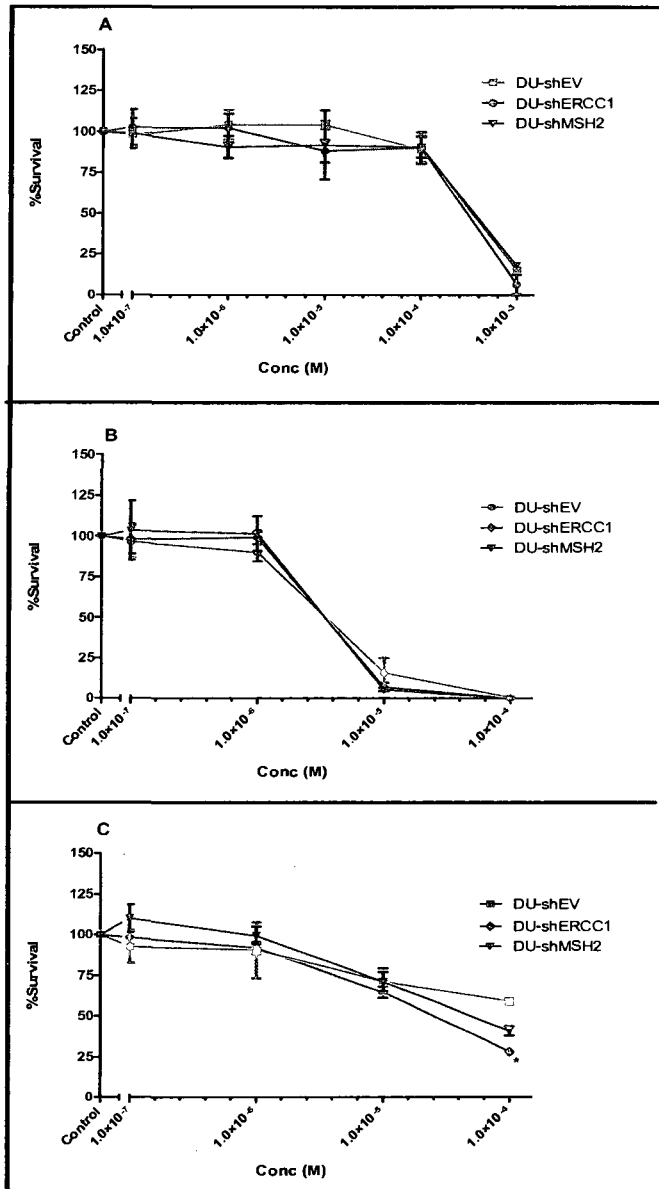


Figure 30: Clonogenic survival using cisplatin (A), 4DB (B) or 4TB (C) in DU-145 transfected cells. Cell survival was measured and compared to control cells after a 1 hr exposure to varying concentrations of the indicated drug. The above figures represent three trials each. Colonies were stained with crystal violet and viability was measured by counting colonies and comparing to the number of colonies in the control sample. A colony is a group of cells with $n \geq 50$.

Agent (μM)	MDA-MB-435 (Wild Type)	MB-shEV	MB-shERCC1	MB-shMSH2
CDDP	311.96	400	402	975*
4DB	2.50	3.00	3.00	3.64
4TB	2.41	7.32	1.85	2.62

Table 16: EC₅₀ values determined of MDA-MB-435 wild type and transfected cells as determined by using the clonogenic survival assay method. *Statistically significant in comparison to wild type and shEV cell line.

Agent (μM)	A-549 (Wild Type)	A-shEV	A-shERCC1	A-shMSH2
CDDP	850	1110	930	>1000*
4DB	8.50	1.33	1.38	1.11
4TB	>100	>100	>100	>100

Table 17: EC₅₀ values determined of A-549 wild type and transfected cells as determined by using the clonogenic survival assay method. *Statistically significant in comparison to wild type and shEV cell line.

Agent (μM)	DU-145 (Wild Type)	DU-shEV	DU-shERCC1	DU-shMSH2
CDDP	490.00	332	309	375
4DB	2.53	3.54	3.54	3.54
4TB	73.72	93.5	25.2*	51.3

Table 18: EC₅₀ values determined of DU-145 wild type and transfected cells as determined by using the clonogenic survival assay method. *Statistically significant in comparison to wild type and shEV cell line.

CHAPTER 5

SUMMARY, CONCLUSIONS AND RECOMMENDATIONS

5.1 Discussion of Results

The purpose of the current study was to determine potential biomarkers and other factors inherent to the three investigated chemotherapeutic drugs that are responsible for the observed variations in lethality upon treatment with cisplatin 4DB and 4TB in different cancer tissue types. The current study generated data relevant to the following tasks:

- 1) Characterize drug uptake and drug clearance over time in whole cells in wild type breast, prostate and lung cancer cell lines;
- 2) Determine the levels of platinum-DNA adducts formed over time with each drug in all wild type cell lines;
- 3) Determine by microarray analysis which genes are expressed in the wild type cell lines in response to drug treatment;
- 4) Suppress DNA repair mechanisms, nucleotide excision repair and mismatch repair, using short hairpin RNA, to determine the effects on drug efficacy.

Determination of drug uptake and clearance over time in the wild type cell lines was achieved by analyzing samples treated with the EC_{50} concentration of each drug

using ICP-MS analysis. Comparing the observed lethality of each drug to the level of initial drug uptake and subsequent clearance of drug from the cells can lend insight into whether or not drug uptake is playing a role in the ability of each drug to induce cell death. To determine the level of uptake, the initial concentration of platinum immediately following treatment was measured in each sample. The concentration in the sample was then compared to the total concentration of platinum in each EC_{50} concentration. The concentration of platinum in the treatment sample was divided by the total concentration of platinum in the EC_{50} concentration to determine the percentage of drug uptake. The results revealed that percentage of drug uptake as well as percentage of drug clearance over a 24 hr period can be correlated to the level of lethality exerted by each drug in each cell line. As shown in Table 1, 4DB is the most lethal drug in all three cell lines investigated. The 4TB drug is effective in both the DU-145 and MDA-MB-435 cell lines but had no effect in the A-549 cell line. Further, the 4TB drug is 30 times more lethal in the MDA-MB-435 cell line compared to the DU-145 cell line. With respect to cisplatin, the drug is effective in inducing cell death, but only at concentrations greater than 300 μ M for all cell lines. Drug uptake studies with 4DB (Figure 13A) revealed that 23.25%, 4.24% and 29.65% of the drug was taken up by MDA-MB-435, A-549 and DU-145 cells, respectively. This trend continued in all cell lines with the other two investigated drugs, 4TB and cisplatin. Levels of drug uptake with 4TB were 8.11%, 0.08% and 2.70% for the MDA-MB-435, A-549 and DU-145 cells, respectively. Levels of drug uptake with cisplatin were 0.16%, 0.27% and 0.15% for the MDA-MB-435, A-549 and DU-145 cells, respectively.

Characterization of nuclear uptake of each drug, lends further support to the idea that the level of drug uptake positively correlates to cytotoxicity (Figure 13B). In the MDA-MB-435 cell line, the percentage of drug that had formed Pt-DNA adducts immediately following drug treatment was 0.0093% with cisplatin, 0.21% with 4TB and 0.41% with 4DB. In the A-549 cell line, the percentage of drug that had formed Pt-DNA adducts was 0.17% with cisplatin, 0.0074% with 4TB and 0.083% with 4DB. In the DU-145 cell line, the percentage of drug that had formed Pt-DNA adducts was 0.0065% with cisplatin, 0.018% with 4TB and 0.27% with 4DB. As with the whole cell platinum accumulation studies, the drugs that induce the highest levels of cytotoxicity also formed the greatest number of Pt-DNA adducts. These data show a positive correlation between Pt-DNA adduct formation and drug lethality.

ICP-MS studies of drug clearance rates also provided insight into the factors that contribute to the observed lethality with each drug. Samples were first analyzed to determine if each cell line was competent to both export the drug from the cell as well as repair Pt-DNA adducts. These studies confirmed that levels of platinum in whole cells as well as levels of Pt-DNA adducts decreased over time with respect to all cell lines and all drugs (Figures 14 and 15). Analysis of drug clearance rates from whole cells revealed that the more efficacious drugs (i.e., lower EC_{50} concentration) were retained at higher concentrations in the cell during the 24 hr period in comparison to the drugs that were less effective at inducing cell kill. Specifically, in MDA-MB-435 cell line, 36% of both 4DB and 4TB remained in the cells 24 hr post treatment. Given that the EC_{50} concentrations for 4DB and 4TB with the MDA-MB-435 cell line are nearly identical,

and the clearance rates of these drugs are also identical, the data suggests that the ability of the cell to export the drug is directly related to its lethality. The studies with MDA-MB-435 further showed that only 28% of cisplatin remained after a 24 hr period (Figure 16A). In the A-549 cell line, the amount of each drug remaining 24 hr following treatment for 4DB, 4TB and cisplatin were 47%, 43% and 30%, respectively. The data for the A-549 cell line (Figure 16B) with respect to 4DB and cisplatin correlate to the given EC_{50} values for each of these drugs. However, the clearance rate for 4TB does not correlate to the established EC_{50} value. The amount of drug remaining 24 hr post drug treatment in DU-145 cells was 29%, 24% and 25% for 4DB, 4TB and cisplatin, respectively (Figure 16C). The studies involving drug uptake and clearance reveal that if an increased concentration of drug gains access to and remains in the cell, the more lethal the drug. These data show that in order for newer generation of cisplatin analogues to have the desired efficacy, the drug must effectively gain access to and be retained with the cell.

The second primary task in the current study was to determine the level of platinum-DNA adducts formed over time with each drug type in all wild type cell lines. ICP-MS studies of platinum present in genomic extracts of cells treated with the EC_{50} concentration of each drug revealed that the drugs with increased levels of uptake also had increased levels of Pt-DNA adduct formation. The studies further showed that the more efficacious drugs had reduced levels of repair in comparison to the drugs with reduced efficacy. Specifically, in the MDA-MB-435 cell line, the percentage of lesions remaining in both the 4DB and 4TB treated samples 24 hr post drug exposure was 48%

compared to only 30% of the lesions remaining in the samples treated with cisplatin (Figure 17A). There is a correlation between drug cytotoxicity and ineffective repair of Pt-DNA adducts. This correlation was also observed in the A-549 and DU-145 cell lines. In the A-549 cell line, the percentage of lesions remaining 24 hr post drug treatment were 63% in 4DB treatment samples, 36% in 4TB treatment samples and 45% in samples treated with cisplatin (Figure 17B). In the DU-145 cell line, the percentage of lesions remaining 24 hr post drug treatment were 80% in 4DB treatment samples, 72% in 4TB treatment samples, and 56% in cisplatin treatment samples (Figure 17C).

The data obtained from the analysis of Pt-DNA adduct clearance from cells suggests that effective repair of Pt-DNA adducts correlates to increased survival. These data lend further insight into the method by which these drugs exert their cytotoxic effects once inside the cell. Further, the analyses of Pt-DNA adduct clearance with the 4TB drug in the A-549 cells indicate that although 43% of the drug remains in the cell 24 hr post drug treatment, only 36% of the Pt-DNA adducts remained. The amount of Pt-DNA adducts remaining is consistent with drugs that are less efficacious in other cell lines. For example, cisplatin is the least efficacious of the three investigated drugs in the DU-145 cell line with 56% of Pt-DNA adducts remained 24 hr post drug treatment. These data reveal that chemotherapeutic drugs that have the capacity to thwart DNA repair processes have the potential to induce greater levels of cytotoxicity.

The third task in the study involved microarray analysis of RNA extracted from wild type cells at 0 hr, 2 hr, 4 hr or 24 hr post drug treatment to determine the genes involved in the observed sensitivity or resistance to each drug. However, the 24 hr time

point with the MDA-MB-435 cell line treated with the EC₅₀ concentration of 4DB had to be abandoned due to insufficient RNA in these samples. As shown in Figures 18 and 19, flow cytometry and fluorescent microscopy studies revealed that the majority of the cells in this treatment group were in the active stages of cell death, apoptosis or necrosis, 4 hr post treatment with 4DB. Due to the increased level of cell death, the 24 hr time point was excluded from these samples and a 2 hr post treatment time point was included in the study.

In order to determine the genes of interest, gene expression levels at each time point were compared to the control sample (wild type cells exposed to the drug vehicle DMSO). The genes with the highest changes in expression levels, up to five, at each time point were identified, resulting in a total of 93 genes with potential involvement in response to drug treatment. Of the 93 total genes, 18 genes were identified as common to all cell lines upon treatment with each of the three investigated drugs (Tables 6 to 14). One common gene to all cell lines with respect to the 4DB treatment was the CHOP gene. Over expression of CHOP in response to 4DB treatment could play a role in DNA damage signalling which has the potential to induce increased levels of apoptosis. Five of the 18 genes common to all cell lines were the heat shock proteins (HSP) HSP72, HSP70, HSP60, HSP40 and HSP32. The activity of heat shock proteins involves protecting cells from stress by binding and refolding client proteins. HSP72 and HSP70 are members of the HSP70 family, which requires the presence of HSP40 to refold client proteins (Goloubinoff et al., 2007). HSP60 is considered a mitochondrial chaperonin protein which is responsible for transporting and refolding proteins from the cytoplasm into the

matrix of the mitochondria (Gupta et al., 2002). HSP32 is classified as a small heat shock protein and is involved in porphyrin metabolism. This protein has also been characterized as a stress related survival protein that has been found in tumours (Sasaki et al., 2005).

As previously stated, the HSPs identified were found in all cell lines in response to each of the drugs. The presence of these proteins in all examined treatment samples suggest that although there is protection afforded from each of these drugs, these proteins are not responsible for differences in the observed cytotoxicity levels with respect to 4TB in the three cell lines. Further analysis of the genes that were over expressed in the treatment samples revealed three genes that have the potential to promote the observed resistance in the A-549 and DU-145 cell lines to cisplatin and 4TB. Cyclin dependent kinase inhibitor (p21), zinc transporter 1 (ZNT1), and metallothionein-1L (MT-1L) were over expressed genes in the DU-145 and A-549 cell lines following treatment with 4TB. These genes were not over expressed in the MDA-MB-435 treatment samples. The p21 gene has been shown to be anti apoptotic. The gene is regulated by the tumor suppressor protein p53 and is responsible for regulation cell cycle progression through the G1 phase. This gene also plays a role in regulating DNA replication and DNA damage repair (Nath, 2005). The MT-1L gene is responsible for binding heavy metals, such as Zn and Pt, that are either physiological or introduced into the cell. MT-1L is believed to provide protection against metal toxicity, oxidative stress and supports regulation of zinc and copper. MT-1L has the capacity to activate transcription factors through regulation of zinc levels (Andrews, 2000; Baraboy et al., 2003). The third gene of interest, ZNT1 is a zinc transporter responsible for supporting homeostasis of intracellular zinc levels (Qin et

al., 2009). Previous studies have linked cation transport activity with the export of platinum containing drugs. Further, increased expression of cation transporters have been identified in cell lines that have been characterized as resistant to cisplatin. ZNT1 is of particular interest because it has been implicated in activation of MT-1L which in turn regulates copper homeostasis by regulation of copper transporters, ATP7A and ATP7B, two proteins that have been identified in cisplatin resistant cell types (Kuo et al., 2007). The anti apoptotic activity of p21, increased binding of the drug in the cytoplasm by MT-1L such that the drug does not have the opportunity to form Pt-DNA adducts and export of the drug via ZNT1 activities are most likely involved in the observed resistance to cisplatin and 4TB in the DU-145 and A-549 wild type cell lines.

The final task in the current study was to determine if disruption of the DNA repair mechanisms, NER and MMR, increased the efficacy of each drug. ERCC1 was the target in the disruption of the NER mechanism and MSH2 was the target in the disruption of the MSH2 mechanism. Prior to disruption of these proteins, wild type MDA-MB-435, DU-145, and A-549 cells were analyzed for each protein using Western blot analysis to confirm that these proteins of interest were expressed in each cell line (Figure 20). Following confirmation of expression, disruption of each DNA repair mechanism was achieved by introducing shRNA inserted in a DNA expression vector (Figure 21) against either ERCC1 or MSH2. Four different non-overlapping constructs against each protein were transiently transfected into each cell line and the construct that resulted in the greatest decrease of protein expression was selected for the creation of a stable cell line. As shown in Figures 22, 23 and 24 a construct that sufficiently reduced protein

expression was successfully identified by either intracellular antigen staining or Western blot analysis. The identified construct as well as positive and negative controls were then used to create stable cell lines from each wild type cell line. The nomenclature for each developed cell line is given in Table 15. Confirmation of reduced protein expression in the cell lines subjected to stable transfection was confirmed was Western blot analysis (Figures 25, 26, 27).

Clonogenic survivals were conducted with the newly developed cell lines to determine if disruption of the DNA repair mechanisms would result in a change in lethality to each of the three drugs. The newly generated survival curves were used to recalculate the EC_{50} values in each of the developed cell lines for cisplatin, 4TB and 4DB. As shown in Figure 28 and Table 16, the results of the clonogenic survivals in MDA-MB-435 transfected cells revealed that the only statistically significant change in the transfected cells compared to wild type or the negative control was in MB-shMSH2 cell line with respect to cisplatin. The newly calculated EC_{50} for cisplatin in the MB-shMSH2 cell line was 975 μ M compared to 311 μ M in the wild type cell line. An increase in the EC_{50} concentration in a cell line with suppressed MSH2 expression was not unexpected. In addition to its role in the MMR mechanism, MSH2 is known to induce cell-cycle arrest in the G2 phase upon recognition of mismatched base pairs or damaged DNA which allows sufficient time for the cell to repair the DNA prior to entering the S phase of the cell cycle. Decreasing levels of MSH2 has the potential to allow continued cell cycle progression in cells with genetic instability, resulting in cell survival as well as increased levels of mutations. However, MSH2 deficient cell lines have also been tested

and results suggest that the effect of MSH2 suppression on drug cytotoxicity warrants empirical determination of untested cell lines (Marquez et al., 2003).

The EC₅₀ values for the A-549 transfected cell lines had similar results to those of the MDA-MB-435 transfected cell lines. As shown in Figure 29 and Table 17, the results of the clonogenic survivals in A-549 transfected cells revealed that the only statistically significant change in the transfected cells compared to wild type or the negative control was in A-shMSH2 cell line with respect to cisplatin. The newly calculated EC₅₀ for cisplatin in the A-shMSH2 cell line was >1000 μM compared to 850 μM in the wild type cell line.

In the DU-145 cell line (Figure 30 and Table 18), results from the clonogenic survivals revealed that the only significant difference in cytotoxicity occurred in the DU-shERCC1 cell line in response to 4TB. The newly calculated EC₅₀ for this cell line with 4TB was 25.2 μM as compared to 73.72 μM in the wild type cell line. The data from the clonogenic survivals suggests that DNA repair alone does not account for the observed resistance or sensitivity to each drug in each cell line.

Review of all the data generated from each of the tasks lends insight into the possible biomarkers and drug characteristics that are responsible for the varying cytotoxicity observed between the investigated cell lines. In the MDA-MB-435 cell line, the data suggests that increased levels of drug uptake are responsible for the observed sensitivity. Changes in levels of gene expression following treatment does not account for the observed sensitivity of MDA-MB-435 to each of the drugs. NER silencing also did not result in any change in lethality. Interruption of MSH2 with this cell line did result in

a significant increase in survival rate upon treatment with 4DB. These data indicate that 4DB exerts its cytotoxic effects by gaining access to the cell at significantly increased levels, 23.25%, and that the MSH2 protein is involved in modulating cellular response to this drug. Upon gaining access to the cell, a significant portion of the drug gains access to DNA, forms Pt-DNA adducts and is not rapidly repaired over a 24 hr period. MSH2 may be responsible for recognizing the DNA damage and committing the cell to apoptosis upon recognizing the lesions induced by the presence of 4DB. Given that there are no changes in gene expression following drug exposure that would account for increased sensitivity (i.e., pro-apoptotic proteins are not over expressed), increased drug uptake appears to be the principle cause of lethality. The experiments conducted with the MDA-MB-435 and the two remaining drugs, 4TB and cisplatin, yield similar results. Sensitivity to each drug is correlated to the amount of drug taken up by the cell. Changes in gene expression and suppression of DNA repair activity did not change the response of the cell line to either of these drugs.

In the A-549 and DU-145 cell lines, drug uptake also appears to be a central cause of cytotoxicity. The cell line's response to each drug is directly correlative to the amount of drug taken up by the cell; with increased drug uptake there is increased lethality. However, gene expression changes in response to treatment, in both cell lines, also appear to play a role in determining sensitivity levels to cisplatin and 4TB. Increased levels of MT-1L, p21 and ZNT1 have the potential to bind cisplatin in the cytoplasm, prevent the initiation of the apoptotic cascade and actively export the drug from the cell.

DNA repair also appears to play a role in the response of these cell lines to these drugs. In the A-shMSH2 cell line, there is increased survival upon treatment with cisplatin in comparison to the wild type, indicating that normal MSH2 expression levels in the cell line, as with MDA-MB-435 cells, may be responsible for recognizing DNA damage and committing the cell to apoptosis when the damage is too overwhelming. In the DU-shERCC1 cell line, there was decreased survival upon treatment with 4TB in comparison to the wild type. These data indicate that normal expression of ERCC1 levels within the DU-145 cell line actively repairs Pt-DNA adducts formed by 4TB. With respect to the 4DB in all cell lines, it appears that the intracellular concentration is so elevated that the cell is unable to overcome the cytotoxic effects exerted by increased protein binding and Pt-DNA adduct formation. Taken together, these data indicate that inhibition of MMR supports increased survival due to reduced cell cycle regulation and inhibition of NER decreases Pt-DNA adduct repair resulting in increased levels of cell death.

5.2 Conclusions and Recommendations for Further Study

The data from the study indicates that drug uptake is positively correlated to drug sensitivity. In the cases of drug resistance, overexpression of an apoptotic inhibitor (p21), cation transporter (ZNT1) and a protein that binds heavy metals (MT-1L) potentially account for resistance. Changes in gene expression levels associated with DNA repair following drug treatment were not observed in any of the cell lines, indicating that efficiency of DNA repair does not play a critical role in drug resistance. Additionally,

levels of HMG proteins were not over expressed in any cell line following drug exposure which eliminates this class of proteins as a potential target for modulating drug response.

Drug uptake levels were identified as critical components of sensitivity or resistance to a chemotherapeutic agent. However, the conditions that render the cell susceptible or not to drug uptake have not been elucidated. The data from the current study suggest a physiological difference inherent in each tissue type with respect to cisplatin and 4TB. However, given that 4DB is uniformly taken up by cells at elevated concentrations, it is likely that the chemical composition of 4DB is responsible for its ability to induce cytotoxicity in the different tissue types, rather than individual characteristics of the cells. Understanding the chemical interactions between 4DB and the surface of the cell is the most likely approach to allow elucidation of the conditions that contribute to the successful entrance and subsequent enhanced cytotoxicity induced by this drug. Understanding the interactions between 4DB and the plasma membrane could lend valuable insight into the rational drug design of new chemotherapeutic drugs. If lower concentrations of the drug are required given their ability to induce increased levels of cell death, side effects are likely be less severely toxic and be more tolerable.

The variations in response to 4TB warrant further study regarding the interactions of the drug and the plasma membrane. If the membranes of DU-145 and A-549 cells have increased concentrations of molecules that support membrane rigidity and tight junctions between cells, these factors could account for decreased levels of drug uptake. For example, if there are increased concentrations of cholesterol in the plasma membrane of these cells, this could explain the reduced drug uptake and therefore reduced efficacy of

4TB. The tertbutyl groups extending from the bipyridine ring system are subject to enhanced steric strain in comparison to the n-butyl groups extending from the bipyridine ring system in the 4DB drug. The differences in rigidity of these functional groups could be responsible for reduction in drug uptake. These factors could not be identified by the microarray data from the current study due to the design of the experiment. Microarray experiments of exponentially growing wild type cells from each cell line should be conducted. The data from each cell line should be used to compare differences between tissue types in order to determine if there are expression changes from one cell line to another that can account for observed drug uptake levels.

The microarray data revealed that increased expression of ZNT1 and MT-1L correlated to increased survival in the DU-145 and A-549 cells following treatment with 4TB or cisplatin. Therefore, disruption of these proteins using shRNA and assessing changes in cytotoxicity using clonogenic survivals should be conducted to determine if these proteins are involved in drug response. Disruption of one or both targets with concurrent improvement in cytotoxicity could indicate that these proteins support survival following drug treatment.

Additional studies using these drugs within normal tissue types also warrants investigation. The success of 4DB at inducing high levels of cell kill is a promising results. Therefore, clonogenic survivals should be conducted to empirically determine the cytotoxic effects of 4DB in tissues that have been identified as particularly susceptible to platinum compounds such as kidney epithelial cells.

In conclusion, it appears that drug sensitivity is only minimally impacted by the disruption of DNA repair mechanisms in the MDA-MB-435, A-549 and DU-145 cells. Increased drug uptake positively correlates to cytotoxicity. In the A-549 and DU-145 cells, the upregulation of p21, MT-1L and ZNT1 are potential contributors to the observed resistance in these cell lines to 4TB and cisplatin. Determining the specific interactions that allow for increased drug uptake will support future efforts in designing new chemotherapeutics which have increased efficacy with less severe side effects in comparison to currently used chemotherapeutics.

REFERENCES

- American Cancer Society. *Cancer Facts & Figures 2008*. Atlanta: American Cancer Society; 2008.
- Andrews GK. 2000. Regulation of metallothionein gene expression by oxidative stress and metal ions. *Biochem. Pharmacol.* 59:95-104.
- Anguiano A, Nevins J, Potti A. 2008. Toward the Individualization of Lung Cancer Therapy. *Cancer* 113:1760-1767.
- Baraboy VA, Petrina LG. 2003. Metallothioneins: The structure and action mechanisms. *Ukrainskii Biokhimicheskii Zhurnal* 75:28-36.
- Biswas SK, Huang J, Persaud S, Basu A. 2004. Down-regulation of Bcl-2 is associated with cisplatin resistance in human small cell lung cancer H69 cells. *Mol. Cancer Ther.* 3:327-334.
- Chaney SG, Campbell SL, Bassett E, Wu Y. 2005. Recognition and processing of cisplatin- and oxaliplatin-DNA adducts. *Crit. Rev. Oncol./Hematol.* 53:3-11.
- Chang IY, Kim MH, Kim HB, Lee DY, Kim SH, Kim HY, You HJ. 2005. Small interfering RNA-induced suppression of ERCC1 enhances sensitivity of human cancer cells to cisplatin. *Biochem. Biophys. Res. Commun.* 327:225-233.
- Eastman A. 1987. The formation, isolation and characterization of DNA adducts produced by anticancer platinum complexes. *Pharmacology and Therapeutics* 34:155-166.
- Elwell KE, Hall C, Tharkar S, Giraud Y, Bennett B, Bae C, Carper SW. 2006. A fluorine containing bipyridine cisplatin analog is more effective than cisplatin at inducing apoptosis in cancer cell lines. *Bioorg. Med. Chem.* 14:8692-8700.
- Farid RS, Bianchi ME, Falciola L, Engelsberg BN, Billings PC. 1996. Differential binding of HMG1, HMG2, and a single HMG box to cisplatin-damaged DNA. *Toxicol. Appl. Pharmacol.* 141:532-539.

- Garelli N, Vierling P. 1992a. Incorporation of new amphiphilic perfluoroalkylated bipyridine platinum and palladium complexes into liposomes: Stability and structure - Incorporation relationships. *Biochimica et Biophysica Acta - Lipids and Lipid Metabolism* 1127:41-48.
- Garelli N, Vierling P. 1992b. Synthesis and characterization of amphiphilic platinum and palladium complexes linked to perfluoroalkylated side-chain disubstituted bipyridines. *Inorganica Chimica Acta* 194:247-253.
- Goloubinoff P, Rios PDL. 2007. The mechanism of Hsp70 chaperones: (entropic) pulling the models together. *Trends Biochem. Sci.* 32:372-380.
- Gonzalez-Mariscal L, Betanzos A, Nava P, Jaramillo BE. 2003. Tight junction proteins. *Progress in Biophysics and Molecular Biology* 81:1-44.
- Gupta S, Knowlton AA. 2002. Cytosolic heat shock protein 60, hypoxia, and apoptosis. *Circulation* 106:2727-2733.
- Jordan P, Carmo-Fonseca M. 2000. Molecular mechanisms involved in cisplatin cytotoxicity. *Cell. Mol. Life Sci.* 57:1229-1235.
- Kuo MT, Chen HHW, Song IS, Savaraj N, Ishikawa T. 2007. The roles of copper transporters in cisplatin resistance. *Cancer and Metastasis Reviews* 26:71-83.
- Marcel Gielen, Tiekink E. 2005. *Metallotherapeutic Drugs and Metal-Based Diagnostic Agents: The Use of Metals in Medicine*. Hoboken: Wiley.
- Marquez N, Chappell SC, Sansom OJ, Clarke AR, Court J, Errington RJ, Smith PJ. 2003. Single cell tracking reveals that Msh2 is a key component of an early-acting DNA damage-activated G2 checkpoint. *Oncogene* 22:7642-7648.
- Mymryk JS, Zaniewski E, Archer TK. 1995. Cisplatin inhibits chromatin remodeling, transcription factor binding, and transcription from the mouse mammary tumor virus promoter in vivo. *Proceedings of the National Academy of Sciences of the United States of America* 92:2076-2080.
- Nath KA. 2005. Provenance of the protective property of p21. *American Journal of Physiology - Renal Physiology* 289:F512-F513.
- Qin Y, Thomas D, Fontaine CP, Colvin RA. 2009. Silencing of ZnT1 reduces Zn²⁺ efflux in cultured cortical neurons. *Neurosci. Lett.* 450:206-210.

Sasaki T, Yoshida K, Kondo H, Ohmori H, Kuniyasu H. 2005. Heme oxygenase-1 accelerates protumoral effects of nitric oxide in cancer cells. *Virchows Archiv* 446:525-531.

Stewart DJ. 2007. Mechanisms of Resistance to Cisplatin and Carboplatin. *Crit. Rev. Oncol./Hematol.* 63:1-11.

Stewart JJ, White JT, Yan X, Collins S, Drescher CW, Urban ND, Hood L, Lin B. 2006. Proteins associated with cisplatin resistance in ovarian cancer cells identified by quantitative proteomic technology and integrated with mRNA expression levels. *Mol. Cell. Proteomics* 5:433-443.

Stojic L, Brun R, Jiricny J. 2004. Mismatch repair and DNA damage signalling. *DNA Repair* 3:1091-1101.

Vo V. 2009 Characterizing Lethality of Novel Cisplatin Analogues. University of Nevada Las Vegas

Wang D, Lippard SJ. 2005. Cellular processing of platinum anticancer drugs. *Nature Reviews Drug Discovery* 4:307-320.

VITA

Graduate College
University of Nevada, Las Vegas

Becky Michelle Hess

Local Address:

4525 Galapagos Avenue
North Las Vegas, NV 89084

Degrees:

Bachelor of Science, Chemistry, 2006
University of Nevada, Las Vegas

Thesis Title:

Identifying Biomarkers for Resistance to Novel Cisplatin Analogues in Human
Lung, Breast and Prostate Cancers

Thesis Examination Committee:

Chairperson, Bryan Spangelo, Ph.D.
Committee Member, MaryKay Orgill, Ph.D.
Committee Member, Ronald Gary, Ph.D.
Graduate College Representative, Lloyd Stark, Ph.D.